The respiratory basis of metabolic rate and life histories

by
Jennifer Sarah Bigman

M.Sc., Moss Landing Marine Laboratories, 2013
B.Sc., (*summa cum laude*) University of North Carolina Wilmington, 2009

Thesis Submitted in Partial Fulfillment of the
Requirements for the Degree of
Doctor of Philosophy

in the
Department of Biological Sciences
Faculty of Science

SIMON FRASER UNIVERSITY
Summer 2021

Declaration of Committee

Name:	**Jennifer Sarah Bigman**
Degree:	**Doctor of Philosophy**
Title:	**The respiratory basis of metabolic rate and life histories**
Committee:	**Chair:** John Reynolds Professor, Biological Sciences
	Nicholas K. Dulvy Supervisor Professor, Biological Sciences
	Nicholas C. Wegner Committee Member Fisheries Research Biologist NOAA Fisheries
	Jonathan W. Moore Committee Member Professor, Biological Sciences
	Arne Ø. Mooers Examiner Professor, Biological Sciences
	William W. L. Cheung External Examiner Professor Institute for the Oceans and Fisheries The University of British Columbia

Ethics Statement

The author, whose name appears on the title page of this work, has obtained, for the research described in this work, either:

a. human research ethics approval from the Simon Fraser University Office of Research Ethics

or

b. advance approval of the animal care protocol from the University Animal Care Committee of Simon Fraser University

or has conducted the research

c. as a co-investigator, collaborator, or research assistant in a research project approved in advance.

A copy of the approval letter has been filed with the Theses Office of the University Library at the time of submission of this thesis or project.

The original application for approval and letter of approval are filed with the relevant offices. Inquiries may be directed to those authorities.

Simon Fraser University Library
Burnaby, British Columbia, Canada

Update Spring 2016

Abstract

Oxygen fuels aerobic metabolism and as such, plays an important role in the physiology, ecology, and evolution of organisms. Traits related to oxygen acquisition (respiratory surface area) and use (metabolic rate) or the balance of oxygen supply and demand (or its mismatch, termed 'oxygen limitation') have been proposed to underlie broad patterns such as the temperature-size rule and the geographic distributions of marine species. Moreover, traits related to oxygen acquisition and use form the central focus of seemingly disparate macroecological theories that aim to explain and predict the structure and dynamics of ecological systems and how these systems and their constituents will respond to a changing climate. While these existing theories and oxygen-related explanations offer a compelling story, the role of oxygen in shaping biological observations, responses, and patterns is hotly debated. Further, much work in this area is experimental in nature and typically focuses on a single species in laboratory settings. Broader scale, macroecological research stemming from meta-analysis and modeling is needed to understand the generality of patterns. To that end, this thesis takes a macroecological approach and examines the generality of the relationships among traits related to oxygen acquisition and use, ecology, and life histories. First, I reveal that respiratory surface area explains patterns of metabolic rate across the vertebrate tree of life. Second, I uncover that larger-bodied, active, pelagic sharks have greater gill surface areas (respiratory surface area in fishes) for a given size compared to their smaller-bodied, less active, benthic counterparts. Conversely, the rate at which gill surface area increases with body mass is the same for all species, regardless of activity level, habitat type, or maximum size. Third, I test a central prediction of the Gill Oxygen Limitation Theory and find that across fishes, growth and maximum size more strongly relate to activity level than gill surface area. Collectively, my thesis highlights the complexities of integrating data across scales and illustrates that oxygen acquisition and use is tightly correlated with activity level, but the relationships with life histories are less straightforward. This body of work builds on existing theory while empirically testing relationships among oxygen acquisition and use, ecological lifestyle, and the life histories among fishes and other vertebrates.

Keywords: Metabolic Theory of Ecology; Gill Oxygen Limitation Theory; respiratory surface area; von Bertalanffy growth function; Bayesian hierarchical modeling; allometry

Acknowledgements

This thesis would not have been possible without the help and support of numerous people. First, I would like to thank my primary supervisor, Nick Dulvy. From the very beginning, Nick helped me achieve things that I did not think I was capable of and always pushed me to do the best I could. I would not be the scientist I am today if it were not for him. Second, I would like to thank Nick Wegner. His input was instrumental to this thesis, and I thank him for his continuous enthusiasm and engagement, as well as enduring amid macroecologists. Although it was challenging to have two supervisors with such divergent views, this experience pushed me to understand a range of topics and research areas, and for that, I am grateful. I would also like to thank my other committee member, Jon Moore, for his insightful comments throughout this process. Importantly, I thank Leithen M'Gonigle for agreeing to work with Nick D. and I on the modeling framework in Chapter 2 and Daniel Pauly for working with me to understand the ins and outs of the Gill Oxygen Limitation Theory. I immensely enjoyed working with both of you.

I would like to thank those who have helped me accomplish this research aside from my committee members. First, thank you to all the researchers, students, and field technicians who made it possible for me to collect all the elasmobranch specimens that went into my dataset. "The Dulvy Lab goes outside" was a trip to remember, and I particularly thank Chris Bedore, Chris Mull, and Pete Kyne. I would also like to thank Erik Mahan for assisting with the caudal fin aspect ratios in my last chapter. Thank you to all E2O, particularly Chris Mull, Seb Pardo, Dan Greenberg, Nicola Smith, Marlene Wagner, Amanda Kissel, Rachel Walls, Serena Wong, Tanya Prinzing, and Wade Vanderwright. Not only were you all great colleagues, but great friends. Thank you to all my friends outside of E2O who had to put up with me during this process, particularly Chris Bedore, Kady Lyons, and Pete Kyne.

Finally, and most importantly, thank you to my family. I could not have accomplished any of this without my amazing husband Nick Hill. Your kindness and encouragement helped me get through this, and my accomplishments are as much yours as mine. I look forward to many years to come. My family, although never failing to ask me how much longer I was going to take to finish my PhD, was always there for me. I thank all of you—Mom, Dad, Linda, David, Fran, Abby, Maura, Hillary, Matthew, and Jeffrey (and spouses and kids) for your support and love over the years. I couldn't ask for a better bunch!

Table of Contents

List of Tables

List of Figures

Chapter 1.

Introduction

Oxygen fuels life on Earth. The marked increase in oxygen levels in the atmosphere and ocean around the late Neoproterozoic Era (850 – 542 million years ago) is thought to have paved the way for the evolution of complex life forms, e.g., metazoans (Nursall 1959; Canfield & Teske 1996). Today, most animals respire aerobically and thus rely on oxygen to fuel metabolic activities, which broadly function to transform resources from the environment into available energy (Brown *et al.* 2004; Mentel *et al.* 2016). This energy is subsequently allocated to life-sustaining processes, such as survival, growth, and reproduction (Brown *et al*. 2004).

Although physiologists have long recognized the important role oxygen plays in the ecology and evolution of organisms, this role has been largely underappreciated in ecology until recently. Traits related to oxygen acquisition (respiratory surface area) and use (metabolic rate) or the balance of oxygen supply and demand (or its mismatch, termed 'oxygen limitation') have recently been proposed to underlie broad, macroecological and macrophysiological patterns (Forster *et al.* 2012; Rubalcaba *et al.* 2020; Deutsch *et al*. 2020). For example, oxygen limitation is one suggested explanation for the inverse relationship between ectothermic body size and temperature seen in the wild (Bergmann's rule/James' Rule) and in the laboratory (temperature-size rule; Forster *et al*. 2012; Hoefnagel & Verberk 2015; Verberk *et al*. 2020). The faster growth to a smaller maximum size observed under warmer temperatures (or in warmer waters) is thought to be related to the difficulty in obtaining oxygen as temperature increases due to higher metabolic demand and decreased oxygen availability (Forster *et al.* 2012; Hoefnagel & Verberk 2015). This explanation is particularly relevant to aquatic ectotherms, especially those that are large-bodied, as this group must deal with the challenge of extracting oxygen from water and not air (Forster *et al*. 2012; Hoefnagel & Verberk 2015). Other broad patterns, such as the geographic distribution of marine species and the body mass- and temperature- dependence of metabolic rate in fishes, have also been linked to the balance of oxygen supply and demand (e.g., Deutsch *et al.* 2020; Rubalcaba *et al*. 2020). Such oxygen-related explanations for these broad patterns align well with predictions of macroecological and macrophysiological theories that invoke oxygen acquisition and use

(i.e., respiratory surface area, metabolic rate) or oxygen limitation to explain and predict the dynamics of biological systems and how they will respond to a changing climate (Brown *et al*. 2004; Pauly 2010; Pörtner 2010).

The Metabolic Theory of Ecology is the cornerstone of metabolic ecology, a field that encompasses the theoretical and empirical foundations connecting organismal aerobic metabolic rate to biological patterns on multiple scales, from cells to the biosphere (Brown *et al*. 2004). This field ultimately aims to leverage the evolutionary allometry (scaling) of metabolic rate, body mass, and temperature to predict patterns and processes across all levels of biological organization, including life histories and population dynamics (Gillooly *et al.* 2001; Brown *et al.* 2004). While the connections among metabolic rate, body mass, and temperature were well-established prior to the emergence of this field, this theory refined the mathematical relationship among these factors, offered a mechanism to explain why metabolic rate may vary with body mass in a predictable way, and proposed a framework to scale up metabolic rate to higher-order biological patterns and processes (Kleiber 1932; West *et al.* 1999; Brown *et al.* 2004). Although the proposed mechanism underlying the relationship of metabolic rate and body mass continues to be debated, the mathematical relationship refined by this theory, as well as the general framework connecting individual metabolic rates to higher-order patterns and processes has proven useful (O'Connor *et al.* 2007; Munch & Salinas 2009; Barneche *et al.* 2014). However, as noted by those who proposed the Metabolic Theory of Ecology, body mass and temperature do not explain all variation in metabolic rate across organisms (Gillooly *et al*. 2001; Brown *et al*. 2004). After accounting for temperature, metabolic rate for organisms of the same body mass still varies by over five orders of magnitude, suggesting that additional factors likely help explain patterns of metabolic rate across species (Gillooly *et al.* 2001; Brown *et al*. 2004).

Other traits related to oxygen acquisition, such as respiratory surface area are intimately related to metabolic rate and as such, play a large role in metabolic processes. As codified in Fick's law of diffusion, the oxygen required to fuel aerobic metabolism is diffused over the respiratory surface (Fick 1855; De Jager & Dekkers 1975; Gillooly *et al.* 2016). Although other factors are also important in determining rates of oxygen flux across a membrane (e.g.., the thickness of the respiratory membrane, the partial pressure gradient of oxygen), respiratory surface area is the only factor to substantially change, or scale, with body size (Fick 1855; De Jager & Dekkers 1975; Gillooly *et al*. 2016). When the

scaling of respiratory surface area with body mass is compared to that of metabolic rate, a remarkable similarity is revealed, both within (ontogenetic or static scaling/allometry) and across (evolutionary allometry) species (Winberg 1956; De Jager & Dekkers 1975; Wegner 2016; Gillooly *et al.* 2016). The scaling of respiratory surface area and metabolic rate, and more broadly, the importance of respiratory surface area in acquiring the oxygen required for metabolic processes has led to the proposal of a theory that argues that respiratory surface area, specifically in aquatic, water-breathing organisms, imposes a physical constraint on oxygen supply and metabolic rate (Pauly 1981, 2010).

The Gill Oxygen Limitation Theory centers on the idea that the gills of aquatic, water-breathing ectotherms limit aerobic metabolic rate and ultimately, growth and other processes that rely on the energy produced by aerobic metabolism (Pauly 1981, 2010). The central tenet of this theory is that the surface area of the gills (as a two-dimensional surface) cannot grow as fast as the body it must supply with oxygen (a three-dimensional volume; Pauly 1981, 2010). In other words, the ontogenetic scaling of gill surface area and body mass should always be less than one, resulting in a mismatch between oxygen supply and demand as an organism increases in size (Pauly 1981, 2010). Thus, the ratio of gill surface area to body mass will decrease throughout an organism's lifetime, and eventually, will not be able to match the demand of a growing body, at which the maximum size of the organism will be reached (Pauly 1981, 2010). Because this theory posits that gill surface area constrains aerobic metabolic rate, and thus processes related to or relying on metabolism, energy, and oxygen, it is multifaceted and explicitly and implicitly generates a range of predictions, including those surrounding growth and other aspects of life history and ecology (e.g., maximum size, timing of maturation and reproduction, geographic distributions, activity level) and those based more on physiological processes (e.g., food consumption and conversion efficiency, the balance of oxidative versus glycolytic enzymes; Pauly 2010, 2021). Although originally proposed in the early 1980s, the Gill Oxygen Limitation Theory has experienced a resurgence in light of research that aims to predict how species will respond to continued environmental change (Cheung *et al.* 2013; Lefevre *et al.* 2017, 2018; Pauly 2010, 2021; Seibel & Deutsch 2020). Studies have invoked the scaling of gill surface area to predict how species will respond to increased temperature and reduced oxygen availability (Cheung *et al.* 2013; Cheung & Pauly 2016). In particular, the maximum body size of fishes is expected to decline, or

‘shrink,’ due to, in part, the proposed mismatch in oxygen supply and demand as temperatures rise (Cheung *et al.* 2013).

In addition to the Gill Oxygen Limitation Theory, other, more general theories and frameworks surrounding oxygen limitation have been proposed. However, these theories differ from the Gill Oxygen Limitation Theory in that they do not propose a specific mechanism underlying oxygen limitation and are more focused on either the physiological performance of an organism (the Oxygen- and Capacity-Limited Thermal Tolerance, OCLTT) or were specifically proposed to explain the temperature-size rule (Maintain Aerobic Scope and Regulate Oxygen Supply, MASROS; the Ghost of Oxygen Limitation Past; Atkinson *et al.* 2006; Pörtner 2010; Pörtner *et al.* 2017; Verberk *et al.* 2020). The Oxygen- and Capacity-Limited Thermal Tolerance concept is primarily focused on how the physiological performance of an organism is mediated by temperature and oxygen, such that temperature imposes constraints on oxygen supply to tissues, affecting aerobic performance and ultimately, determining thermal limits (Pörtner 2010; Pörtner *et al*. 2017). The Maintain Aerobic Scope and Regulate Oxygen Supply and the Ghost of Oxygen Limitation Past concepts are related to each other and broadly suggest that reductions in maximum size (and thus faster growth, the temperature-size rule) are an adaptive response to increasing temperatures to ensure that oxygen supply will meet oxygen demand (Atkinson *et al*. 2006; Verberk *et al*. 2020).

While existing theories and oxygen-related explanations for broad scale macroecological and macrophysiological patterns present a compelling story, these theories and explanations, and more generally, the role of oxygen in shaping proposed biological phenomena and species’ responses to climate change are hotly debated (Lefevre *et al.* 2017, 2018, 2021; Marshall & White 2019; Seibel & Deutsch 2020). Moreover, most studies examining links among oxygen, temperature, physiology, and ecology are experimental in nature and focus on observations or responses of a single species in laboratory settings (e.g., Clark *et al.* 2013; Lefevre *et al.* 2021). While this work is most certainly necessary, it generates pieces of a much larger puzzle that can be ‘put together’ by meta-analysis and modeling. Doing so will allow us to understand the generality of observations or responses and thus identify whether they are consistent across species (i.e., the existence of patterns). Identifying whether patterns exist and understanding how pervasive an observation or response is will go far in helping identify why a particular response or observation may occur (i.e., the underlying mechanism or driver of such a

pattern). Such broad scale, macroecological and macrophysiological work has gained momentum in recent months, yet much remains to be examined (Audzijonyte *et al.* 2020; Deutsch *et al.* 2020, Rubalcaba *et al.* 2020). Specifically, there is a lack of clarity regarding the generality of the relationships among traits related to oxygen acquisition and use, ecology, and life histories.

To that end, this thesis takes a largely macroecological approach to examining the respiratory basis of metabolic rate and life histories in fishes and other vertebrates. Specifically, I couple field collections, laboratory dissections, and meta-analysis and modeling to examine the generality of the relationships between traits related to oxygen acquisition (respiratory surface area) and use (metabolic rate, Chapter 2), among oxygen acquisition (gill surface area) and ecological lifestyle (activity, habitat, and maximum size, Chapter 3), and finally, I test a central prediction of The Gill Oxygen Limitation Theory centered on the relationship between oxygen acquisition (gill surface area) and life history (Chapter 4, Figure 1.1). In doing so, I (along with my collaborators) (1) collect > 200 individual elasmobranch specimens for gill surface area measurements, (2) measure gill surface area for twelve species (> 71 individuals) that previously did not have these data, and (3) develop quantitative methods that enable me to address knowledge gaps by combining data across scales (individuals, species), multiple size-dependent phenomena (metabolic rate, respiratory surface area), and salient covariates including the evolutionary history among species.

1.1. Main objectives of the thesis

The main objectives of this thesis are:

1. To assess whether respiratory surface area is important in understanding patterns of metabolic rate across the vertebrate tree of life. Specifically, through a novel phylogenetic Bayesian hierarchical modeling framework that allowed me to combine size-mismatched metabolic rate and respiratory surface area data, as well as salient covariates, I test whether respiratory surface area explains additional variation in metabolic rate after accounting for body mass and temperature (Chapter 2).

2. To quantify how gill surface area (respiratory surface area in fishes) relates to ecological lifestyle across shark species. Here, I examine how gill surface area in the context of its allometry (ontogenetic intercept [gill surface area for a given body size] and ontogenetic slope [rate at which gill surface area increases with body mass ontogenetically]) varies with activity level, habitat type, and maximum size (Chapter 3).

3. To test a central prediction of the Gill Oxygen Limitation Theory – that gill surface area relates to growth and maximum size across fishes. For this chapter, I re-examine the original dataset used to first establish this relationship over 40 years ago, and then conduct a meta-analysis and expand the phylogenetic Bayesian hierarchical modeling framework to assess whether gill surface area is closely tied to the von Bertalanffy growth model (growth coefficient and asymptotic size, Chapter 4).

1.2. Contributions

The main data chapters in this thesis (Chapters 2, 3, and 4) are the result of collaborations with other researchers. Each chapter is either published (Chapters 2 and 3) or submitted for publication (Chapter 4) with other co-authors. For all chapters, I was responsible for either conceptualizing the idea or contributing to the conceptualization of the idea with my co-authors, writing the manuscript, collecting and analyzing data, writing all code, and generating all figures and tables. However, all the various parts of each manuscript greatly benefited from collaboration with my committee members and other colleagues (noted in the acknowledgements and introductory citation).

1.3. Figures

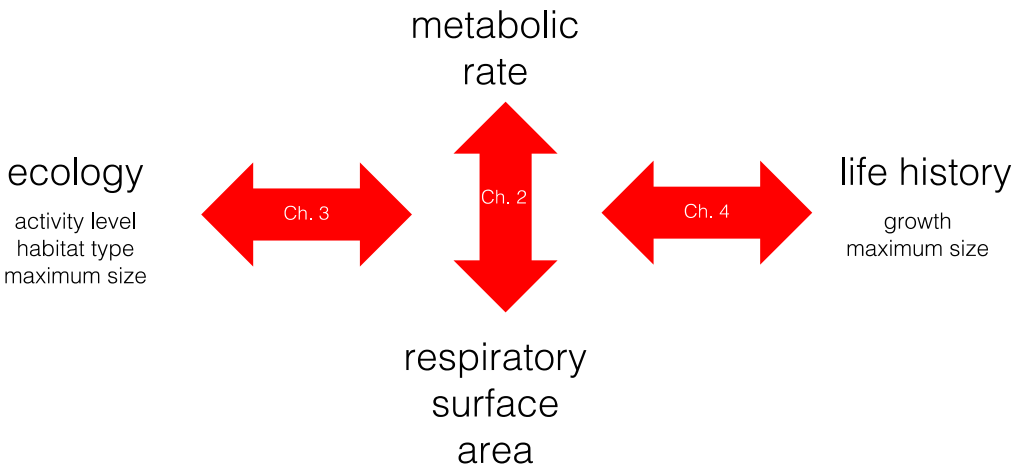

Figure 1.1 The links among oxygen acquisition (respiratory surface area) and use (metabolic rate), ecology, and life histories examined in this thesis, as well as the corresponding chapters.

1.4. References

Atkinson, D., Morley, S. A., & Hughes, R. N. (2006). From cells to colonies: at what levels of body organization does the 'temperature-size rule' apply? *Evol. Dev*., *8*(2), 202-214.

Audzijonyte, A., Richards, S. A., Stuart-Smith, R. D., Pecl, G., Edgar, G. J., Barrett, N. S., Payne, N., & Blanchard, J. L. (2020). Fish body sizes change with temperature but not all species shrink with warming. *Nat. Ecol. Evol*., *4*(6), 809-814.

Barneche, D. R., Kulbicki, M., Floeter, S. R., Friedlander, A. M., Maina, J., & Allen, A. P. (2014). Scaling metabolism from individuals to reef-fish communities at broad spatial scales. *Ecol. Lett*., *17*(9), 1067-1076.

Brown, J. H., Gillooly, J. F., Allen, A. P., Savage, V. M., & West, G. B. (2004). Toward a metabolic theory of ecology. *Ecology*, *85*(7), 1771–1789.

Canfield, D. E. & Teske, A. (1996). Late Proterozoic rise in atmospheric oxygen concentration inferred from phylogenetic and sulphur-isotope studies. *Nature*, 382(6587), 127-132.

Cheung, W. & Pauly, D. *in* Explaining ocean warming: Causes, Scale, Effects and Consequences (eds. Laffoley, D. & Baxter, J.) 239–253. International Union for Conservation of Nature. (2016).

Cheung, W. W., Sarmiento, J. L., Dunne, J., Frölicher, T. L., Lam, V. W., Palomares, M. D., Watson, R., & Pauly, D. (2013). Shrinking of fishes exacerbates impacts of global ocean changes on marine ecosystems. *Nat. Clim. Change*, *3*(3), 254-258.

Clark, T. D., Sandblom, E., & Jutfelt, F. (2013). Aerobic scope measurements of fishes in an era of climate change: respirometry, relevance and recommendations. J*. Exp. Biol*., *216*(15), 2771-2782.

De Jager, S. & Dekkers, W. (1975). Relation between gill structure and activity in fish. *Neth. J. Zool*., *25*, 276–308.

Deutsch, C., Penn, J.L., & Seibel, B. (2020). Metabolic trait diversity shapes marine biogeography. *Nature*, *585*, 557–-562.

Fick, A. (1855). Ueber diffusion. *Ann. Phys*., *170*(1), 59-86.

Forster, J., Hirst, A. G., & Atkinson, D. (2012). Warming-induced reductions in body size are greater in aquatic than terrestrial species. *Proc. Nat. Acad. Sci*. *U.S.A*, *109*(47), 19310–19314.

Gillooly, J. F., Brown, J. H., West, G. B., Savage, V. M., & Charnov, E. L. (2001). Effects of size and temperature on metabolic rate. *Science*, *293*(5538), 2248–2251.

Gillooly, J. F, Gomez, J. P., Mavrodiev, E. V., Rong, Y., & McLamore, E. S. (2016). Body mass scaling of passive oxygen diffusion in endotherms and ectotherms. *Proc. Nat. Acad. Sci., U.S.A.*, *113*(19), 5340–5345.

Hoefnagel, K. N. & Verberk, W. C. E. P. (2015). Is the temperature-size rule mediated by oxygen in aquatic ectotherms? *J. Therm. Biol.*, *54*, 56–65.

Kleiber, M. (1932). Body size and metabolism. *Hilgardia*, *6*(11), 315–353.

Lefevre, S., McKenzie, D. J., & Nilsson, G. E. (2017). Models projecting the fate of fish populations under climate change need to be based on valid physiological mechanisms. *Glob. Chang. Biol*., *23*(9), 3449-3459.

Lefevre, S., McKenzie, D. J., & Nilsson, G. E. (2018). In modelling effects of global warming, invalid assumptions lead to unrealistic projections. *Glob. Chang. Biol.*, *24*(2), 553-556.

Lefevre, S., Wang, T., & McKenzie, D. J. (2021). The role of mechanistic physiology in investigating impacts of global warming on fishes. *J. Exp. Biol., 224, jeb238840.* doi:10.1242/jeb.238840.

Marshall, D. J. & White, C. R. (2019). Aquatic life history trajectories are shaped by selection, not oxygen limitation. *Trends Ecol. Evol*., *34*(3), 182-184.

Mentel, M., Tielens, A. G., & Martin, W. F. (2016). Animals, anoxic environments, and reasons to go deep. *BMC Biol.*, *14*(1), 1-3.

Munch, S. B. & Salinas, S. (2009). Latitudinal variation in lifespan within species is explained by the metabolic theory of ecology. *Proc. Nat. Acad. Sci., U.S.A*., *106*(33), 13860-13864.

Nursall, J. R. (1959). Oxygen as a prerequisite to the origin of the Metazoa. *Nature*, *183*(4669), 1170-1172.

O'Connor, M. P., Kemp, S. J., Agosta, S. J., Hansen, F., Sieg, A. E., Wallace, B. P., Mcnair, J. N., & Dunham, A. E. (2007). Reconsidering the mechanistic basis of the metabolic theory of ecology. *Oikos*, *116*(6), 1058-1072.

Pauly, D. (1981). The relationship between gill surface area and growth performance in fish: a generalization of von Bertalanffy's theory of growth. Berichte der Deutschen Wissenschaftlichen Kommission für Meeresforschung, *28*, 251-282.

Pauly, D. (2010). Gasping fish and panting squids: oxygen, temperature, and the growth of water-breathing animals. International Ecology Institute.

Pauly, D. (2021). The gill-oxygen limitation theory (GOLT) and its critics. *Sci. Adv*., *7*(2), eabc6050.

Pörtner, H. O. (2010). Oxygen-and capacity-limitation of thermal tolerance: a matrix for integrating climate-related stressor effects in marine ecosystems. *J. Exp. Biol*., *213*(6), 881-893.

Pörtner, H. O., Bock, C., & Mark, F. C. (2017). Oxygen-and capacity-limited thermal tolerance: bridging ecology and physiology. *J. Exp. Biol*., *220*(15), 2685-2696.

Rubalcaba, J. G., Verberk, W. C., Hendriks, A. J., Saris, B., & Woods, H. A. (2020). Oxygen limitation may affect the temperature and size dependence of metabolism in aquatic ectotherms. *Proc. Nat. Acad. Sci. U.S.A*., *117*(50), 31963-31968.

Seibel, B. A. & Deutsch, C. (2020). Oxygen supply capacity in animals evolves to meet maximum demand at the current oxygen partial pressure regardless of size or temperature. *J. Exp. Biol*., *223*(12).

Verberk, W. C., Atkinson, D., Hoefnagel, K. N., Hirst, A. G., Horne, C. R., & Siepel, H. (2020). Shrinking body sizes in response to warming: explanations for the temperature–size rule with special emphasis on the role of oxygen. *Biol. Rev*., *96*(1), 247-268.

Wegner, N. C. (2015). Elasmobranch gill structure. In Fish Physiology (Vol. 34, pp. 101-151). Academic Press.

West, G B, Brown, J. H., & Enquist, B. J. (1999). The fourth dimension of life: fractal geometry and allometric scaling of organisms. *Science*, *284*(5420), 1677–1679.

Winberg, G. G. (1956). Rate of metabolism and food requirements of fishes. *Res. Bd. Can. Transl. Ser*. *No. 194.*

Chapter 2.

Respiratory capacity is twice as important as temperature in explaining patterns of metabolic rate across the vertebrate tree of life[1]

2.1. Abstract

Metabolic rate underlies a wide range of phenomena from cellular dynamics to ecosystem structure and function. Models seeking to statistically explain variation in metabolic rate across vertebrates are based largely on body size and temperature. Surprisingly, such models overlook variation in the size of gills and lungs that acquire the oxygen needed to fuel aerobic processes. Here, we assess the importance of respiratory surface area in explaining patterns of metabolic rate across the vertebrate tree of life using a novel phylogenetic Bayesian multilevel modeling framework coupled with a species-paired dataset of metabolic rate and respiratory surface area. We reveal that respiratory surface area explains twice as much variation in metabolic rate, compared to temperature, across the vertebrate tree of life. Understanding the combination of oxygen acquisition and transport provides a significant opportunity to understand the evolutionary history of metabolic rate and improve models that quantify the impacts of climate change.

[1] A version of this chapter appears as: Bigman JS, M'Gonigle LK, Wegner NC, & Dulvy NK. (2021). Respiratory capacity is twice as important as temperature in explaining patterns of metabolic rate across the vertebrate tree of life. *Science Advances.* Due to the unusual formatting of this journal, this chapter is formatted as follows: Introduction, Results, Discussion, and Methods, and key elements of the paper, such as the tables, are presented in the Supplementary Information.

2.2. Introduction

The power of the Metabolic Theory of Ecology (MTE) is that it uses metabolism to explain and predict phenomena at population, community, and ecosystem scales (Brown *et al.* 2004). In this theory, organismal metabolic rate is mathematically connected to broader ecosystem attributes through its dependence on body mass and temperature (Gillooly *et al.* 2001; Brown *et al.* 2004). While the mechanism surrounding the body mass component of the MTE continues to be debated (i.e., the fractal distribution network), the mathematical relationship has proven useful (O'Connor *et al.* 2007; Munch & Salinas 2009; Barneche *et al.* 2014). However, this relationship seeks to provide only a "zeroth-order" approximation; even after accounting for body mass and temperature, a considerable amount of variation in metabolic rate across species still remains to be explained statistically (Gillooly *et al.* 2001; Brown *et al.* 2004). Specifically, metabolic rate for organisms of the same body mass varies over five orders of magnitude, after accounting for temperature (Gillooly *et al.* 2001; Brown *et al.* 2004). Although the MTE acknowledges that exchange surfaces are important in metabolic scaling, the nature of these surfaces is rarely elaborated upon (West *et al.* 1999). One particular trait that may explain variation in the scaling of metabolic rate are the surfaces of the respiratory system. Indeed, many have long recognized the importance of such respiratory surfaces to metabolism, for example as codified in Fick's law of diffusion (Fick 1855; Hughes 1984; Wegner 2011).

Respiratory organs—lungs and gills—comprise the exchange surfaces that are used to acquire oxygen from the external environment, which is subsequently distributed throughout the body via the circulatory system (Nilsson 2010). Two lines of inference have shown that metabolic rate and respiratory surface area are highly intertwined both within and across species – experimental manipulations and allometric comparisons (i.e., comparing body mass-scaling exponents; Hughes 1984; Brown & Shick 1979; Gillooly *et al.* 2016). First, experiments on Rainbow Trout (*Oncorhynchus mykiss*) and other organisms reveal that the physical reduction or blockage of respiratory surface area results in concomitant reductions in oxygen uptake and metabolic scope (Brown & Shick 1979; Duthie & Hughes 1987). Second, allometric inference has revealed that ontogenetic body mass-scaling exponents for metabolic rate and respiratory surface area are often similar when compared within and across species (Winberg 1956; De Jager & Dekkers 1975). The same pattern holds when evolutionary body mass-scaling exponents (i.e.,

estimated across different species that differ in size) are compared (Gillooly *et al.* 2016; Killen *et al.* 2016). A recent study found that the body mass-scaling exponent of oxygen diffusion capacity (combined area and thickness) of the respiratory surfaces matches the body mass-scaling exponent of metabolic rate (as measured by oxygen consumption) across differing subsets of vertebrate species (Gillooly *et al.* 2016). However, our understanding of the intimate relationship between metabolic rate and respiratory surface area both within and across species is largely limited to these experimental manipulations and comparisons of body mass-scaling exponents. There has not yet been a robust test of whether respiratory surface area *explains variation* in the scaling of metabolic rate across vertebrates, beyond what can be accounted for by body mass, temperature, thermoregulatory strategy, and evolutionary history. The lack of an adequate test likely stems from the profound analytical challenges as both metabolic rate and respiratory surface area are almost never measured at the same body mass in the same species.

Here, we ask whether respiratory surface area explains additional variation in the scaling of metabolic rate across the vertebrate tree of life. To do so, we first compile a dataset with paired species' estimates of metabolic rate and respiratory surface area that includes all major vertebrate lineages—fishes, amphibians, reptiles, birds, and mammals. Such species-paired datasets have enabled a breakthrough in our understanding of the metabolic basis of species' responses to climate change (e.g., Sunday *et al.* 2012). Second, to solve the problem that traits are often measured at mismatched body sizes—an unresolved issue in many macroecological analyses, we develop a phylogenetic Bayesian multilevel modeling framework. The first level of this model estimates the residual effect of respiratory surface area when regressed against the body mass associated with respiratory surface area. The second level then examines whether residual respiratory surface area explains significant variation in the scaling of metabolic rate, while simultaneously accounting for the additional effects of temperature, thermoregulatory strategy, and evolutionary history. A strength of our quantitative framework is that it propagates uncertainty across levels of the model as each iteration happens in succession. Finally, we examine the differences in the scaling relationships of metabolic rate and respiratory surface area between species that vary in thermoregulatory strategy (i.e., endotherms versus ectotherms), as well as the type of respiratory organ (i.e., lungs versus gills).

2.3. Results

We compiled a dataset of metabolic rate, respiratory surface area, body mass measurements for both metabolic rate and respiratory surface area, and the temperature associated with metabolic rate for 109 species from all major vertebrate lineages: eight chondrichthyan and 63 teleost fishes, ten amphibians, four reptiles, six birds, and 18 mammals. To our knowledge, this is the first extensive vertebrate-wide paired species dataset containing all species that have published estimates for *both* metabolic rate and respiratory surface area.

In compiling this dataset, we found that metabolic rates and respiratory surface areas have rarely been measured for individuals of the same body mass in the same species, complicating comparison of mean trait values (Fig. 2.1). There were only three species with both traits measured at the same body mass (Fig. 2.1a). The mean body masses for metabolic rate and respiratory surface area differed by more than a tolerable amount (10%) for most (85%) species (n = 93/109; Fig. 2.1a). Further, for approximately one-third of species, the mean body masses for both traits differed by over an order of magnitude (n = 34/109; Fig. 2.1a-c). Macroecology is founded on analyses of endothermic birds and mammals that grow little after fledging or weaning ('determinate growers'). However, generalizing these types of analyses to include ectotherms, resulting in fully comparative vertebrate-wide analyses, poses a problem as this group of vertebrates generally grow throughout life (i.e., 'indeterminate growers'). Almost all (84 of 85) ectothermic species in our dataset had size-mismatched traits, with 34 of these species (40%) having a mean body mass mismatch greater than an order of magnitude (Fig. 2.1 a-c). To overcome this mismatch in body mass for metabolic rate and respiratory surface area, we developed a Bayesian multilevel analytical framework that enabled a vertebrate-wide comparison of multiple size-dependent phenomena (metabolic rate and respiratory surface area) while simultaneously accounting for additional covariates (e.g., body mass, temperature, thermoregulatory strategy, and evolutionary history).

2.3.1. Does respiratory surface area statistically explain variation in metabolic rate across vertebrates?

Our results show that the surface area of lungs and gills explains substantial variation in metabolic rate across the vertebrate tree of life. First, species with greater respiratory

surface areas had higher metabolic rates (Fig. 2.2). This was exemplified by organisms of the same body mass—species that had higher relative respiratory surface area (i.e., positive residual respiratory surface area) had higher metabolic rates (both observed metabolic rate as well as fitted metabolic rate values estimated by the model), even after differences in thermoregulatory strategy were accounted for (Fig. 2.2). For example, the body mass of the endothermic Kowari *Dasyuroides byrnei* (a rat-like marsupial) was nearly identical to that of the ectothermic White Sucker *Catostomus commersonii* (a teleost fish), yet the Kowari had ~32 times greater relative respiratory surface area and ~16 times greater metabolic rate compared to the White Sucker (Fig. 2.2, orange and purple lines). Second, the addition of respiratory surface area consistently improved our explanatory models of metabolic rate across vertebrates (compare *looic* and $elpd_{loo}$ for all "MR" models and all "C" models; Table S1). Third, the addition of respiratory surface area was significant in all six models that included it as a covariate (95% Bayesian Credible Interval [BCI] of the effect sizes for respiratory surface area did not include zero; Table S2, column "residual RSA"). Fourth, evidence ratios (i.e., the weight of evidence of one model divided by that of another) show that including respiratory surface area to explain variation in metabolic rate was, on average, 18.5 times more likely than excluding respiratory surface area, after accounting for body mass, temperature, thermoregulatory strategy, and evolutionary relatedness (this evidence ratio ranged from 12.3 to 22.3 according to model run; Table S3). Fifth, the standardized effect size of residual respiratory surface area was twice as large as that of temperature, indicating that respiratory surface area is twice as important in explaining variation in metabolic rate across vertebrates compared to temperature (Fig. 2.3; comparing the absolute value of standardized effect sizes of residual respiratory surface area and temperature in Table S4). Collectively, these results show that respiratory surface area explains substantial variation in metabolic rate *even after* accounting for body mass, thermoregulatory strategy, temperature, and the evolutionary relatedness among species.

2.3.2. Is respiratory surface area simply a recasting of the known difference in metabolic rates between endotherms and ectotherms?

We know empirically that ectotherms have lower metabolic rates for a given size than endotherms, which retain metabolically produced heat to maintain their body temperature within a narrow thermal range. However, it is unlikely that thermoregulatory strategy alone

explains the observed variation in metabolic rate that exists after body mass and temperature have been accounted for. First, the inclusion of respiratory surface area in models explaining variation in metabolic rate substantially improved the fit of the model, even after accounting for thermoregulatory strategy (see previous section). Second, the models that included respiratory organ (i.e., lungs versus gills) in place of thermoregulatory strategy (i.e., endotherm versus ectotherm) provided a poor fit to the data (Table S5). Third, if respiratory surface area and thermoregulatory strategy were interchangeable in explaining the same variance in the scaling of metabolic rate across vertebrates, we would expect to see similar body mass-scaling relationships of metabolic rate and respiratory surface area across all species, regardless of thermoregulatory strategy. However, we see a mismatch in the body mass-scaling of metabolic rate and respiratory surface area for endotherms (Fig. 2.4). For endotherms, the mean body mass-scaling exponent (i.e., allometric slope) of metabolic rate was shallower than the mean body mass-scaling exponent of respiratory surface area, although the 95% BCIs marginally overlapped (compare Fig. 2.4c and 2.4d and body mass-scaling exponents [and their 95% BCIs] for endotherms from models “MR3” and “RSA3” in Table S2). In contrast, the body mass-scaling exponent of metabolic rate and respiratory surface area was nearly identical for ectotherms (compare Fig. 2.4e and 2.4f and body mass-scaling exponents [and their 95% BCIs] for ectotherms from models “MR3” and “RSA3” in Table S2). This mismatch in scaling for metabolic rate and respiratory surface area for endotherms persisted even when respiratory surface area was included in the model; the body mass-scaling exponent for metabolic rate was still shallower than that of respiratory surface area (compare metabolic rate and respiratory surface area body mass-scaling exponents [and their 95% BCIs] for endotherms and ectotherms from models “C5” and “RSA3”, Table S2). Together, these results suggest that respiratory surface area is not simply a recasting of thermoregulatory strategy.

2.3.3. Is respiratory organ (i.e., lungs versus gills) a better characterization of the known difference in metabolic rate and respiratory surface area between endotherms and ectotherms?

The difference in the type of respiratory organ—having lungs or gills—does not explain the differences in metabolic rate and respiratory surface area between endotherms and ectotherms. Specifically, using thermoregulatory strategy (endotherm versus ectotherm) as a covariate *instead* of the type of respiratory organ (lungs versus gills) provided a far

better fit for all models (compare the *looic* of models with thermoregulatory strategy to those with respiratory organ instead of thermoregulatory strategy in Table S5). As such, the characterization of the differences in respiratory surface area and metabolic rate between endotherms and ectotherms is far better explained by thermoregulatory strategy than by whether an organism has lungs versus gills (Table S5, S6). See Supplementary Information for further results of the respiratory organ analyses.

2.4. Discussion

We have shown here that respiratory surface area plays a critical role in understanding variation in metabolic rate across the vertebrate tree of life. This is supported by two main findings. First, respiratory surface area substantially improved our ability to explain variation in metabolic rate across 109 vertebrate species from all major lineages, while simultaneously accounting for differences in body mass, temperature, thermoregulatory strategy, and evolutionary relatedness. Indeed, we found that respiratory surface area was twice as important in explaining variation in metabolic rate compared to temperature. Second, we confirmed that respiratory surface area was not simply a recasting of the differences in metabolic rate between endotherms and ectotherms. Answering these questions was only possible due to our paired dataset in which each species had estimates of both respiratory surface area and metabolic rate, as well as a novel Bayesian multilevel modeling approach that propagates uncertainty in the effect of body mass on respiratory surface area to all levels of the model. This modeling framework offers a breakthrough in dealing with multiple size-dependent phenomena while accounting for evolutionary relatedness and can be applied to many types of comparative questions. Importantly, our paired dataset and modeling framework allowed us to extend the mathematical framework of the Metabolic Theory of Ecology by examining whether additional size-dependent phenomena—here, respiratory surface area—explain variation in metabolic rate across species. Together, our results show that respiratory surface area, in addition to body mass, temperature, and thermoregulatory strategy, underpins the scaling of metabolic rate across vertebrates. We focus our discussion on three key issues, (1) the importance of respiratory surface area and oxygen uptake in ecological and physiological phenomena, (2) the differences in the body mass-scaling of metabolic rate and respiratory surface area between endotherms and ectotherms, and (3) the limitations of modeling studies in uncovering mechanistic relationships. Finally, we lay out a research

agenda to further dissect the relationship between metabolic rate and respiratory surface area.

Respiratory surface area appears to play a central role in several ecological and physiological phenomena including symmorphosis and oxygen limitation (including the temperature-size rule (TSR) and the Gill Oxygen Limitation Theory [GOLT]). First, symmorphosis is the hypothesis that organismal structures (e.g., respiratory surface area) are perfectly matched to their function (e.g., acquiring oxygen to meet metabolic demand) (Weibel *et al.* 1991; Hillman *et al.* 2013). While some work has found that the respiratory system appears to be 'over-designed' for the function of acquiring oxygen, others have found that the body mass-scaling of resting metabolic rate and respiratory surface area are closely matched across a broad size range of vertebrates (Weibel *et al.* 1991; Hillman *et al.* 2013; Gillooly *et al.* 2016). In our study, we found that the body mass-scaling of metabolic rate and respiratory surface area matched closely for ectotherms, but not endotherms, suggesting the potential importance of additional traits in sculpting this relationship. Direct tests of symmorphosis would ideally be conducted *within* and not *across* species and using maximum rather than resting metabolic rate. Additionally, it is important to recognize that oxygen diffusion across the respiratory surface is only one step in a series of steps involved in the acquisition of oxygen for aerobic metabolism ('oxygen cascade'). Many other steps – including oxygen binding to hemoglobin, oxygen delivery to the tissues through the circulatory system, and the density of mitochondria (the final oxygen receptor) – must be considered in a direct test of symmorphosis (Weibel *et al.* 1991). Second, oxygen limitation is the idea that geometric and physiological constraints on oxygen supply will affect aerobic metabolism, particularly for larger organisms or those in warmer waters (Forster *et al.* 2012; Rubalcaba *et al.* 2020). This phenomenon is one of the proposed explanations that is thought to underlie the widespread inverse relationship between rearing temperature and ectothermic body size (Forster *et al.* 2012*;* Hoefnagel & Verberk 2015; Audzijonyte *et al.* 2019). Specifically, the smaller maximum size and faster growth rate observed under warmer temperatures is thought to be due to the difficulty in obtaining oxygen as temperature increases due to higher metabolic demand and decreased oxygen availability, particularly for aquatic ectotherms (e.g., Hoefnagel & Verberk 2015). The GOLT proposes that respiratory surface area limits metabolic rate in fishes and other water-breathing organisms because an individual's respiratory surface area (gill surface area) cannot grow as fast as the body mass it must supply with oxygen

(i.e., a hypoallometric ontogenetic scaling of respiratory surface area) (Pauly 2010, 2021). This theory—while largely empirically untested—further predicts that respiratory surface area in fishes may be related to several metabolism-related phenomena, such as the 'shrinking' of fish body size with climate warming (Pauly 2010, 2021; Cheung *et al.* 2013). However, the GOLT is based on an allometric relationship (the ontogenetic scaling of gill surface area with body mass for a fish), and as such, cannot be used to determine mechanism by itself (see discussion below; Pauly 2010, 2021). While the role of oxygen in the physiology, ecology, and evolution of organisms is debated, broad, cross-species studies have shown that oxygen may shape marine species' geographic distributions and affect the relationship among metabolic rate, body mass, and temperature in fishes (Rubalcaba *et al.* 2020; Deutsch *et al.* 2020). However, many within species studies show a much more complicated relationship between oxygen acquisition, distribution, and use (Clark *et al.* 2008; Farrell *et al.* 2009). While our results show that respiratory surface area substantially improves our ability to explain variation in metabolic rate across species, further experimental and modeling work—especially work that is able to incorporate variation across evolutionary timescales (i.e., selection experiments and additional cross-species analyses)—is needed to assess if the diffusion of oxygen via the respiratory structures is a valid mechanism that underlies the GOLT and TSR. Indeed, a coordinated effort among organismal physiologists, macrophysiologists, and comparative evolutionary ecologists would greatly enhance our ability to understand the role that oxygen plays in ecological and physiological phenomena, both within and across species.

We found that although respiratory surface area vastly improved our understanding of metabolic rate across both endotherms and ectotherms, ectothermic organisms had a tighter coupling of the scaling of metabolic rate and respiratory surface area than that observed for endotherms. These differences in scaling of metabolic rate and respiratory surface area were not explained by the type of respiratory organ itself (i.e., lungs versus gills), as all models that included respiratory organ in place of thermoregulatory strategy fit the data less well. Instead, our results suggest that attributes related to thermoregulatory strategy likely underlie the differences in the relationship of metabolic rate and body mass between endotherms and ectotherms. For example, the body mass-scaling exponent of metabolic rate found here for endothermic organisms may support the Heat Dissipation Theory, which suggests that there is an upper limit to metabolic rate in endothermic organisms (Speakman & Król 2010). Endothermic organisms maintain their

body temperature within a target range and have to dissipate excess heat produced by metabolism across their body surface area. Thus, endothermic organisms must balance heat production and heat loss, which is constrained by the body mass-to-surface area ratio (Speakman & Król 2010). As organisms increase in size, the ratio of body surface area to body mass decreases, resulting in a decreased heat dissipation capacity (Speakman & Król 2010*;* Brown & Lasiewski 1972). The Heat Dissipation theory suggests that the body mass-scaling exponent of field metabolic rate for endothermic organisms will not significantly differ from ~0.63-0.67, following surface area to volume geometry (field metabolic rate is a measure of energy expenditure in a free-living organism; Speakman & Król 2010). While the mean body mass-scaling exponent for resting metabolic rate—both with and without respiratory surface area—for endotherms found in this study was higher than 0.63-0.67, the 95% BCIs of both models included the 0.63 value (models "MR3" and "C5" in Table S2; these intervals also included the predicted ¾ slope of the MTE; *1*). Because ectothermic organisms do not retain metabolically produced heat, dissipation is not an issue, and hence this may explain the steeper body mass-scaling exponent of metabolic rate in ectotherms. Additionally, some work has shown that the evolutionary body mass-scaling exponent of maximum metabolic rate, and not resting metabolic rate as used here, is more similar to the evolutionary body mass-scaling exponent of respiratory surface area (e.g., Killen *et al.* 2016). However, we found a match in the body mass-scaling of resting metabolic rate and respiratory surface area for ectotherms and not endotherms (this is also an evolutionary allometry), and thus, our examination of resting metabolic rate versus maximum metabolic rate cannot explain the observed difference in body mass-scaling of metabolic rate and respiratory surface area in endotherms.

We provide compelling evidence that—to a first approximation—respiratory surface area, in addition to body size and temperature, explains significant variation in metabolic rate across vertebrates. Yet, we have much to learn about the causal relationships between metabolic rate and respiratory surface area. Correlative or scaling studies such as ours serve to identify broad, general patterns, which can then inspire other studies that aim to understand the underlying or driving mechanisms (e.g., experimental or selection studies). While our results show that respiratory surface area (in addition to body mass, temperature, and thermoregulatory strategy) underlies *patterns* of metabolic rate across vertebrates, we cannot say from our results—or other scaling studies—whether organismal metabolic rate constrains or shapes organismal respiratory surface area or

vice versa (e.g., Gillooly *et al.* 2016). A major step forward in understanding the mechanistic relationship between organismal metabolic rate and organismal respiratory surface area would be to understand the relationships among ontogenetic allometries (i.e., within an individual of a single species across its lifetime or, for traits that require lethal sampling, across individuals of the same species that span the size range of the species), static allometries (i.e., across individuals of the same species of the same life stage), and evolutionary allometries (i.e., across different species that differ in size) of both metabolic rate and respiratory surface area. For example, a recent study examining the relationships among ontogenetic, static, and evolutionary brain and body size allometries suggested that developmental constraints governed scaling relationships within and across species rather than geometric/physical constraints or physiological mechanisms (Tsuboi *et al.* 2018). What are the constraints and causal mechanisms that underlie the relationship between metabolic rate and respiratory surface area within and across species?

To this end, we outline six specific avenues of research that would help us to understand causality between organismal metabolic rate and organismal respiratory surface area. First, the advance in phylogenetic methods has opened the door to comparing evolutionary transitions of metabolic rate to transitions in respiratory mode (Uyeda *et al.* 2018). Second, common-garden and long-term selection experiments, particularly of aquatic organisms, offer the opportunity to understand the phenotypic and genotypic response of organismal metabolic rate and organismal respiratory surface area to food availability, temperature, and oxygen (e.g., Audzijonyte *et al.* 2019). Third, a deeper understanding of allometries—including the relationships examined in this study—has been profoundly hindered by a lack of available estimates of individual (i.e., raw) data for metabolic rate, respiratory surface area, and other traits. We urge experimental scientists to publish their raw data alongside means and other summaries. This would allow the statistical propagation of uncertainty using the approach we have developed here, which can be easily modified to include data at both individual and species scales. Additionally, this would also enhance datasets such as ours and facilitate the identification of patterns across broad groups of species. Fourth, activity, metabolic rate (both resting and maximum, as these two measures are correlated), respiratory surface area, and temperature are deeply intertwined (Pauly 2010; Killen *et al.* 2016; Bigman *et al.* 2018). Are metabolic rate and respiratory surface area simply proxies for activity or are metabolic rate and respiratory surface area capturing total energy availability for growth and

reproduction in addition to activity? Additionally, which measures of metabolic rate (i.e., standard/basal, resting, routine, field, maximum) are suitable to test the interrelationships between metabolic rate, respiratory surface area, temperature, and activity? Finally, there is an incredible, but widely overlooked, diversity of respiratory systems, modes, and types of ventilation. We were unable to tackle this diversity with our dataset beyond examining respiratory organ as a potential predictor of metabolic rate. Studies that explore ventilation types and the diversity of respiratory modes even within the coarse categorizations of respiratory organs (e.g., unidirectional flow of water across fish gills, unidirectional flow of air through bird lungs, and tidal air flow in mammalian and reptilian lungs) could begin to examine this question. Air-breathing and cutaneous respiration in aquatic organisms and amphibians provide further contrasts to explore. Blood flow across these respiratory surfaces also differs (i.e., counter-current in fish gills, cross-current in bird lungs, etc.) providing another avenue for exploration. Combining more advanced modeling approaches such as the one presented here with detailed physiological and ecological data both within and across species will allow us to further understand the role that oxygen plays in the ecology, physiology, and evolution of organisms.

2.5. Methods

2.5.1. Trait data

We compiled a species-paired dataset of vertebrates that had both metabolic rate and respiratory surface area data. To do so, we collated mean estimates of whole-organism aerobic metabolic rate (termed here, 'metabolic rate'), as measured by oxygen consumption (mg O_2/min, mg O_2/g/hr, mg O_2/kg/hr, ml O_2/hr, ml O_2/min, ml O_2/g/hr, ml O_2/kg/h, ml O_2/kg/min, joules/hr, and watts), body mass (grams, g, or kilograms, kg) associated with the metabolic rate estimates, temperature (˚C) associated with the metabolic rate measurements, whole-organism respiratory surface area (cm^2 or mm^2; termed here, "respiratory surface area"), and body mass (g or kg) associated with the respiratory surface area measurements for as many vertebrate species as possible. If raw data (i.e., measurements for multiple individuals of the same species) were available, these estimates were averaged to generate a species mean. Our ability to incorporate raw data into our modeling framework was limited because the majority of species in our dataset only had published mean estimates of metabolic rate and respiratory surface area

(only nine species of the 109 vertebrates have published raw data for both metabolic rate and respiratory surface area).

Much of our data came from two existing datasets: metabolic rate data from (White *et al.* 2012) and respiratory surface area from (Gillooly *et al.* 2016). We searched the primary literature to fill gaps for species missing either metabolic rate or respiratory surface area estimates. If we found more than one estimate of either mean metabolic rate or mean respiratory surface area for a given species, we included the value from the study with the larger sample size. Metabolic rate estimates are from individuals at rest (resting or standard for ectotherms, basal for endotherms), with the exception of four teleost species for which we could only find estimates of routine metabolic rate (oxygen consumption during volitional movement): *Anabas testudineus* Climbing Perch*, Brevoortia tyrannus* Atlantic Menhaden*, Channichthys rhinoceratus* Unicorn Icefish*,* and *Hoplerythrinus unitaeniatus* Trahira. These four species, specifically, and other species with routine metabolic rates are regularly included in metabolic allometry studies, as the variation of metabolic rate among individuals of the same species is substantially smaller than the variation across different species (e.g., Bokma 2004). For the purposes of this study, the thermoregulatory strategy of five fish species that are regionally endothermic (*Carcharodon carcharias* White Shark, *Euthynnus affinis* Kawakawa, *Isurus oxyrinchus* Shortfin Mako, *Katsuwonus pelamis* Skipjack Tuna, and *Thunnus albacares* Yellowfin Tuna) were classified as ectotherms. However, rerunning the three top models (MR3, RSA2, and C5 in Table S1) without the five regionally endothermic species did not significantly change any coefficient value (i.e., the effect size of any parameter in a model). For analyses, all estimates of metabolic rate were converted to watts, respiratory surface area to cm^2, body mass for both metabolic rate and respiratory surface area to grams, and temperature to inverse temperature for model parameterization as the Boltzmann factor (see 'Basic modeling framework and analysis' section). Metabolic rate, respiratory surface area, and both associated body masses were natural log-transformed prior to analyses.

2.5.2. Phylogeny

We included a phylogenetic random effect in all models that allowed for a phylogenetic signal among residuals (i.e., error). To do so, we first constructed a new supertree from a database of molecular phylogenies, TimeTree (Hedges *et al.* 2006), and a recently published molecular phylogeny for Chondrichthyans (Stein *et. al.* 2018). As the

evolutionary position of all species in our dataset has not yet been fully resolved, we opted to use a genera-level phylogeny for all species except the Chondrichthyans (as a phylogeny for this group was recently published). In the infrequent (n = 7) case that two species from the paired dataset were in the same genus, the branch length was split equally among those two species. This use of a genera-level tree with a few equally split branches to accommodate species from the same genus—as opposed to a tree with all species at the tips—will yield the same conclusion, as divergence times between species in the paired dataset are quite high across the phylogeny due to the number of species included in our dataset relative to all extant vertebrates.

2.5.3. Modeling framework and statistical analysis

Metabolic rate and respiratory surface area are mass-dependent traits, meaning that they change as an individual grows and increases in size. However, both traits do not increase at the same rate as body mass (i.e., the body mass-scaling exponent of an ontogenetic allometry for these traits does not equal one) and therefore, the body mass at which these traits were measured must be included in all models. Mass-dependent traits are typically examined in an allometric context using a power-law, or scaling, relationship such as

$$t = \beta_0 M^{\beta_{mass}}, \quad (1)$$

where t is the mass-dependent trait (in this case, either metabolic rate or respiratory surface area), β_0 is the intercept (i.e., the value of t at a given body mass, often called the 'normalization constant'), M is body mass, and β_{mass} is the body mass-scaling exponent (i.e., allometric slope; Kleiber 1932). This equation is most often examined on a logarithmic scale, resulting in a linear relationship for log-transformed data,

$$\ln(t) = \ln(\beta_0) + \beta_{mass} \ln(M). \quad (2)$$

We used the equation above as a starting point and adjusted the parameterization to test (1) whether respiratory surface area explained variation in metabolic rate across vertebrates, after accounting for body mass, temperature, thermoregulatory strategy, and evolutionary relatedness across species and (2) compared the scaling relationships of metabolic rate and respiratory surface area, while accounting for differences in thermoregulatory strategy to assess whether respiratory surface area was directly related to thermoregulatory strategy. We also assessed whether respiratory organ (lungs in

amphibians, reptiles, mammals, and birds and gills in fishes) was a better characterization of the differences in metabolic rates between endotherms and ectotherms as opposed to thermoregulatory strategy. Following the MTE, we used the Boltzmann factor as a covariate to examine the effect of temperature on metabolic rate resulting in the classic MTE equation:

$$\ln(t) = \ln(\beta_0) + \beta_{mass} \ln(M) + \frac{-E_i}{kT} \quad (3)$$

where E_i is the activation energy for the biochemical reactions of metabolism, k is the Boltzmann constant (8.617×10^{-5} eV) and T is temperature in Kelvin (Gillooly *et al.* 2001; Brown *et al.* 2004). Temperature is parameterized as the Boltzmann factor (i.e., inverse temperature) for metabolic rate scaling relationships as it best approximates how temperature affects metabolic reactions (Gillooly *et al.* 2001; Brown *et al.* 2004). For endotherms, temperature data is body temperature and for ectotherms, temperature data is the temperature at which metabolic rate was experimentally measured. Importantly, this temperature-dependence does not capture the fundamental differences in metabolic rates between endotherms and ectotherms as temperature has the same effect on the biochemical reactions of respiration for both groups (Gillooly *et al.* 2001, 2016).

All models were fit in a Bayesian framework in Stan with the *rstan* package in R v.3.5.1 and v.4.0.1 (R Core Team 2013; Stan Development Team 2019). To ensure our results were robust to model run, we ran each model a total of four times. The results of each additional model run (after the first one) are in Table S7. We also ran all models without one possible outlier, but this did not significantly change any coefficient estimates. A detailed outline of all models, their parameterization, and choice of priors is included in the Supplementary Information. The results of the models with respiratory organ (lungs versus gills) *in place of* thermoregulatory strategy are expanded upon in the Supplementary Information. Below, we detail the parameterization of models specific to each research question.

2.5.4. Does respiratory surface area explain variation in metabolic rate across vertebrates?

To assess whether respiratory surface area explains variation in metabolic rate across vertebrates, above and beyond that explained by the other covariates (e.g., body mass, temperature, and thermoregulatory strategy) we compared candidate models that described variation in metabolic rate with and without respiratory surface area (Table S1). For models that examined variation in metabolic rate without respiratory surface area ('metabolic rate models'), we compared the classic MTE model to that with the addition of thermoregulatory strategy as a covariate (Table S1). To do this, we examined models that allowed just the intercept to vary by thermoregulatory strategy (i.e., metabolic rate for a given body mass differed for endotherms and ectotherms) and models that allowed both the slope and intercept to vary by thermoregulatory strategy (i.e., metabolic rate for a given body mass differed for endotherms and ectotherms and the effect of body mass varied between endotherms and ectotherms). In total, we parameterized three candidate models to examine the body mass-scaling of metabolic rate without respiratory surface area ("MR" models, Table S1). Second, we built on these three metabolic rate models above (the classic MTE model with and without thermoregulatory strategy) by adding in respiratory surface area as a covariate ('combined models'). To do this, we used a multilevel model where we first calculated the residual respiratory surface area by regressing respiratory surface area against the measurement body mass. We subsequently incorporated this residual respiratory surface area as a covariate in the next level, in addition to other covariates. This approach allows for the uncertainty in estimated residual respiratory surface area to be propagated across levels of the model, as opposed to simply including a mean estimate of residual respiratory surface area per species (which does not incorporate the uncertainty in that estimate). In total, we parameterized six candidate models to examine the body mass-scaling of metabolic rate with respiratory surface area ("C" models, Table S1).

We used model selection to identify a single best model that explains variation in metabolic rate without respiratory surface area (termed here, 'best metabolic rate model') and a single best model with respiratory surface area (termed here, 'best combined model'). To do this, we used Pareto-smoothing Leave-one-out Cross Validation (PSIS-LOO). This model selection framework is based on the predictive accuracy of a model, as estimated by iteratively leaving out one observation at a time and then predicting that observation

based on the model fit to the remaining data (Vehtari *et al.* 2017). An assumption of using PSIS-LOO is that the joint likelihood of the model observed over all observations is factorizable, or pairwise conditionally independent, given the model parameters (Sundararajan & Keethi 2001; Vehtari *et al.* 2017*;* Bürkner *et al.* 2019). As phylogenetic models do not meet this assumption, we instead computed the pointwise log-likelihood for non-factorizable models (Sundararajan & Keethi 2001*;* Bürkner *et al.* 2019). We then used the *loo* package in R v 5.3.1 to estimate the expected log predictive density ($elpd_{loo}$), the LOO information criterion value (*looic*)*,* the effective number of parameters (p_{loo}), the standard error of the expected log predictive density (se_{elpd_loo}), the difference in the expected log predictive density ($elpd_{diff}$) for a given model compared to the best model, and finally, the weight of evidence for each model as estimated by the Bayesian stacking method (Vehtari *et al.* 2017; Yao *et al.* 2018). The model with the lowest $elpd_{loo}$ value is the best fit to the data. Additionally, we used a z-score standardization to standardize the predictors of the best combined model to identify and compare the relative importance of these predictors in explaining variation in metabolic rate across vertebrates (i.e., comparing standardized effect sizes; Gelman & Hill 2007). We also computed evidence ratios to measure how much more likely one model is over the other(s). Evidence ratios are simply the weight of evidence of the best model divided by the weight of evidence of the other model(s) of interest (Burnham & Anderson 2002).

2.5.5. Is respiratory surface area simply a recasting of the difference in metabolic rate between endotherms and ectotherms?

To assess whether respiratory surface area is simply a recasting of the difference in metabolic rate between endotherms and ectotherms, we compared the scaling relationships of metabolic rate and respiratory surface area, while accounting for differences in thermoregulatory strategy. First, we parameterized three candidate models ('respiratory surface area models') to examine the body mass-scaling of respiratory surface area ("RSA" models, Table S1). We then selected the single best model (termed here, 'best respiratory surface area model') from these candidate models using PSIS-LOO (see above, Table S1). Second, we compared the body mass-scaling of the best metabolic rate model (model "MR3", Table S2) and the best respiratory surface area model (model "RSA2", Table S2) by comparing the 95% Bayesian Credible Interval (BCI).

2.5.6. Is respiratory organ (i.e., lungs versus gills) a better characterization of the known difference in metabolic rate and respiratory surface area between endotherms and ectotherms?

To examine whether respiratory organ (i.e., lungs versus gills) was a better predictor of the differences in metabolic rates between endotherms and ectotherms *instead* of thermoregulatory strategy, we replaced thermoregulatory strategy in all models that included it with respiratory organ (Table S5). We did this in favor of simply adding respiratory organ as covariate in addition to thermoregulatory strategy, which would not be feasible with our dataset as the ectothermic species in our dataset were largely fishes and thermoregulatory strategy is almost entirely correlated with respiratory organ (i.e., fishes have gills). Specifically, we examined the effect of lungs versus gills in the scaling of metabolic rate (models “MR2_LG” and “MR3_LG” in Table S5, S6), the scaling of respiratory surface area (models “RSA2_LG”, “RSA3_LG” in Table S5, S6), and how respiratory organ affected the scaling of metabolic rate with the effect of residual respiratory surface area included (models “C3_LG”, “C4_LG”, “C5_LG”, “C6_LG”, Table S5, S6). All model comparison was conducted using PSIS-LOO (see above).

2.6. Figures

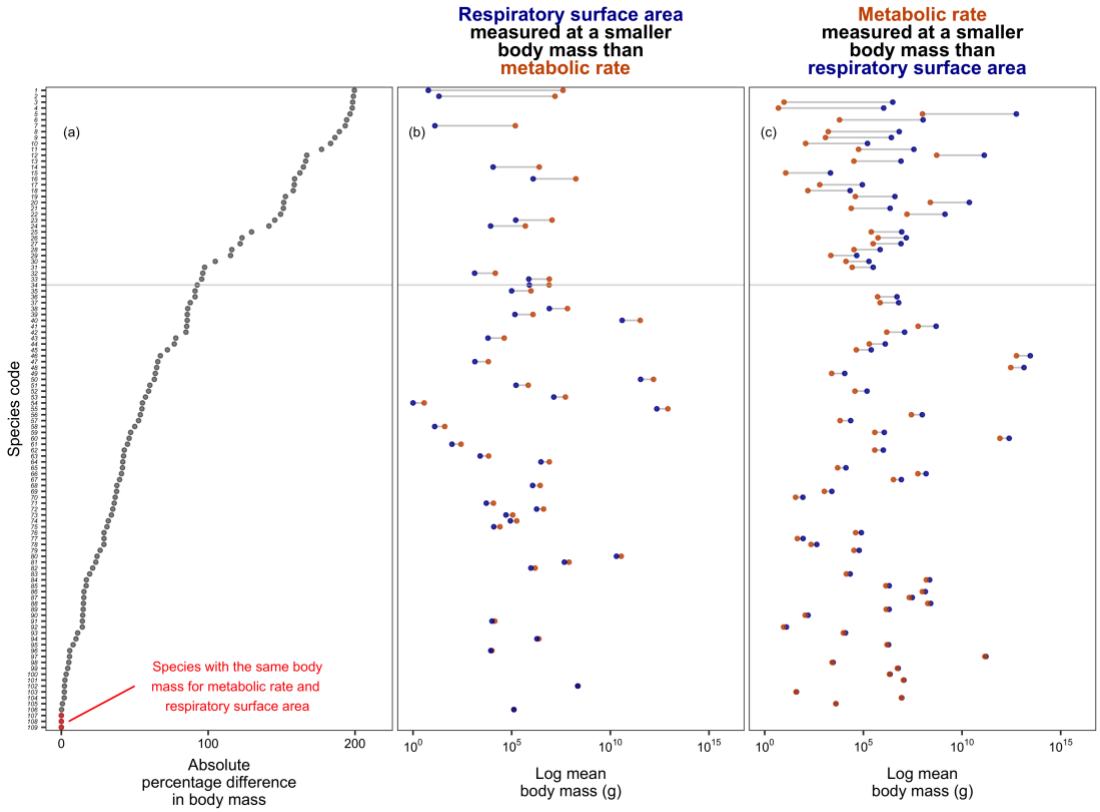

Figure 2.1. Metabolic rate and respiratory surface area were measured at different body masses for the majority of the 109 vertebrate species included in this study—a common issue with macroecological studies.
(a) The absolute percentage difference between mean body mass for mean (whole-organism) metabolic rate and mean (whole-organism) respiratory surface area for all species included in this study. Only three species had equal mean body masses associated with both metabolic rate and respiratory surface area (red data points). The difference between the mean log body mass associated with mean metabolic rate (dark orange) and the mean log body mass associated with mean respiratory surface area (dark blue) for each species when (b) the body mass associated with metabolic rate was larger, and (c) when body mass associated with respiratory surface area was larger. For approximately one-third of species, the mean body mass associated with metabolic rate and respiratory surface area differed by over an order of magnitude (grey line, a-c). Species code (y-axis) corresponds to species identity in Table S8.

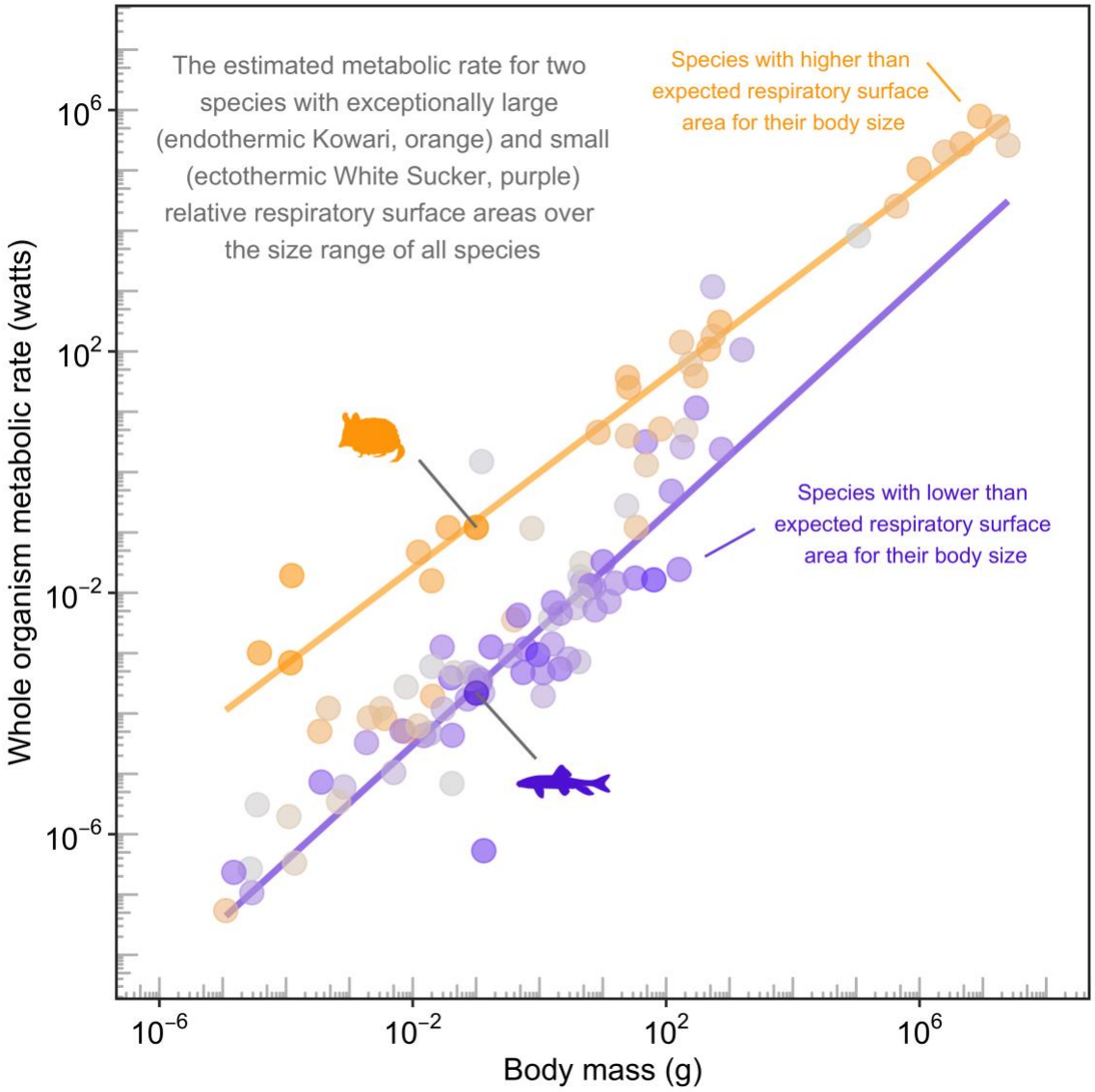

Figure 2.2 Species with high metabolic rates for their body size have large respiratory surface areas for their body size.
Log mean (whole organism) metabolic rate in relation to log mean body mass for 109 vertebrate species from all major lineages. Relative respiratory surface area (i.e., residual respiratory surface area) is indicated by a gradient of color, with orange indicating species with higher-than-expected respiratory surface area for their body size, grey indicating expected respiratory surface area for their body size, and purple indicating lower-than-expected respiratory surface area for their body size. Lines show the estimated metabolic rate (including the effect of body mass, temperature, thermoregulatory strategy, respiratory surface area, and evolutionary history) for species with exceptionally large and small relative respiratory surface areas, based on two species with almost identical body mass: the Kowari *Dasyuroides byrnei* (orange) and the White Sucker *Catostomus commersonii* (purple).

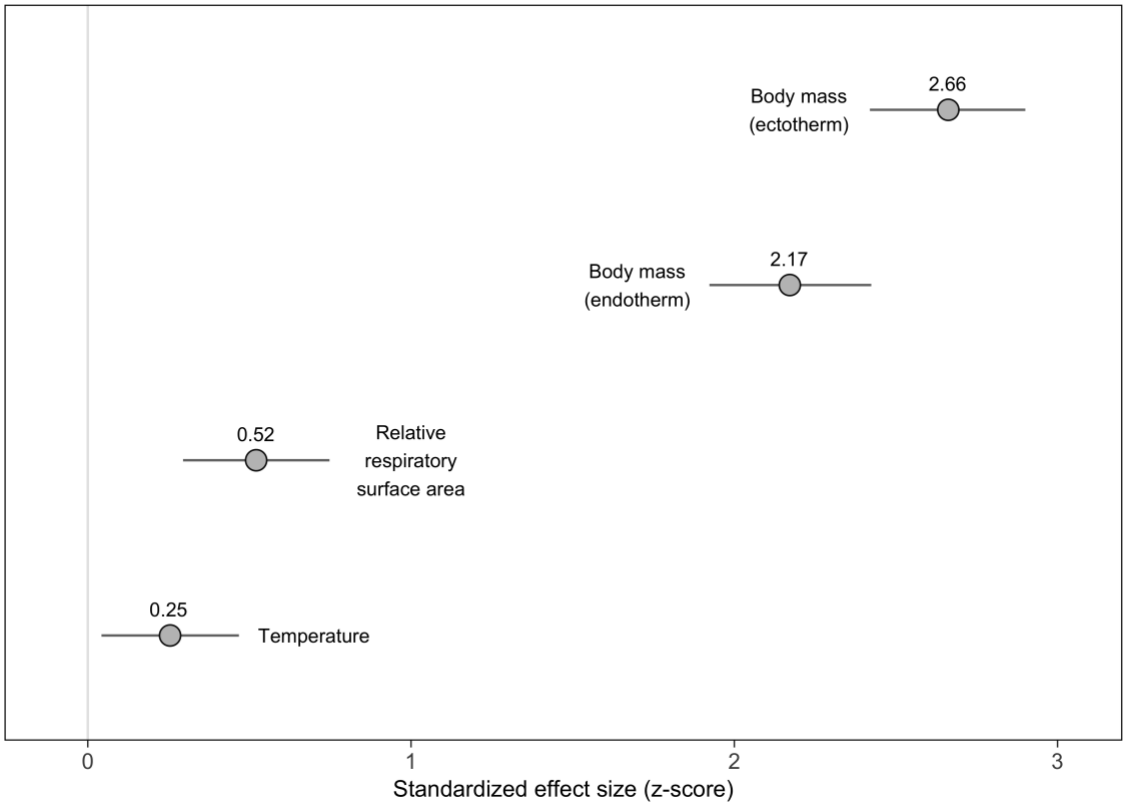

Figure 2.3 Compared to temperature, respiratory surface area explains twice as much variation in metabolic rate across the vertebrate tree of life.
The mean (grey dot) and 95% Bayesian Credible Interval (BCI, black line) of the standardized effect sizes for body mass (for both endotherms and ectotherms), relative respiratory surface area (i.e., residual respiratory surface area) and temperature (model C5, Table S4). For comparison, the standardized effect size of temperature is presented as the absolute value because temperature was modeled as the inverse temperature (see text) and thus had a negative effect size. The z-score standardization was used to estimate standardized effect sizes.

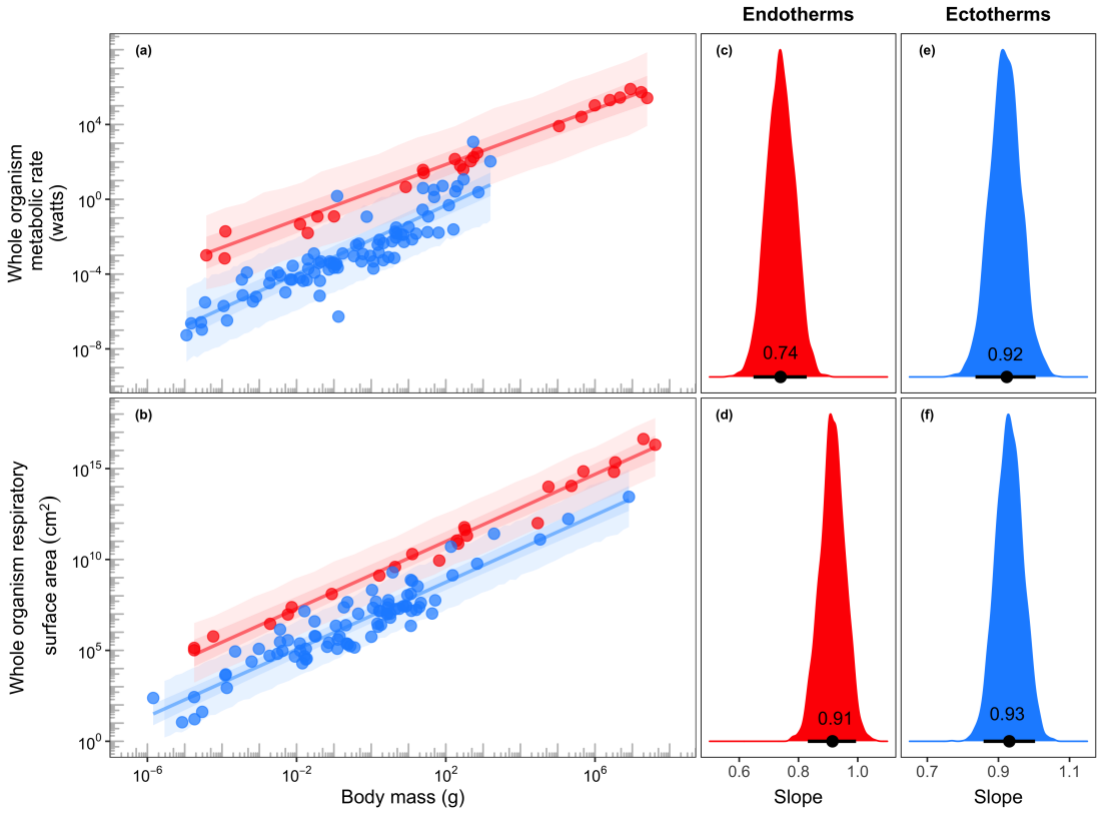

Figure 2.4 The body mass scaling of metabolic rate and respiratory surface across the same 109 vertebrate species differed for endotherms but was similar for ectotherms.

While (whole-organism) metabolic rate body mass-scaling exponents (i.e., allometric slopes) differed between endotherms (red) and ectotherms (blue; a, c, e, model MR3) the (whole organism) respiratory surface area body mass-scaling exponents did not (b, d, f, model RSA3). (c-f) The posterior distributions of the metabolic rate (c, e) and respiratory surface area (d, f) body mass-scaling exponents for endotherms and ectotherms, respectively. The black dot and line in each of the posterior distributions indicates the mean body mass-scaling exponent and 95% Bayesian Credible Interval (BCI), respectively. Lines are shown from the model that allowed body mass-scaling exponents (i.e., slopes) to vary by thermoregulatory strategy (model "RSA3", Table S1). We note that these body mass-scaling exponents are nearly identical to that from the best model that explains variation in respiratory surface area ("RSA2", Table S1), which did not allow for slopes to vary by thermoregulatory strategy.

2.7. References

Audzijonyte, A., Barneche, D. R., Baudron, A. R., Belmaker, J., Clark, T. D., Marshall, C. T., Morrongiello, J.R., & van Rijn, I. (2019). Is oxygen limitation in warming waters a valid mechanism to explain decreased body sizes in aquatic ectotherms? *Glob. Ecol. Biogeogr.*, 1–31.

Barneche, D. R., Kulbicki, M., Floeter, S. R., Friedlander, A. M., Maina, J., & Allen, A. P. (2014). Scaling metabolism from individuals to reef-fish communities at broad spatial scales. *Ecol. Lett.*, *17*(9), 1067-1076.

Bigman, J. S., Pardo, S. A., Prinzing, T. S., Dando, M., Wegner, N. C., & Dulvy, N. K. (2018). Ecological lifestyles and the scaling of shark gill surface area. *J. Morphol.*, *279*(12), 1716–1724.

Bigman, J.S., M'Gonigle, L.K., Wegner, N.C., & Dulvy, N.K. (2021). Assessing patterns of metabolic rate and respiratory surface area data across the vertebrate tree of life. figshare, dataset and code. https://doi.org/10.6084/m9.figshare.13821968.

Bokma, F. (2004). Evidence against universal metabolic allometry. *Funct. Ecol. 18*(2), 184–187.

Brown, J. H., Gillooly, J. F., Allen, A. P., Savage, V. M., & West, G. B. (2004). Toward a metabolic theory of ecology. *Ecology*, *85*(7), 1771–1789.

Brown, J. H. & Lasiewski, R. C. (1972). Metabolism of weasels: the cost of being long and thin. *Ecology*, *53*(5), 939–943.

Brown, W. & Shick, J. M. (1979). Bimodal gas exchange and the regulation of oxygen uptake in holothurians. *Biol. Bull.*, *156*(3), 272–288.

Bürkner, P. C., Gabry, J., & Vehtari, A. (2019). Bayesian leave-one-out cross-validation for non-factorizable normal models. *ArXiv:1810.10559v3*.

Burnham, K. P., and Anderson, D. R. (2002). *Model selection and multimodel inference*. New York, NY: Springer.

Cheung, W. W., Sarmiento, J. L., Dunne, J., Frölicher, T. L., Lam, V. W., Palomares, M. D., Watson, R, & Pauly, D. (2013). Shrinking of fishes exacerbates impacts of global ocean changes on marine ecosystems. *Nat. Clim. Change*, *3*(3), 254-258.

Clark, T. D., Sandblom, E., Cox, G. K., Hinch, S. G., & Farrell, A. P. (2008). Circulatory limits to oxygen supply during an acute temperature increase in the Chinook salmon (Oncorhynchus tshawytscha). *Am J Physiol Regulatory Integrative Comp Physiol* , *295*(5), R1631-R1639.

De Jager, S. & Dekkers, W. (1975). Relation between gill structure and activity in fish. *Neth. J. Zool.*, *25*, 276–308.

Deutsch, C., Penn, J.L., & Seibel, B. (2020). Metabolic trait diversity shapes marine biogeography. *Nature*, 585, 557–-562.

Duthie, G. & Hughes, G. (1987). The effects of reduced gill area and hyperoxia on the oxygen consumption and swimming speed of rainbow trout. *J. Exp. Biol.*, *127*, 349–354.

Farrell, A. P., Eliason, E. J., Sandblom, E., & Clark, T. D. (2009). Fish cardiorespiratory physiology in an era of climate change. *Can. J. Zool.*, *87*(10), 835-851.

Fick, A. (1855). Ueber diffusion. *Ann. Phys.*, *170*(1), 59-86.

Forster, J., Hirst, A. G., & Atkinson, D. (2012). Warming-induced reductions in body size are greater in aquatic than terrestrial species. *Proc. Nat. Acad. Sci.*, *109*(47), 19310–19314.

Frishkoff, L. O., de Valpine, P., & M'Gonigle, L. K. (2017). Phylogenetic occupancy models integrate imperfect detection and phylogenetic signal to analyze community structure. *Ecology*, *98*(1), 198-210.

Gelman, A. & Hill, J. (2007). *Data analysis using regression and multilevelhierarchical models* (Vol. 1). New York, NY, USA: Cambridge University Press.

Gillooly, J. F., Brown, J. H., West, G. B., Savage, V. M., & Charnov, E. L. (2001). Effects of size and temperature on metabolic rate. *Science*, *293*(5538), 2248–2251.

Gillooly, J. F, Gomez, J. P., Mavrodiev, E. V., Rong, Y., & McLamore, E. S. (2016). Body mass scaling of passive oxygen diffusion in endotherms and ectotherms. *Proc. Nat. Acad. Sci., U.S.A., 113*(19), 5340–5345.

Hedges, S. B., Dudley, J., & Kumar, S. (2006). TimeTree: a public knowledge-base of divergence times among organisms. *Bioinformatics*, *22*(23), 2971–2972.

Hillman, S. S., Hancock, T. V., & Hedrick, M. S. (2013). A comparative meta-analysis of maximal aerobic metabolism of vertebrates: implications for respiratory and cardiovascular limits to gas exchange. *J. Comp. Phys. B*, *183*(2), 167-179.

Hoefnagel, K. N. & Verberk, W. C. E. P. (2015). Is the temperature-size rule mediated by oxygen in aquatic ectotherms? *J. Therm. Biol.*, *54*, 56–65.

Hughes, G. M. (1984). Scaling of respiratory areas in relation to oxygen consumption of vertebrates. *Experientia*, *40*(6), 519–524.

Killen, S. S., Glazier, D. S., Rezende, E. L., Clark, T. D., Atkinson, D., Willener, A. S. T., & Halsey, L. G. (2016). Ecological Influences and Morphological Correlates of Resting and Maximal Metabolic Rates across Teleost Fish Species. *Am. Nat. 187*(5), 592–606.

Kleiber, M. (1932). Body size and metabolism. *Hilgardia*, *6*(11), 315–353.

Munch, S. B. & Salinas, S. (2009). Latitudinal variation in lifespan within species is explained by the metabolic theory of ecology. *Proc. Nat. Acad. Sci., U.S.A., 106*(33), 13860-13864.

Nilsson, G. E. (Ed.). (2010). Respiratory physiology of vertebrates: life with and without oxygen. Cambridge University Press.

O'Connor, M. P., Kemp, S. J., Agosta, S. J., Hansen, F., Sieg, A. E., Wallace, B. P., Mcnair, J. N. & Dunham, A. E. (2007). Reconsidering the mechanistic basis of the metabolic theory of ecology. *Oikos*, *116*(6), 1058-1072.

Pauly, D. (2010). Gasping fish and panting squids: oxygen, temperature, and the growth of water-breathing animals. International Ecology Institute.

Pauly, D. (2021). The gill-oxygen limitation theory (GOLT) and its critics. *Sci. Adv.*, *7*(2), eabc6050.

R Core Team (2013). R: A language and environment for statistical computing. R Foundation for Statistical Computing, Vienna, Austria. URL http://www.R-project.org/.

Rubalcaba, J. G., Verberk, W. C., Hendriks, A. J., Saris, B., & Woods, H. A. (2020). Oxygen limitation may affect the temperature and size dependence of metabolism in aquatic ectotherms. *Proc. Nat. Acad. Sci. U.S.A.*, *117*(50), 31963-31968.

Speakman, J. R. & Król, E. (2010). Maximal heat dissipation capacity and hyperthermia risk: neglected key factors in the ecology of endotherms. *J. Anim. Ecol., 79*(4), 726-746.

Stan Development Team. 2019. *Stan Modeling Language Users Guide and Reference Manual*, Version 2.19.2. http://mc-stan.org.

Stein, R. W., Mull, C. G., Kuhn, T. S., Aschliman, N. C., Davidson, L. N. K., Joy, J. B., Smith, G.J., Dulvy, N. K., & Mooers A. Ø. (2018). Global priorities for conserving the evolutionary history of sharks, rays and chimaeras. *Nat. Ecol. Evol.*, *2*(2), 288–298.

Sundararajan, S. & Keerthi, S. S. (2001). Predictive Approaches for Choosing Hyperparameters in Gaussian Processes. *Neural Comput*., *13*, 1103–1118.

Sunday, J.M., Bates, A.E., & Dulvy, N.K. (2012). Thermal tolerance and the global redistribution of animals. *Nat. Clim. Change* 2, 686–690.

Tsuboi, M., van der Bijl, W., Kopperud, B. T., Erritzøe, J., Voje, K. L., Kotrschal, A., Yopak, K. E., Collin, S. P., Iwaniuk A. N., Kolm, N. (2018). Breakdown of brain-body allometry and the encephalization of birds and mammals. *Nat. Ecol. Evol.*, *2*(9), 1492–1500.

Uyeda, J. C., Zenil-Ferguson, R., & Pennell, M. W. (2018). Rethinking phylogenetic comparative methods. *Syst. Biol.*, *67*(6), 1091–1109.

Vehtari, A., Gelman, A., & Gabry, J. (2017). Practical Bayesian model evaluation using leave-one-out cross-validation and WAIC. *Stat. and Comput.*, *27*(5), 1413–1432.

Wegner, N. C. (2011). Gill morphometrics. In A. P. Farrell (Ed.), *Encyclopedia of fish physiology: from genome to environment* (Vol. 2, pp. 803–811). San Diego, CA: Academic Press.

Weibel, E. R., Taylor, C. R., & Hoppeler, H. (1991). The concept of symmorphosis: a testable hypothesis of structure-function relationship. *Proc. Nat. Acad. Sci. U.S.A*, *88*(22), 10357-10361.

West, G B, Brown, J. H., & Enquist, B. J. (1999). The fourth dimension of life: fractal geometry and allometric scaling of organisms. *Science*, *284*(5420), 1677–1679.

White, C. R., Frappell, P. B., & Chown, S. L. (2012). An information-theoretic approach to evaluating the size and temperature dependence of metabolic rate. *Proc. R. Soc. B.*, *279*(1742), 3616–3621.

Winberg, G. G. (1956). Rate of metabolism and food requirements of fishes. *Res. Bd. Can. Transl. Ser. No. 194*.

Yao, Y., Vehtari, A., Simpson, D., & Gelman, A. (2018). Using stacking to average bayesian predictive distributions. *Bayesian Anal*., *13*(3), 917-1007.

2.8. Supplementary Information

2.8.1. Supplementary Results

Is respiratory organ (i.e., lungs versus gills) a better characterization of the known difference in metabolic rate and respiratory surface area between endotherms and ectotherms?

The intercept—the metabolic rate for a given body size—did not differ significantly between organisms with lungs versus gills for all models explaining variation in metabolic rate without the inclusion of respiratory surface area (compare the overlapping 95% Bayesian Credible Intervals [BCIs] for the intercept for organisms with lungs versus gills in models “MR2_LG”, “MR3_LG” in Table S6). Similarly, the body mass-scaling exponent did not differ between organisms with lungs versus gills when the body mass-scaling exponent was allowed to vary between these two groups (compare the overlapping 95% BCIs for the “mass” effect size for organisms with lungs versus gills in model “MR3_LG” in Table S6). For all models explaining variation in metabolic rate with the inclusion of respiratory surface area, neither the intercept, nor the body mass-scaling exponents (if allowed to vary, model C6_LG) differed between organisms with lungs and those with gills (models “C3_LG”, “C4_LG”, “C5_LG”, and “C6_LG” in Table S6). Thus, the metabolic rate for a given body size and the body mass-scaling of metabolic rate did not differ between lunged- and gilled-organisms, regardless of the inclusion of respiratory surface area as a covariate (Table S6).

For the models assessing the scaling of respiratory surface area and body size—only the intercept, or respiratory surface area for a given size—was significantly different between species with lungs versus species with gills (models “RSA2_LG”, “RSA3_LG” in Table S6). When the body mass-scaling exponent was allowed to vary between organisms with lungs versus gills, the difference was not significant, suggesting that the body mass-scaling of respiratory surface area does not differ between lunged- and gilled-organisms (model “RSA3_LG” in Table S6).

2.8.2. Supplementary Methods

Model overview

We constructed and compared phylogenetic Bayesian multilevel linear regression models in R v.3.5.1 and v.4.0.1 in Stan using the package rstan (R Core Team 2013; Stan Development Team 2019).

Model parameterization

Metabolic Rate Models ("MR" models in Table S1)

We fitted three candidate models to examine the effects of mean body mass, mean (inverse) temperature, and thermoregulatory strategy on whole-organism metabolic rate (MR_i) (see Table S1).

General model parameterization:

$MR_i = \alpha + \Sigma_j \beta_j x_{i,j} + \varepsilon_i$

$\hat{\varepsilon} \sim$ multivariate normal $(\hat{0}, \sigma_e^2 * C_{phylo})$

$C_{phylo} = \lambda * V + (1 - \lambda) * I$

$\alpha \sim$ student-t (3, 0, 10)

$\beta_j \sim$ student-t (3, 0, 10)

$\sigma_e^2 \sim$ half-Cauchy (0, 10)

Here, MR_i is the response variable (mean whole-organism metabolic rate), α is the intercept, and β_j is the slope of the *jth* predictor, and $x_{i,j}$ is species *i*'s trait value for the *j*th trait (see below for predictors in each model). The priors on the intercept, α, slope, β_j, and error, σ_e^2, are also reported (see above) and our choice of priors is explained below.

Following (Frishkoff *et al.* 2017), we assumed the residual error, ε_i, to be distributed according to a multivariate normal distribution, where $\hat{0}$ is a vector with length *N*, σ_e^2 is the variation in responses to the predictors ($\beta_j x_{i,j}$), and C_{phylo} is the $N \times N$ correlation matrix resulting from the phylogeny. The strength of the phylogenetic signal, λ, in the residuals

under a model of evolution of Brownian motion is estimated according to $C_{phylo} = \lambda * V + (1 - \lambda) * I$, where V is the variance covariance matrix from the phylogeny, and I is an identify matrix of $N \times N$ values with σ_e^2 on the diagonal.

Model 1: $\beta_{mass} * x_{mass} + \beta_{temp} * x_{temp}$

Model 2: $\beta_{mass} * x_{mass} + \beta_{temp} * x_{temp} + \beta_{therm} * x_{therm}$

Model 3: $\beta_{mass} * x_{mass} + \beta_{temp} * x_{temp} + \beta_{therm} * x_{therm} + \beta_{mass\_therm} * x_{therm} * x_{tmass}$,

where *mass* is the mean body mass associated with metabolic rate, *temp* is the mean inverse temperature associated with metabolic rate (for ectotherms, this is the temperature at which metabolic rate was experimentally measured and for endotherms, this is body temperature), and *therm* is thermoregulatory strategy. Following (*2*), temperature is parameterized as the Boltzmann factor (1/(Boltzmann constant * temperature in Kelvin)) and thus, β_{temp} is the activation energy.

Respiratory surface area models ("RSA" models in Table S1)

We fitted three candidate models to examine the effects of mean body mass and thermoregulatory strategy on whole-organism respiratory surface area (RSA_i) (see Table S1).

General model parameterization:

$RSA_i = \alpha + \Sigma_j \beta_j x_{i,j} + \varepsilon_i$

$\hat{\varepsilon} \sim$ multivariate normal $(\hat{0}, \sigma_e^2 * C_{phylo})$

$C_{phylo} = \lambda * V + (1 - \lambda) * I$

$\alpha \sim$ student-t (3, 0, 10)

$\beta_j \sim$ student-t (3, 0, 10)

$\sigma_e^2 \sim$ half-Cauchy (0, 10)

Here, RSA_i is the response variable (mean whole-organism respiratory surface area), α is the intercept, and β_j is the slope of the *jth* predictor, and $x_{i,j}$ is species *i*'s trait value for the *j*th trait (see below for predictors in each model). The priors on the intercept, α, slope, β_j, and error, σ_e^2, are also reported and our choice of priors is explained below.

The parameterization of the phylogenetic components is the same as above for the Metabolic Rate models.

Model 1: $\beta_{mass} * x_{mass}$

Model 2: $\beta_{mass} * x_{mass} + \beta_{therm} * x_{therm}$

Model 3: $\beta_{mass} * x_{mass} + \beta_{therm} * x_{therm} + \beta_{mass\_therm} * x_{therm} * x_{mass}$,

where *mass* is the mean body mass associated with respiratory surface area and *therm* is as defined above. For the models with respiratory organ, "*organ*" replaced "*therm*" and was designated as either lung or gill.

Combined models ("C" models in Table S1)

We fitted six candidate models to examine the effects of mean body mass, mean temperature, residual respiratory surface area, and thermoregulatory strategy on whole-organism metabolic rate (MR_i) (see Table S1). The first level of the model regressed mean whole-organism respiratory surface (RSA_i) against mean body mass associated with respiratory surface area. The residuals from this model indicate whether a species had a higher respiratory surface area (positive residual) or lower respiratory surface area (negative residual) than would be expected based on its body mass. The second level modeled metabolic rate as a function of different combinations of covariates (body mass associated with metabolic rate, temperature, thermoregulatory strategy, as well as respiratory surface area, see Table S1). The entire posterior distribution of residual respiratory surface area estimated in the first level of the model was included as the respiratory surface area covariate in the second level of the model. Importantly, each iteration of both models happens in succession so estimates and uncertainty of residual respiratory surface area are propagated across levels of the model.

General model parameterization:

First level of the model:

$RSA_i = \alpha + \Sigma_j \beta_j x_{i,j} + \varepsilon_i$

$\hat{\varepsilon} \sim$ multivariate normal $(\hat{0}, \sigma_e^2 * C_{phylo})$

$C_{phylo} = \lambda * V + (1 - \lambda) * I$

$\alpha \sim$ student-t (3, 0, 10)

$\beta_{mass} \sim$ student-t (3, 0, 10)

$\sigma_e^2 \sim$ half-Cauchy (0, 10)

Here, RSA_i is the response variable (mean whole-organism respiratory surface area), α is the intercept, and β_{mass} is the slope of the body mass associated with respiratory surface area, x_{mass}. The priors on the intercept, α, slope, β_{mass}, and error, σ_e^2, are also reported and our choice of priors is explained below.

Second level of the model:

$MR_i = \alpha + \Sigma_j \beta_j x_{i,j} + \varepsilon_i$

$\hat{\varepsilon} \sim$ multivariate normal $(\hat{0}, \sigma_e^2 * C_{phylo})$

$C_{phylo} = \lambda * V + (1 - \lambda) * I$

$\alpha \sim$ student-t (3, 0, 10)

$\beta_j \sim$ student-t (3, 0, 10)

$\sigma_e^2 \sim$ half-Cauchy (0, 10)

Here, MR_i is the response variable (mean whole-organism metabolic rate), α is the intercept, and β_j is the slope of the *jth* predictor, and $x_{i,j}$ is species *i*'s trait value for the *j*th trait (see below for predictors in each model). The priors on the intercept, α, slope, β_j, and error, σ_e^2, are also reported and our choice of priors is explained below.

The parameterization of the variance and phylogeny is the same as above in the "Metabolic Rate Models" and "Respiratory Surface Area Models".

Model 1: $\beta_{Rrsa} * x_{Rrsa} + \beta_{mass} * x_{mass} + \beta_{temp} * x_{temp}$

Model 2: $\beta_{Rrsa} * x_{Rrsa} + \beta_{mass} * x_{mass} + \beta_{mass\_Rrsa} * x_{mass} * x_{Rrsa} + \beta_{temp} * x_{temp}$

Model 3: $\beta_{Rrsa} * x_{Rrsa} + \beta_{mass} * x_{mass} + \beta_{temp} * x_{temp} + \beta_{therm} * x_{therm}$

Model 4: $\beta_{Rrsa} * x_{Rrsa} + \beta_{mass} * x_{mass} + \beta_{mass\_Rrsa} * x_{mass} * x_{Rrsa} + \beta_{temp} * x_{temp} + \beta_{therm} * x_{therm}$

Model 5: $\beta_{Rrsa} * x_{Rrsa} + \beta_{mass} * x_{mass} + \beta_{therm} * x_{therm} + \beta_{mass\_therm} * x_{mass} * x_{therm} + \beta_{temp} * x_{temp}$

Model 6: $\beta_{Rrsa} * x_{Rrsa} + \beta_{mass} * x_{mass} + \beta_{therm} * x_{therm} + \beta_{mass\_therm} * x_{mass} * x_{therm} +$

$\beta_{mass\_Rrsa} * x_{mass} * x_{Rrsa} + \beta_{temp} * x_{temp}$

Choice of priors

We used weakly informative regularizing priors based on recommendations for Stan (https://github.com/stan-dev/stan/wiki/Prior-Choice-Recommendations).

As λ (phylogenetic signal) has an equal chance of taking any value within the bounds of zero to one, we used a prior with a uniform distribution from zero to one. As σ_e^2 (variation in responses to the predictors ($\beta_j x_{i,j}$) can only be positive, we used a half-Cauchy prior with a location of zero and a scale of ten. Priors are also shown below for each set of models.

2.8.3. Supplementary Tables

Table S1. Comparison of all models using Pareto-smoothing importance sampling leave-one-out cross validation (PSIS-LOO).

Values reported are for the first model run and include the LOO information criterion value (similar to Akaike Information Criterion [AIC]) *looic,* the effective number of parameters (p_{loo}), the expected log predictive density ($elpd_{loo}$), the standard error of the expected log predictive density (se_{elpd_loo}), the difference in the expected log predictive density ($elpd_{diff}$) for a given model compared to the best model, and the Bayesian stacking weight (similar to Akaike weight). The model with the lowest *looic* has the most support and is emboldened and highlighted in grey for each group. Any model with $elpd_{diff} < 2$ is also highlighted in grey. PSIS-LOO was conducted using the *loo* package.

	Model	**looic**	**p_{loo}**	**$elpd_{loo}$**	**se_{elpd_loo}**	**$elpd_{diff}$**	**Weight**
	Metabolic rate:						
MR1	MR ~ $mass_{MR}$ + temperature	299.5	11.6	-149.7	5.9	-9.8	0.230
MR2	MR ~ $mass_{MR}$ + temperature + thermoregulatory strategy	285.9	8.4	-142.9	13.1	-3.0	0
MR3	**MR ~ $mass_{MR}$ * thermoregulatory strategy + temperature**	**279.9**	**9.9**	**-140.0**	**13.9**	**0.0**	**0.770**
	Respiratory surface area:						
RSA1	RSA ~ $mass_{RSA}$	346.4	3.0	-173.2	5.6	-46.3	0
RSA2	**RSA ~ $mass_{RSA}$ + thermoregulatory strategy**	**253.8**	**3.2**	**-126.8**	**7.3**	**0.0**	**1.00**
RSA3	RSA ~ $mass_{RSA}$ * thermoregulatory strategy	255.7	4.0	-127.8	7.2	-0.9	0
	Combined:						
C1	MR ~ residual RSA + $mass_{MR}$ + temperature	277.9	10.6	-139.0	13.5	-7.2	0
C2	MR ~ residual RSA * $mass_{MR}$ + temperature	278.6	12.6	-139.3	12.6	-7.6	0.071
C3	MR ~ residual RSA + $mass_{MR}$ + temperature + thermoregulatory strategy	271.6	11.2	-135.8	13.9	-4.1	0.118
C4	MR ~ residual RSA * $mass_{MR}$ + temperature + thermoregulatory strategy	270.0	12.2	-135.0	14.1	-3.3	0
C5	**MR ~ residual RSA + $mass_{MR}$ * thermoregulatory strategy + temperature**	**263.4**	**11.7**	**-131.7**	**14.6**	**0.0**	**0.811**
C6	MR ~ residual RSA * $mass_{MR}$ * thermoregulatory strategy + temperature	267.5	13.5	-133.7	14.8	-2.0	0

Table S2. Coefficient means and 95% Bayesian Credible Intervals (BCI, in parentheses) for all models examined.
Model names correspond to those in Table S1. Intercepts are back transformed from the natural log scale. The models with the most support from each group are highlighted in grey (see Table S1). The coefficient means reported here are from the first model run. Pagel's λ indicates the strength of the phylogenetic signal in the residuals of the response variable. RSA = respiratory surface area.

Model		Intercept	Mass	Temperature	Residual RSA	Mass: Residual RSA	Sigma	Pagel's λ
MR1		0.18 (0.10 to 0.38)	0.89 (0.82 to 0.96)	-1.60 (-2.00 to -1.17)	NA	NA	1.37 (0.90 to 2.24)	0.33 (0.03 to 0.72)
MR2	*Ectotherm*	0.12 (0.07 to 0.21)	0.84 (0.77 to 0.90)	-0.53 (-1.00 to -0.06)	NA	NA	0.95 (0.65 to 1.50)	0.29 (0.02 to 0.68)
	Endotherm	0.81 (0.28 to 2.61)						
MR3	*Ectotherm*	0.13 (0.07 to 0.22)	0.93 (0.84 to 1.02)	-0.59 (-1.05 to -0.14)	NA	NA	0.89 (0.59 to 1.43)	0.31 (0.02 to 0.70)
	Endotherm	0.95 (0.32 to 3.01)	0.74 (0.53 to 0.95)					
RSA1		1597.59 (787.52 to 3201.40)	1.05 (0.97 to 1.13)	NA	NA	NA	1.74 (1.18 to 2.86)	0.26 (0.01 to 0.70)
RSA2	*Ectotherm*	1002.16 (679.33 to 1524.50)	0.92 (0.87 to 0.98)	NA	NA	NA	0.70 (0.49 to 1.09)	0.22 (0.01 to 0.63)
	Endotherm	9407.04 (4428.47 to 20574.87)						
RSA3	*Ectotherm*	1005.28 (673.15 to 1611.09)	0.93 (0.86 to 1.00)	NA	NA	NA	0.71 (0.49 to 1.11)	0.23 (0.01 to 0.62)
	Endotherm	9615.49 (4404.45 to 22723.31)	0.91 (0.74 to 1.10)					
C1		0.18 (0.10 to 0.32)	0.93 (0.86 to 1.00)	-0.75 (-1.14 to -0.34)	0.63 (0.47 to 0.79)	NA	0.77 (0.55 to 1.19)	0.21 (0.01 to 0.58)
C2		0.18 (0.10 to 0.32)	0.96 (0.88 to 1.04)	-0.81 (-1.21 to -0.40)	0.60 (0.44 to 0.76)	0.05 (-0.10 to 0.01)	0.75 (0.53 to 1.13)	0.21 (0.01 to 0.57)
C3	*Ectotherm*	0.14 (0.08 to 0.26)	0.90 (0.83 to 0.97)	-0.45 (-0.90 to 0.00)	0.46 (0.27 to 0.66)	NA	0.75 (0.53 to 1.17)	0.25 (0.01 to 0.63)
	Endotherm	0.37 (0.11 to 1.31)						
C4	*Ectotherm*	0.14 (0.09 to 0.26)	0.92 (0.84 to 1.00)	-0.51 (-0.94 to -0.06)	0.42 (0.22 to 0.61)	-0.05 (-0.10 to 0.00)	0.73 (0.51 to 1.12)	0.25 (0.01 to 0.62)
	Endotherm	0.37 (0.12 to 1.33)						
C5	*Ectotherm*	0.15 (0.09 to 0.26)	0.96 (0.88 to 1.04)	-0.51 (-0.92 to -0.07)	0.45 (0.26 to 0.64)	NA	0.69 (0.48 to 1.07)	0.24 (0.01 to 0.62)
	Endotherm	0.44 (0.14 to 1.52)	0.80 (0.60 to 1.01)					
C6	*Ectotherm*	0.15 (0.09 to 0.28)	0.98 (0.89 to 1.08)	-0.50 (-0.91 to -0.08)	0.45 (0.27 to 0.66)	0.02 (-0.06 to 0.09)	0.70 (0.48 to 1.08)	0.24 (0.02 to 0.61)
	Endotherm	0.45 (0.14 to 1.57)	0.77 (0.49 to 1.05)					

Table S3. Comparison of the best models with and without respiratory surface area that explained variation in metabolic rate across 109 vertebrate species (i.e., "best metabolic rate model" and "best combined model").
Model names correspond to those in Table S1. Each model was run a total of four times to ensure the robustness of results. All model comparison was conducted using Pareto-smoothing importance sampling leave-one-out cross validation (PSIS-LOO) using the *loo* package. Values reported are the LOO information criterion value (similar to Akaike Information Criterion [AIC]) *looic,* the effective number of parameters (p_{loo}), the expected log predictive density ($elpd_{loo}$), the standard error of the expected log predictive density (se_{elpd_loo}), the difference in the expected log predictive density ($elpd_{diff}$) for a given model compared to the best model, the Bayesian stacking weight (similar to Akaike weight), and the evidence ratio (weight of evidence of the best model divided by the weight of evidence of the other model(s) of interest).

Model	Model run	looic	p_{loo}	$elpd_{loo}$	se_{elpd_loo}	$elpd_{diff}$	Weight	Evidence ratio
MR3	1	279.9	9.9	-140.0	13.9	-8.2	0.043	22.3
C5		263.4	11.7	-131.7	14.6	0	0.957	
MR3	2	279.6	9.6	-139.8	13.8	-8.0	0.054	17.5
C5		263.6	11.8	-131.8	14.7	0	0.946	
MR3	3	279.6	9.7	-139.8	14	-7.8	0.044	21.7
C5		264	12	-132	14.9	0	0.956	
MR3	4	279.7	9.7	-139.8	13.9	-8.1	0.075	12.3
C5		263.4	11.7	-131.7	14.8	0	0.925	
							average	18.5

Table S4. Standardized coefficient means (i.e., effect sizes) and 95% Bayesian Credible Intervals (BCIs, in parentheses) for the top model that explains metabolic rate as a function of body mass, temperature, respiratory surface area, thermoregulatory strategy, and the interaction of body mass and thermoregulatory strategy, while accounting for evolutionary history.

The model name corresponds to that in Table S1. Intercepts are back transformed from the natural log scale. Pagel's λ indicates the strength of the phylogenetic signal in the residuals of the response variable. RSA = respiratory surface area.

Model		Intercept	Mass	Temperature	Residual RSA	Sigma	Pagel's λ
				-0.25	0.52	0.69	0.24
	Ectotherm	0.15	2.66	(-0.47 to -0.04)	(0.29 to 0.75)	(0.48 to 1.09)	(0.01 to 0.61)
C5		(0.10 to 0.25)	(2.42 to 2.90)				
	Endotherm	0.44	2.17				
		(0.14 to 1.41)	(1.61-0. to 2.73)				

Table S5. Comparison of models using thermoregulatory strategy *or* respiratory organ to characterize the differences in metabolic rate and respiratory surface area between endotherms and ectotherms.

Values reported are the LOO information criterion value (similar to Akaike Information Criterion [AIC]) *looic*, the effective number of parameters (p_{loo}), the expected log predictive density ($elpd_{loo}$), the standard error of the expected log predictive density (se_{elpd_loo}), and the difference in the expected log predictive density ($elpd_{diff}$) for a given model compared to the best model. The model with the lowest *looic* of each group has the most support and is highlighted in grey. Model comparison was conducted using Pareto-smoothing importance sampling leave-one-out cross validation (PSIS-LOO) with the loo package. MR = metabolic rate, RSA = respiratory surface area, $mass_{MR}$ = mass associated with the metabolic rate estimate and $mass_{RSA}$ = mass associated with respiratory surface area estimate.

	Model	looic	p_{loo}	$elpd_{loo}$	se_{elpd_loo}	$elpd_{diff}$
MR2	MR ~ $mass_{MR}$ + temperature + thermoregulatory strategy	286.8	8.5	-143.3	13	0
MR2_LG	MR ~ $mass_{MR}$ + temperature + respiratory organ	302.8	6.9	-151.4	11.7	-8.0
MR3	MR ~ $mass_{MR}$ * thermoregulatory strategy + temperature	281.3	9.9	-140.7	13.9	0
MR3_LG	MR ~ $mass_{MR}$ * respiratory organ + temperature	304.1	8.3	-152.1	12.0	-11.4
RSA2	RSA ~ $mass_{RSA}$ + thermoregulatory strategy	253.7	3.2	-126.8	7.3	0
RSA2_LG	RSA ~ $mass_{RSA}$ + respiratory organ	269.3	2.7	-134.7	5.8	-7.8
RSA3	RSA ~ $mass_{RSA}$ * thermoregulatory strategy	255.6	4.0	-127.8	5.8	0
RSA3_LG	RSA ~ $mass_{RSA}$ * respiratory organ	272.3	4.0	-136.2	5.8	-8.4
C3	MR ~ residual RSA + $mass_{MR}$ + temperature + thermoregulatory strategy	271.6	11.2	-135.8	13.9	0
C3_LG	MR ~ residual RSA + $mass_{MR}$ + temperature + respiratory organ	283.3	11.4	-141.6	13.6	-5.9
C4	MR ~ residual RSA * $mass_{MR}$ + temperature + thermoregulatory strategy	270.0	12.2	-135.0	14.1	0
C4_LG	MR ~ residual RSA * $mass_{MR}$ + temperature + respiratory organ	284.3	13.8	-142.2	14.4	-7.2
C5	MR ~ residual RSA + $mass_{MR}$ * thermoregulatory strategy + temperature	263.4	11.7	-131.7	14.6	0
C5_LG	MR ~ residual RSA + $mass_{MR}$ * respiratory organ + temperature	283.9	12.9	-142.0	13.9	-10.2
C6	MR ~ residual RSA * $mass_{MR}$ * thermoregulatory strategy + temperature	267.5	11.7	-133.7	14.8	0
C6_LG	MR ~ residual RSA * $mass_{MR}$ * respiratory organ + temperature	294.0	17.2	-147.0	14.7	-13.3

Table S6. Coefficient means and 95% Bayesian Credible Intervals (BCIs, in parentheses) for all models that included respiratory organ (i.e., lungs or gills) in place of thermoregulatory strategy (i.e., ectotherm or endotherm).

Model names correspond to those in Table S5. Intercepts are back-transformed from the natural log scale. Pagel's λ indicates the strength of the phylogenetic signal in the residuals of the response. RSA = respiratory surface area.

Model		Intercept	Mass	Temeprature	Residual RSA	Mass: Residual RSA	Sigma	Pagel's λ
MR2_LG	Gills	0.14 (0.07 to 0.27)	0.89 (0.82 to 0.97)	-1.23 (-1.71 to -0.75)	NA	NA	1.24 (0.84 to 2.00)	0.30 (0.02 to 0.68)
	Lungs	0.26 (0.09 to 0.82)						
MR3_LG	Gills	0.14 (0.08 to 0.29)	0.94 (0.82 to 1.07)	-1.31 (-1.81 to -0.80)	NA	NA	1.27 (0.85 to 2.05)	0.31 (0.02 to 0.70)
	Lungs	0.26 (0.09 to 0.84)	0.86 (0.58 to 1.15)					
RSA2_LG	Gills	820.00 (395.54 – 1671.05)	1.02 (0.96 to 1.07)	-0.59 (-1.05 to -0.14)	NA	NA	1.17 (0.75 to 1.85)	0.49 (0.11 to 0.77)
	Lungs	4147.50 (1432.91 – 11917.25)						
RSA3_LG	Gills	825.27 (403.64 – 1706.42)	1.02 (0.93 to 1.12)	NA	NA	NA	1.19 (0.76 to 1.89)	0.49 (0.10 to 0.78)
	Lungs	4175.97 (1454.04 – 12183.13)	1.01 (0.79 to 1.23)					
C3_LG	Gills	0.19 (0.10 to 0.38)	0.93 (0.86 to 1.00)	-0.80 (-1.20 to -0.39)	0.67 (0.48 to 0.86)	NA	0.79 (0.55 to 1.21)	0.23 (0.01 to 0.59)
	Lungs	0.15 (0.05 to 1.48)						
C4_LG	Gills	0.19 (0.10 to 0.37)	0.96 (0.88 to 1.05)	-0.86 (-1.27 to -0.44)	0.64 (0.45 to 0.83)	-0.05 (-0.10 to 0.01)	0.76 (0.54 to 1.17)	0.22 (0.01 to 0.58)
	Lungs	0.16 (0.05 to 0.48)						
C5_LG	Gills	0.19 (0.10 to 0.37)	0.95 (0.85 to 1.06)	-0.84 (-1.27 to -0.39)	0.66 (0.48 to 0.85)	NA	0.79 (0.55 to 1.20)	0.22 (0.01 to 0.59)
	Lungs	0.15 (0.05 to 0.48)						
C6_LG	Gills	0.18 (0.10 to 0.36)	0.92 (0.80 to 1.04)	-0.80 (-1.23 to -0.37)	0.63 (0.45 to 0.82)	-0.07 (-0.14 to 0.01)	0.77 (0.54 to 1.17)	0.22 (0.01 to 0.58)
	Lungs	0.16 (0.05 to 0.49)	1.00 (0.70 to 1.29)					

Table S7. Model comparison for the three additional runs per model.

Model names correspond to those in Table S1. All model comparison was conducted using Pareto-smoothing importance sampling leave-one-out cross validation (PSIS-LOO) using the *loo* package. Values reported are the LOO information criterion value (similar to Akaike Information Criterion [AIC]) *looic,* the effective number of parameters (p_{loo}), the expected log predictive density ($elpd_{loo}$), the standard error of the expected log predictive density (se_{elpd_loo}), the difference in the expected log predictive density ($elpd_{diff}$) for a given model compared to the best model, and the Bayesian stacking weight (similar to Akaike weight). The grey shading serves as a visualization tool for separating models being compared.

Model	Model run	looic	p_{loo}	$elpd_{loo}$	se_{elpd_loo}	$elpd_{diff}$	Weight
MR1	1	306.5	14.8	-153.2	6.2	-13.4	0.207
MR2		286.7	8.8	-143.4	13.3	-3.5	0
MR3		279.6	9.6	-139.8	13.8	0	0.793
MR1	2	305.4	14.4	-152.7	6.2	-12.9	0.208
MR2		286.4	8.7	-143.2	13.2	-3.4	0
MR3		279.6	9.7	-139.8	14	0	0.792
MR1	3	302.8	13.1	-151.4	6.1	-11.6	0.219
MR2		285.9	8.4	-143	13.2	-3.1	0
MR3		279.7	9.7	-139.8	13.9	0	0.781
RSA1	1	346.5	3.1	-173.2	5.6	-46.3	0
RSA2		253.9	3.3	-127	7.3	0	1
RSA3		255.8	4.1	-127.9	7.3	-0.9	0
RSA1	2	346.5	3.2	-173.3	5.6	-46.3	0
RSA2		253.9	3.3	-126.9	7.3	0	1
RSA3		255.9	4.1	-128	7.2	-1	0
RSA1	3	346.3	3.1	-173.2	5.6	-46.3	0
RSA2		253.7	3.2	-126.8	7.2	0	1
RSA3		255.6	4	-127.8	7.2	-0.9	0
C1	1	276.5	10	-138.2	13.2	-6.5	0.002
C2		277.4	12	-138.7	14	-6.9	0.08
C3		271.7	11.4	-135.8	14	-4.1	0.108
C4		270.7	12.7	-135.4	14.2	-3.6	0
C5		263.6	11.8	-131.8	14.7	0	0.809
C6		267.2	13.3	-133.6	14.8	-1.8	267.2
C1	2	276.6	9.9	-138.3	13.3	-6.3	0
C2		275.8	11.2	-137.9	13.3	-5.9	0.118
C3		270.8	11	-135.4	13.9	-3.4	0.138
C4		269.1	11.7	-134.5	13.7	-2.6	0
C5		264	12	-132	14.9	0	0.744
C6		266.8	13.1	-133.4	14.6	-1.4	0
C1	3	278.1	10.5	-139.1	13.3	-7.1	0
C2		277.3	11.8	-138.7	13.8	-7	0.069
C3		270.8	10.8	-135.4	13.8	-3.7	0.14
C4		271.9	13.3	-136	14.8	-4.3	0
C5		263.4	11.7	-131.7	14.8	0	0.791
C6		267	13.3	-133.5	14.6	-1.8	0

Table S8. The corresponding species identity to the species code (number) along the y-axis in Figure 1.

Species code	Scientific name	Common name
1	*Seriola lalandi*	Yellowtail
2	*Euthynnus affinis*	Mackerel Tuna
3	*Ctenopharyngodon idella*	Grass Carp
4	*Sebastes diploproa*	Rockfish
5	*Carcharodon carcharias*	White Shark
6	*Morone saxatilis*	Striped Bass
7	*Pagrus auratus*	Silver Seabream
8	*Cirrhinus mrigala*	Mrigal Carp
9	*Brevoortia tyrannus*	Menhaden
10	*Carassius auratus*	Goldfish
11	*Conger conger*	Conger Eel
12	*Isurus oxyrinchus*	Shortfin Mako
13	*Hoplias malabaricus*	Wolf Fish
14	*Sander lucioperca*	Pikeperch
15	*Cottus gobio*	European Bullhead
16	*Varanus exanthematicus*	Savannah Monitor Lizard
17	*Tinca tinca*	Tench
18	*Labeo rohita*	Rohu Carp
19	*Pseudopleuronectes americanus*	Winter Flounder
20	*Carcharhinus plumbeus*	Sandbar Shark
21	*Anguilla anguilla*	European Eel
22	*Thunnus albacares*	Yellowfin Tuna
23	*Scomber scombrus*	Atlantic Mackerel
24	*Merlangius merlangus*	Whiting
25	*Pomatomus saltatrix*	Bluefish
26	*Oncorhynchus mykiss*	Rainbow Trout
27	*Hoplerythrinus unitaeniatus*	Trahira
28	*Catostomus commersonii*	White Sucker
29	*Misgurnus fossilis*	Weatherfish
30	*Gekko gecko*	Tokay Gecko
31	*Centropristis striata*	Black Sea Bass
32	*Gymnocephalus cernua*	Ruffe
33	*Scomber japonicus*	Chub Mackerel
34	*Seriola quinqueradiata*	Amberjack
35	*Platichthys flesus*	European Flounder
36	*Trachemys scripta*	Pond Slider Turtle
37	*Sander vitreus*	Walleye

Species code	Scientific name	Common name
38	*Coryphaena hippurus*	Dolphinfish
39	*Salmo trutta*	Brown Trout
40	*Struthio camelus*	Common Ostrich
41	*Rhinoptera bonasus*	Cownose Ray
42	*Pollachius virens*	Coalfish Pollock
43	*Callionymus lyra*	Dragonet
44	*Channichthys rhinoceratus*	Unicorn Icefish
45	*Sebastolobus altivelis*	Longspine Thornyhead
46	*Bos taurus*	Cow
47	*Mus musculus*	Mouse
48	*Equus caballus*	Horse
49	*Heteropneustes fossilis*	Stinging Catfish
50	*Connochaetes taurinus*	Blue Wildebeest
51	*Limanda limanda*	Common Dab
52	*Ameiurus nebulosus*	Brown Bullhead Catfish
53	*Scyliorhinus stellaris*	Nursehound
54	*Notophthalmus viridescens*	Eastern Newt
55	*Camelus dromedarius*	Camel
56	*Katsuwonus pelamis*	Skipjack Tuna
57	*Rutilus rutilus*	Common Roach
58	*Sorex minutus*	Pygmy Shew
59	*Anguilla rostrata*	American Eel
60	*Taurotragus oryx*	Eland Antelope
61	*Perca flavescens*	Yellow Perch
62	*Opsanus tau*	Oyster Toadfish
63	*Bufo bufo*	Common Toad
64	*Larus argentatus*	Herring Gull
65	*Anabas testudineus*	Climbing Perch
66	*Oryctolagus cuniculus*	Rabbit
67	*Esox lucius*	Northern Pike
68	*Cavia porcellus*	Guinea Pig
69	*Perca fluviatilis*	European Perch
70	*Lipophrys pholis*	Shanny Blenny
71	*Phyllotis darwini*	Darwin's Mouse
72	*Scyliorhinus canicula*	Lesser Spotted Dogfish
73	*Oreochromis niloticus*	Nile Tilapia
74	*Pleuronectes platessa*	European Plaice
75	*Channa striata*	Snakehead Murrel
76	*Zoarces viviparus*	Eelpout
77	*Ambystoma opacum*	Marbled Salamander

Species code	Scientific name	Common name
78	*Taricha granulosa*	Rough Skinned Newt
79	*Dasyuroides byrnei*	Kowari Rat
80	*Dromaius novaehollandiae*	Emu
81	*Gallus gallus*	Chicken
82	*Echeneis naucrates*	Sharksucker
83	*Dicamptodon ensatus*	Giant California Salamander
84	*Vulpes lagopus*	Arctic Fox
85	*Amphiuma means*	Two Toed Amphiuma Salamander
86	*Setonix brachyurus*	Quokka
87	*Torpedo marmorata*	Marbled Electric Ray
88	*Spheniscus humboldti*	Chilean Penguin
89	*Balistes capriscus*	Grey Triggerfish
90	*Hyla arborea*	European Tree Frog
91	*Channa punctata*	Spotted Snakehead
92	*Rhyacotriton olympicus*	Olympic Torrent Salamander
93	*Myoxocephalus scorpius*	Shortfin Sculpin
94	*Cyprinus carpio*	Common Carp
95	*Dasyatis sabina*	Atlantic Stingray
96	*Clarias batrachus*	Walking Catfish
97	*Homo sapiens*	Human
98	*Bagre cavasius*	Gangetic Catfish
99	*Python regius*	Ball Python
100	*Gadus morhua*	Cod
101	*Chaenocephalus aceratus*	Blackfin Icefish
102	*Madoqua kirkii*	Dik Dik Antelope
103	*Pipistrellus pipistrellus*	Bat
104	*Anas platyrhynchos*	Mallard Duck
105	*Rana temporaria*	Common Frog
106	*Mugil cephalus*	Grey Mullet
107	*Cynopterus brachyotis*	Fruit Bat
108	*Rana arvalis*	Moor Frog
109	*Suncus etruscus*	Shrew

Chapter 3.

Ecological lifestyles and the scaling of shark gill surface area[2]

3.1. Abstract

Fish gill surface area varies across species and with respect to ecological lifestyles. The majority of previous studies only qualitatively describe gill surface area in relation to ecology and focus primarily on teleosts. Here, we quantitatively examined the relationship of gill surface area with respect to specific ecological lifestyle traits in elasmobranchs, which offer an independent evaluation of observed patterns in teleosts. As gill surface area increases ontogenetically with body mass, examination of how gill surface area varies with ecological lifestyle traits must be assessed in the context of its allometry (scaling). Thus, we examined how the relationship of gill surface area and body mass across 11 shark species from the literature and one species for which we made measurements, the Gray Smoothhound *Mustelus californicus,* varied with three ecological lifestyle traits: activity, habitat, and maximum body size. Relative gill surface area (gill surface area at a specified body mass; here we used 5 000 g, termed the 'standardized intercept') ranged from 4 724.98 to 35 694.39 cm^2 (mean and standard error: 17 796.65 ± 2 948.61 cm^2) and varied across species and the ecological lifestyle traits examined. Specifically, larger-bodied, active, oceanic species had greater relative gill surface area than smaller-bodied, less active, coastal species. In contrast, the rate at which gill surface area scaled with body mass (slope) was generally consistent across species (0.85 ± 0.02) and did not differ statistically with activity level, habitat, or maximum body size. Our results suggest that ecology may influence relative gill surface area, rather than the rate at which gill surface area scales with body mass. Future comparisons of gill surface area and ecological lifestyle traits using the quantitative techniques applied in this study can provide further insight into patterns dictating the relationship between gill surface area, metabolism, and ecological lifestyle traits.

[2] A version of this chapter appears as: Bigman, J. S., Pardo, S. A., Prinzing, T. S., Dando, M., Wegner, N. C., & Dulvy, N. K. (2018). Ecological lifestyles and the scaling of shark gill surface area. *Journal of morphology*, *279*(12), 1716-1724.

3.2. Introduction

In most fishes, gills function as the primary site of oxygen uptake used to support aerobic metabolism, resulting in an intimate relationship between gill surface area and metabolic rate (Hughes 1966; Hughes & Morgan 1973; Wegner 2011). The diffusive flux of oxygen across the gills is dependent upon their surface area, such that an increase in gill surface area augments oxygen uptake (Hughes 1970; Hughes & Morgan 1973; Hughes 1984a). Fishes with higher metabolic demands thus have greater gill surface areas, with active species in oceanic habitats typically having greater gill surface areas than less active species in coastal, benthic habitats (Gray 1954; Hughes 1966; Hughes 1984a). These patterns have led to several reviews of gill morphology to categorize fishes into ecological lifestyle groupings (i.e., groups of species that have similar habitats and activity) based primarily on their gill surface area.

Such categorizations of gill surface area, activity, and habitat began with Gray (1954), who descriptively categorized 31 teleost species into three ecological groups based on relative gill surface area (i.e., gill surface area at a specified body mass). These groups included (1) active, pelagic species with the greatest relative gill surface areas, (2) fishes of "moderate" activity with "intermediate" relative gill surface areas, and (3) "sluggish," benthic species with the lowest relative gill surface areas. Since then, subsequent reviews have further elaborated upon and attempted to define these groups (Hughes 1984a; Palzenberger & Pohla 1992; Wegner 2011). However, such comparisons of gill surface area across large species groups in relation to ecological lifestyle have mostly been descriptive or qualitative in nature, rather than analyzed quantitatively.

The quantitative assessment of how gill surface area varies across species and with respect to ecological lifestyle requires a thorough understanding of how gill surface area scales ontogenetically with body growth, or the allometry of gill surface area. This allows for both an understanding of the relative gill surface area (gill surface area at a specified mass, or the intercept of the allometric relationship) and the rate at which gill surface area scales with body mass (slope of the allometric relationship). For many species, gill surface area has not been examined for a sufficient size range of individuals to establish such relationships. For those species with sufficient gill surface area data across a size range of individuals, it is standard practice to estimate and report the regression equation for this

scaling relationship (Hughes 1984b; Emery & Szczepanski 1985; Palzenberger & Pohla 1992). However, comparisons of gill surface area across species or with respect to ecological lifestyle are generally discussed in descriptive or qualitative terms (Emery & Szczepanski 1985; Palzenberger & Pohla 1992; Wegner 2011). Thus, it remains largely untested if observed differences in gill surface area across species with diverse ecological lifestyles are statistically significant, and if the intercept, the slope, or both allometric regression coefficients vary with specific ecological lifestyle traits.

This study thus seeks to quantitatively assess how the allometry of gill surface area varies with specific ecological lifestyle traits. We focused our efforts on elasmobranch fishes as the majority of previous studies examining gill surface area across species and ecological lifestyles focus primarily on teleost fishes (De Jager & Dekkers 1975; Palzenberger & Pohla 1992; Satora & Wegner 2012). Chondrichthyans, and specifically elasmobranchs, offer an opportunity to evaluate the generality of gill surface area patterns as they are one of three taxonomic classes of fishes and have evolved separately for over 420 million years (Heinicke *et al.* 2009; Stein *et al.* 2018). Additionally, the elasmobranch gill differs from that of teleosts in their evolutionary retention of the plate-like interbranchial septum that gave rise to their name, “elasmobranch,” which translates into “plate-gill” (Wilson & Laurent 2002; Wegner 2016). This structure, which is largely absent from the teleost gill, has important consequences for gill function and morphology (Wegner *et al.* 2010a; Wegner *et al.* 2012; Wegner 2016).

Here, we examine if specific ecological lifestyle traits are quantitatively related to shark gill surface area, and if so, ask if these traits are related to the relative gill surface area (standardized intercept), the rate at which gill surface area scales with body mass (slope), or both. First, we estimated gill surface area allometries for 11 shark species from the literature, and one species for which we made measurements, the Gray Smoothhound *Mustelus californicus.* We then assessed if the allometric regression coefficients (standardized intercept and slope) were related to the ecological lifestyle traits of activity level, habitat type, or maximum body size, all of which likely influence gill surface area.

3.3. Methods

3.3.1. Gill surface area measurement and statistical analysis of the Gray Smoothhound

Eight Gray Smoothhound specimens were collected opportunistically off the coast of southern California from anchored benthic gillnet surveys for other scientific studies. For each specimen, mass (kg), total length (TL, cm), and fork length (FL, cm) were measured, and the gills were fixed in 10% formalin buffered in seawater for later processing. Only limited tissue shrinkage is associated with fixation and storage in 10% buffered formalin (Wootton *et al.* 2015).

Total gill surface area (A) of each specimen was estimated following Muir and Hughes (1969) and Hughes (1984c):

$$A = L_{fil} \times 2n_{lam} \times A_{lam}, \quad (1)$$

where L_{fil} is the total length of all the gill filaments, n_{lam} is the average number of lamellae per unit length on one side of the filament (lamellar frequency), and A_{lam} is the mean bilateral surface area of a lamella.

First, total filament length was estimated. All filaments on each of the nine hemibranchs from the right side of the branchial chamber were counted using a dissecting scope (Zeiss Stemi 2000-C) fitted with a digital camera (Lumenera INFINITYLite). Filaments were then binned into groups of approximately 10 filaments, beginning at the dorsal margin and moving ventrally along the arch. Consistent with previous work, the medial filament of each bin was assumed to be representative of all filaments in that bin (Muir & Hughes 1969; Wegner 2011). A magnified photograph was taken of each medial filament, and image-processing software (Image J, NIH) was used to measure the length of the filament from its base, embedded under the branchial canopy, to the tip. The total length of all filaments in each bin was estimated by multiplying the length of the medial filament by the number of filaments in the bin (typically 10). Total filament lengths for each bin were then summed to estimate the total filament length of each hemibranch. To determine the total filament length of the entire fish, the total filament lengths for each hemibranch were summed, and then doubled to account for the filaments from hemibranchs on the other side of the branchial chamber.

Second, we determined average lamellar frequency and the mean bilateral surface area of a lamella from the most representative hemibranch. This was the hemibranch with the smallest difference in average filament length compared to the average filament length for all hemibranchs. To estimate average lamellar frequency, the medial filament of each bin on the representative hemibranch was removed from the interbranchial septum and dissected into two sections, a base half and tip half. Magnified photographs were taken of one side of the filament at approximately the midpoint of the base section and midpoint of the tip section. The number of lamellae per millimeter at both locations were then counted using Image J and averaged to obtain a mean lamellar frequency for each medial filament. The mean lamellar frequency of each medial filament was multiplied by the total filament length of its respective bin, and each bin was then summed. This number was then divided by the total filament length of the representative hemibranch to estimate the average lamellar frequency for the entire hemibranch and gills.

To estimate the mean bilateral surface area of an individual lamella, cross-sections were made at the midpoint of the base section and midpoint of the tip section of each medial filament on the representative hemibranch. These cross-sections were then laid flat to expose the lamellae, which were photographed under magnification. The surface area of one side of these base and tip lamella were measured using ImageJ, averaged, and doubled to obtain the mean bilateral lamellar surface area of a lamella in that bin. Each mean bilateral lamellar surface area from each medial filament was then multiplied by the total number of lamellae within its respective bin, and these measurements were summed to estimate the total bilateral lamellar surface area of all lamellae for the entire hemibranch. This was then divided by the total number of lamellae on the representative hemibranch to determine the mean bilateral surface area for the entire gills.

The relationships of gill surface area and associated dimensions in the Gray Smoothhound (total filament length, average lamellar frequency, and mean bilateral lamellar surface area) in relation to body mass were determined by Ordinary Least Squares Regression using the lm function in R v. 3.3.2 (R Core Team 2016). To linearize the expected power law relationship, body mass, gill surface area, total filament length, average lamellar frequency, and the mean bilateral lamellar surface area were $\log_{10}$-transformed.

3.3.2. Comparative gill surface area analyses

Data

Gill surface area and body mass data for the 11 other shark species were compiled from previously published studies (Table 3.1). We conducted a literature search using Google Scholar and Web of Science with combinations of the following keywords: “shark,” “elasmobranch, “gill surface area,” “respiratory surface area,” “gill surface area allometry,” “respiratory surface area allometry,” “gill morphometrics,” and “gill dimensions.” Three species (Common Thresher Shark *Alopias vulpinus,* Shortfin Mako *Isurus oxyrinchus*, and Sandbar Shark *Carcharhinus plumbeus*) had more than one study reporting gill surface area and body mass data, and for these species, data were combined resulting in one dataset per species. Raw data were obtained from Wegner *et al.* (2010a) and Wootton *et al.* (2015) for four species (Pelagic Thresher *Alopias pelagicus,* Bigeye Thresher *Alopias superciliosus,* Common Thresher Shark*,* and Shortfin Mako). When raw gill surface area and body mass data were not available from the remaining studies, an image-digitizing software was used to extract these data points from published graphs (Plot Digitizer: http://plotdigitizer.sourceforge.net/). Including the Gray Smoothhound (Table 3.1), we know of sufficient data to estimate gill surface area allometric regressions for 12 shark species. In three other shark species for which published gill surface area data exist (Scalloped Hammerhead *Sphyrna lewini,* Blacktip Shark *Carcharhinus limbatus*, and Spiny Dogfish *Squalus acanthias;* Boylan & Lockwood 1962; Emery & Szczepanski 1985; Hata 1993), the sample sizes were too low (i.e., three or fewer individual estimates) to compute reliable regression coefficients. Rays (superorder Batoidea) were not included in this study as there are only three species that have published gill surface area data from more than a few individuals, and only one species where this data covers a range of body masses (Wegner 2016).

Estimation of regression coefficients

Both linear and nonlinear regression frameworks are commonly used to fit power-law relationships, such as those between body mass and morphological traits, e.g., gill surface area. Linear regression on log-transformed data applies a model with additive error on the transformed scale and multiplicative error when back-transformed to the original scale (White & Kearney 2014). In contrast, nonlinear regression applies a model with additive error on the untransformed or original scale (White & Kearney 2014). To estimate whether

a linear or non-linear regression was most appropriate for our particular dataset, we compared error structures of a linear regression on $\log_{10}$-transformed data and a nonlinear regression on raw data following Xiao *et al.* (2011). We concluded that the additive error structure on a transformed scale (i.e., using linear regression on $\log_{10}$-transformed data) provided a better fit to our comparative dataset (Burnham & Anderson 2002; AICc for linear regression = -73.2, AICc for nonlinear regression = 3550.4). Nonlinear regression was performed using the *nls* function in R and linear regressions were performed using the lm function (R Core Team 2016). All statistical analyses were performed in R v 3.2.2 (R Core Team 2016).

Comparison of coefficients across species

Allometric regressions estimate the intercept at 1 gram (g) of body mass, but for most species, particularly elasmobranchs, 1 g lies far outside the range of body masses of the actual specimens measured. Hence, intercepts and slopes are often correlated and centering the data can help reduce this correlation (Quinn & Keough 2002). We thus estimated a meaningful intercept of gill surface area at 5 000 g, which we termed the "standardized intercept". The body mass of 5 000 g was chosen as it is approximately the midpoint of the range of body masses for all shark specimens compared in this study and thus, the $\log_{10}$ of 5 000 g was subtracted from all individual body mass estimates for all species. To compare slopes and intercepts across species, the R-language pseudo-code, "$\log_{10}$(gill surface area) ~ $\log_{10}$(body mass) * species" was used, where the response variable was $\log_{10}$-transformed gill surface area and the explanatory variables were $\log_{10}$-transformed and centered body mass (i.e., centered around 5 000 g), species identity (as a factor), and the interaction term of $\log_{10}$-transformed and centered body mass and species. The inclusion of this interaction term allowed us to estimate standardized intercepts and slopes for each species. Species-specific coefficients were assessed to be significantly different if p <0.05. For further comparison, regression coefficients were bootstrapped to estimate the distribution of slopes and standardized intercepts for each species; this provided a better idea of the uncertainty for each coefficient. To do this, the coefficients and corresponding covariance for each species were extracted from the linear models, values were drawn from a multivariate normal distribution, and coefficients were bootstrapped 500 times.

Comparison of coefficients across ecological traits

Standardized intercepts and slopes of gill surface area allometries were compared across three ecological lifestyle traits: activity level, habitat type, and maximum body size (Table 3.1). These three traits were chosen based on data availability and their inclusion in studies examining differences in gill surface area with respect to ecological lifestyles. Due to data limitations in terms of not only gill surface area but also metabolic rate, swimming speed, ventilation strategy, etc., we were limited in our ability to assess other ecological lifestyle traits as well as how these traits act in concert to shape gill surface area.

We used caudal fin aspect ratio as a quantitative metric for activity level as this has been shown to relate to swimming speed (Thomson & Simanek 1977; Sambilay 1990), daily ration (Palomares & Pauly 1989), and metabolic rate (Killen *et al.* 2016; Campos *et al.* 2018). Caudal fin aspect ratio (*A*) was calculated for each species as $A = h^2/s$, where *h* is the height and *s* is the surface area of the caudal fin (Palomares & Pauly 1989, Sambilay 1990; Table 1). As fresh caudal fins are difficult to obtain, caudal fin aspect ratios are often calculated from anatomically correct drawings (Palomares & Pauly 1989; Sambilay 1990; Campos *et al.* 2018). Here, we calculated caudal fin aspect ratios using anatomically correct drawings published in *Sharks of the World* (Ebert *et al.* 2016). Although we recognize there are shortcomings with this approach (e.g. there is potential for modest changes to tail shape with growth; caudal fin morphology in the thresher sharks also represents specialization to aid in feeding), using caudal fin aspect ratio as a quantitative metric to infer activity level improves the rigor of analyses regarding the relationship of gill surface area and activity, as most previous gill surface area studies have only examined broad, descriptive categories of activity level (i.e. “sluggish,” “moderate activity”) based on the perceived activity of each species rather than a quantitative metric.

For each species, habitat type was assigned based on methodology in Dulvy *et al.* (2014), where species were categorized as coastal and continental shelf, pelagic, or deepwater, based on a species-specific depth distribution and to a lesser extent, position in the water column (Table 3.1). The 12 species examined in this study did not include any representatives from the deepwater habitat type, so only the two habitat types of (1) coastal and continental shelf and (2) pelagic were included. To simplify, we used the term “coastal” for the coastal and continental shelf habitat type and the term “oceanic” for the pelagic habitat type. The maximum body size (mass) for each species (not to be confused

with the largest individual for which gill surface was determined) was obtained from Fishbase (Table 3.1; Froese & Pauly 2000). As maximum body mass reported for the Gray Smoothhound was larger in Castro (2010), this estimate was used in favor of the Fishbase estimate. The body mass of the largest individual Nursehound, *Scyliorhinus stellaris*, specimen examined in Hughes *et al.* (1986) was greater than the maximum body mass reported for this species in Fishbase, so it was used in favor of the Fishbase estimate.

To assess if standardized intercepts and slopes differed with respect to ecological lifestyle traits, mixed-effects models were performed using the lme function in the nmle package (Pinheiro & Bates 2000). Separate models were performed for each ecological lifestyle trait following R-language pseudo-code, "log10(gill surface area) ~ log10(body mass) * ecological lifestyle trait + (body mass | species) ", where the response variable was log10-transformed gill surface area and the explanatory variables were the fixed effects of log10-transformed, centered body mass, the ecological lifestyle trait (e.g. caudal fin aspect ratio, habitat type, or maximum body size), and the interaction between the two. We also included a random effect of "(body mass | species)", which allowed a separate slope and standardized intercept to be estimated for each species, yet the effect of the ecological lifestyle trait on the coefficients was the same. Coefficients were assessed to be significantly different if $p < 0.05$.

3.4. Results

3.4.1. Gray Smoothhound gill surface area

Gill surface area for the eight Gray Smoothhounds examined in this study ranged from 1,103.68 to 4,762.70 cm^2 over the body mass range of 560 to 2,600 g. The standardized intercept, or gill surface area at 5,000 g, was 7,297.94 cm^2 and the slope of the relationship of gill surface area and body mass was 0.7840 (95 % CI = 0.4784 to 1.0896; Table 3.1, Fig. 3.1a). For purposes of comparison with previous studies, the allometric slopes for the gill dimensions of filament length, lamellar frequency, and lamellar bilateral surface area were 0.2567 (95% CI = 0.1396 to 0.3738), -0.1808 (95% CI = -0.2891 to -0.0724), and 0.6983 (95% CI = 0.4795 to 0.9171), respectively (Fig. 3.1b – 1d). Complete regression equations for gill surface area and associated dimensions are reported in Fig. 3.1a – 1d.

3.4.2. Comparison of coefficients across species

The standardized intercepts varied considerably across species and ranged from 4,724.98 cm^2 in the Nursehound to 35,694.39 cm^2 in the Bigeye Thresher, with a mean and standard error of 17,796.65 $\pm$ 2,948.61 cm^2 (Table 3.1, Fig. 3.2). The slopes of gill surface area allometries were fairly consistent across species with all species ranging between 0.7590 in the Shortfin Mako to 0.9555 in the Lesser Spotted Dogfish *Scyliorhinus canicula*, with a mean and standard error of 0.8512 $\pm$ 0.0193 (Table 3.1, Fig. 3.2).

3.4.3. Comparison of coefficients across ecological lifestyle traits

Standardized intercepts differed with respect to all three ecological lifestyle traits (Fig. 3.3 a, c, e). More active species with higher caudal fin aspect ratios had significantly greater gill surface area at 5,000 g than less active species ($t = 2.54$, $df = 10$, $p = 0.03$; Fig. 3.3a). Oceanic species exhibited a significantly greater gill surface area at 5,000 g than coastal species ($t = 4.36$, $df = 10$, $p = 0.001$; Fig. 3.3c). Lastly, larger-bodied species had significantly greater gill surface area at 5 000 g than smaller-bodied species ($t = 3.92$, $df = 124$, $p = 0.001$; Fig. 3.3e). Slopes of gill surface area allometries did not differ across the three ecological lifestyle traits assessed (Fig. 3.3 b, d, f). Specifically, slopes did not differ with respect to caudal fin aspect ratio ($t = 0.07$, $df = 125$, $p = 0.94$; Fig. 3.3b), habitat type ($t = -1.49$, $df = 125$, $p = 0.14$; Fig. 3.3d), or maximum body size ($t = -0.45$, $df = 124$, $p = 0.65$; Fig. 3.3f).

3.5. Discussion

Our results quantitatively confirm that gill surface area varies with ecological lifestyle traits. Specifically, we found that relative gill surface area (i.e., the gill surface area at a specified mass; here we used 5,000 g and termed this the standardized intercept) varied with activity level, habitat type, and maximum body size. Larger-bodied, oceanic, active species had greater relative gill surface area than smaller-bodied, coastal, less active species. However, the rate at which gill surface area scaled with body mass (i.e., slope) did not differ with the same ecological lifestyle traits. These results suggest that relative gill surface area, as opposed to the rate at which gill surface area scales with body mass, is influenced by the ecology and environment of a species. First, we compare the relative

gill surface area across shark species and ecological lifestyle traits, and then discuss these results in the context of other fishes. Second, we consider the consistency of slope values across species and ecological lifestyle traits and note exceptions among fishes. We then discuss the allometry of gill surface area of the species for which we made new measurements, the Gray Smoothhound. Finally, we highlight future questions to consider once more gill surface area data are available.

Relative gill surface area ranged about an order of magnitude across the 12 shark species. On average, we found that oceanic species had approximately 2.6 times greater relative gill surface area than coastal species, more active species had 1.3 times greater relative gill surface area than less active species, and larger-bodied species had 1.6 times greater relative gill surface area than smaller-bodied species. The Bigeye Thresher Shark had the largest relative gill surface area out of the 12 species examined. In addition to being an active and oceanic shark, this species also spends considerable time diving to depth where exposure to subsurface hypoxia may also provide selective pressure for increased gill surface area (Wootton *et al.* 2015). The Nursehound had the lowest relative gill surface area which reflects its less-active lifestyle, coastal and benthic habitat, and small maximum body size.

The order of magnitude difference in relative gill surface area observed in this study across the 12 shark species is considerably less than the two orders of magnitude range in relative gill surface area documented in teleost fishes (De Jager & Dekkers 1975; Palzenberger & Pohla 1992; Wegner 2011). This appears to partially reflect the more diverse ecological roles observed in teleost fishes. For example, the lowest relative gill surface areas for teleost fishes are found in “sluggish” freshwater or estuarine species that have developed facultative or even obligate air-breathing capacities, and thus are not solely dependent on the gills for respiration (Palzenberger & Pohla 1992; Graham 1997; Graham *et al.* 2007). In addition to differences in ecological radiations, fundamental differences in the gill morphology may also play a role in the more limited range of relative gill surface areas observed for sharks. Despite the similarity in ecological lifestyles between regionally endothermic teleosts (i.e., tunas) and regionally endothermic sharks (i.e., lamnid sharks) in terms of their high activity, oceanic habitat, and streamlined, fusiform body types, relative gill surface areas are two to three times greater in tunas compared to lamnid sharks (Muir & Hughes 1969; Wegner *et al.* 2010b). This apparent upper limit to elasmobranch gill surface area has been suggested to reflect constraints on

water flow imposed by the elasmobranch interbranchial septum that appear to affect lamellar spacing and ultimately, limit gill surface area (Wegner *et al.* 2010a; Wegner *et al.* 2012; Wegner 2016). Finally, the more limited range of gill surface areas observed in sharks compared to teleosts may also reflect the much smaller number of shark species for which gill surface area data have been acquired to date. The addition of gill surface area measurements for new elasmobranch species from more diverse habitats (e.g., freshwater and estuarine species) and activity levels, may increase the range of relative gill surface areas observed for this group.

The rate at which gill surface area scaled with body mass (slope) did not differ across shark species or ecological lifestyle traits examined in this study, and as such, were consistent across species that differed in activity level, habitat type, and maximum body size. The range of slopes observed in this study (0.76 to 0.96) was relatively small and fell within the 0.33 to over 1.00 range exhibited by freshwater and marine teleost fishes (De Jager & Dekkers 1975; Palzenberger & Pohla 1992; Wegner 2011). It has long been noted that the slope of the gill surface area and body mass relationship mirrors that of the scaling relationship of metabolic rate and body mass (Hughes & Morgan 1973; Palzenberger & Pohla 1992; Wegner 2011). Accordingly, the mean slope of the relationship of gill surface area and body mass determined in this study (0.85 ± 0.02) is strikingly close to the mean slope of the scaling relationship of metabolic rate (0.84 ± 0.05), which was estimated for a limited number of elasmobranchs with metabolic rate data (six total: four batoids and two sharks; Wegner 2016). This similarity in the allometry of metabolic rate and that of gill surface area is consistent with the idea that gill surface area and oxygen diffusion capacity (i.e. rate of gas transfer across the respiratory surface per unit of gas partial pressure) have evolved to match metabolic demand (Wegner 2011; Gillooly *et al.* 2016; Lefevre *et al.* 2017). Alternatively, it has been suggested that this intimate scaling relationship may reflect a constraint of metabolic rate based on geometric constraints of gill surface area growth within the space-limited opercular / parabranchial cavities (Pauly 2010; Pauly & Cheung 2018), although this hypothesis has been highly contested (see Lefevre *et al.* 2017).

While our results did not show any relationship between the ecological lifestyle traits examined and the slope of the gill surface area allometries for the 12 sharks in this study, there are clear examples from the teleost literature in which the slope does appear to be affected by other underlying physiological and ecological stressors. For example, the

blackfin icefish *Chaenocephalus aceratus* (a hemoglobin-lacking species) has a high gill surface area allometric slope of 1.09, which is thought to reflect the need for a disproportionately large respiratory surface area to help mitigate the effects of a greatly reduced blood-oxygen carrying capacity which becomes increasingly problematic with growth (Holeton 1976; Nilsson 2010). On the other end of the spectrum, low gill surface area allometric slope values of less than 0.33 have been observed in some air-breathing fishes that reflect their increased capacity for breathing air and thus reduced reliance on the gills for oxygen uptake as they grow (Hakim *et al.* 1987; Santos *et al.* 1994; Perna & Fernandes 1996). Thus, while the narrow bounds of the gill surface area allometric slope that we found in this study as well as those seen in other studies are likely explained by the relationship between gill surface area and metabolic rate, there are clear exceptions.

Gill surface area data determined in this study for the Gray Smoothhound were similar to those of the Nursehound and Lesser Spotted Dogfish from the literature (Hughes 1972; Hughes *et al.* 1986). Despite the broad ecological similarity of these three species being coastal, smaller-bodied, and less active, the Gray Smoothhound had the highest estimated activity level based on caudal fin aspect ratio, as well as the largest maximum body size. While the Gray Smoothhound had 1.5 times greater relative gill surface area than the Nursehound, its relative gill surface area was 0.77 times lower than that of the Lesser Spotted Dogfish. Gill surface area data for the Lesser Spotted Dogfish were from a more limited size range than for both the Gray Smoothhound and the Nursehound, and this may have affected the estimates of regression coefficients (Hughes 1972; Hughes *et al.* 1986). For many species examined in this and other gill surface area allometry studies, the sample sizes are small and the body mass ranges do not fully represent the size range of the species. Future work should thus focus not only on adding additional species that have diverse ecological lifestyles but also ideally incorporate gill surface area measurements for the entire size range of the species to provide the most accurate comparative data possible.

Overall, our findings indicate that ecological lifestyle differences among species are reflected in the relationships of gill surface area and body mass in sharks. Specifically, we found that activity level, habitat type, and maximum body size may all act to help shape gill surface area. However, such ecological and environmental influences appear to primarily affect the gill surface area at a given body mass (intercept), rather than the rate at which gill surface area scales with body mass (slope). The rate at which gill surface

area scaled with body mass was narrowly-bounded in the 12 shark species examined likely reflecting its tight relationship with metabolic rate. Due to the nature of only having 12 species with sufficient gill surface area data, we were limited in our ability to test other hypotheses and ask additional questions. For example, we could not tease apart the influence of ecological lifestyle and evolutionary relatedness on gill surface area. Phylogenetic analyses are needed to examine if any of the differences in the relative gill surface area or lack of differences in the rate at which gill surface area increases with body mass are related to shared evolutionary history, but such analyses will only be meaningful once more gill surface area data are available from additional species. Additional gill surface area data, including from more ecologically diverse shark and batoids species (e.g., those inhabiting estuarine environments, or additional species dwelling in chronic hypoxia) as well as larger body size ranges within species, should allow for a more thorough understanding of how elasmobranch gill surface area allometries relate to other fish groups. Additionally, these data could inform how ecological lifestyle traits act in concert to shape gill surface area.

3.6. Tables

Table 3.1 Gill surface area allometric regression coefficients and three ecological lifestyle traits (caudal fin aspect ratio, habitat type, maximum body mass) for 12 shark species.

Species	Common name	Standardized intercept	Slope	Caudal fin aspect ratio	Habitat type	Max. body mass (kg)	Source for gill area data
Alopias superciliosus	Bigeye Thresher	35,694.39	0.8061	4.67	oceanic	363.8	Wootton et al. 2015
Carcharodon carcharias	White Shark	30,040.00	0.7715	3.12	oceanic	2,080.4	Emery and Szczepanski 1985
Isurus oxyrinchus	Shortfin Mako	29,248.26	0.7590	2.52	oceanic	505.8	Emery and Szczepanski 1985, Wegner et al. 2010a
Alopias pelagicus	Pelagic Thresher	24,547.09	0.8946	5.63	oceanic	127.7	Wootton et al. 2015
Galeocerdo cuvier	Tiger Shark	20,141.88	0.9136	3.19	oceanic	807.4	Hata 1993
Alopias vulpinus	Common Thresher Shark	19,404.39	0.8918	5.54	oceanic	348.0	Emery and Szczepanski 1985, Wootton et al 2015
Carcharhinus obscurus	Dusky Shark	12,336.73	0.8761	3.18	coastal	346.5	Emery and Szczepanski 1985
Carcharhinus plumbeus	Sandbar Shark	11,040.79	0.9012	3.17	coastal	117.9	Emery and Szczepanski 1985, Hata 1993
Prionace glauca	Blue Shark	9,667.184	0.8820	3.48	oceanic	205.9	Emery and Szczepanski 1985
Scyliorhinus canicula	Lesser Spotted Dogfish	9,423.24	0.9555	1.63	coastal	1.3	Hughes 1972
Mustelus californicus	Gray Smoothhound	7,297.94	0.7840	2.14	coastal	4.8	This Study
Scyliorhinus stellaris	Nursehound	4,724.98	0.7783	1.63*	coastal	2.6	Hughes et al. 1986

Coefficients were re-estimated from $\log_{10}$-transformed gill surface area and $\log_{10}$-transformed and centered body mass data. Intercepts are back-transformed and represent the gill surface area (cm^2) at 5,000g.

*The caudal fin aspect ratio for S. canicula was used for S. stellaris

3.7. Figures

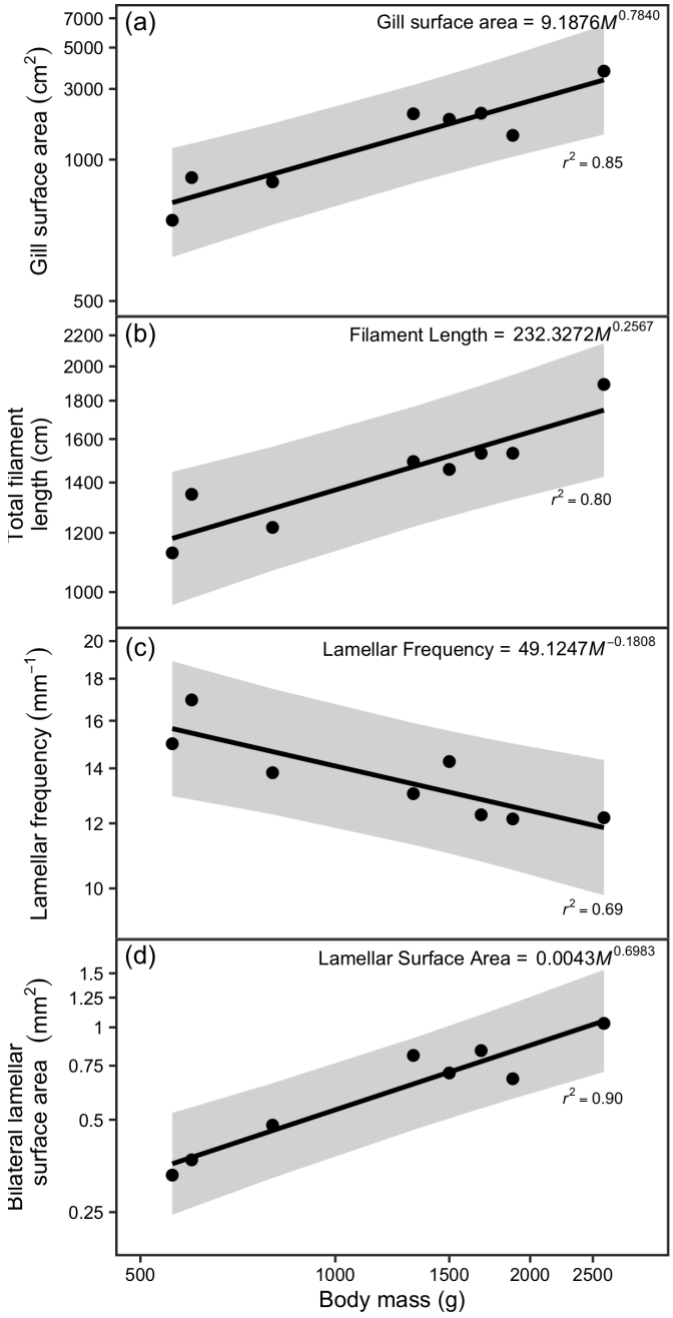

Figure 3.1 The relationship of (a) gill surface area (cm^2), (b) total filament length (cm), (c) average lamellar frequency (mm^{-1}), and (d) mean bilateral lamellar surface area (mm^2) and body mass (g) for eight Gray Smoothhounds, *Mustelus californicus*.

The fitted regression lines and equations are from linear models of log_{10}-transformed gill surface area (and components) data as functions of log_{10}-transformed body mass. Shaded grey region indicates the 95% prediction interval.

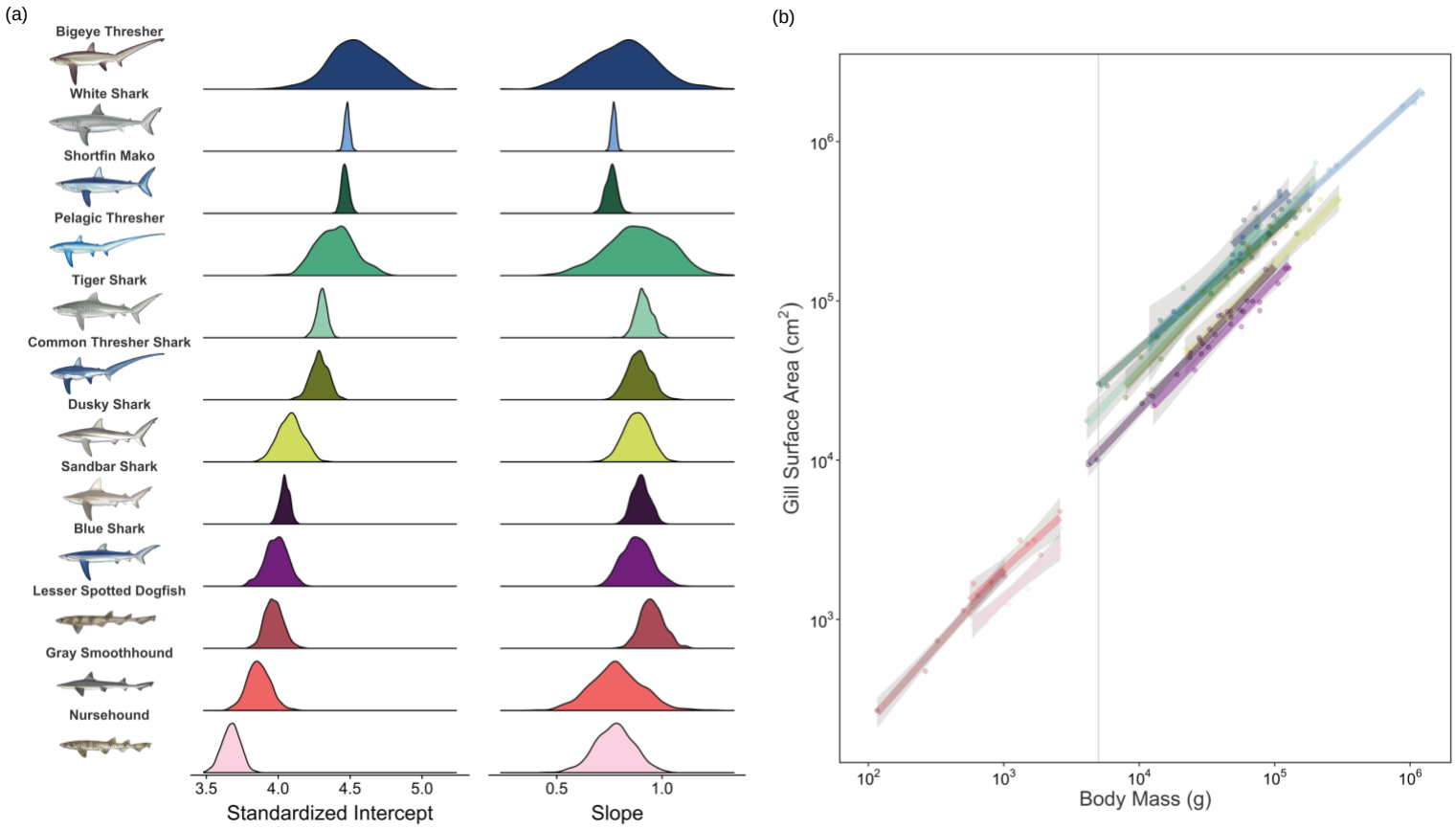

Figure 3.2 The distribution of regression coefficients and gill surface area allometries for 12 shark species showing highly variable standardized intercepts (i.e. gill surface area at 5,000 g) yet consistent slopes.
(a) The distribution of regression coefficients for the allometry of gill surface area in 12 shark species, as estimated by bootstrapping standardized intercepts and slopes from species-specific linear regressions computed with log_{10}-transformed gill surface area and log_{10}-transformed and centered body mass data at 5,000 g. (b) The relationship of gill surface area (cm^2) and body mass (g) for 12 species of sharks. The fitted regression lines are from a linear model of log_{10}-transformed gill surface area as a function of log_{10}-transformed and centered body mass for each species. The vertical grey line represents a body mass of 5,000 g. The shaded grey region indicates the 95% confidence interval.

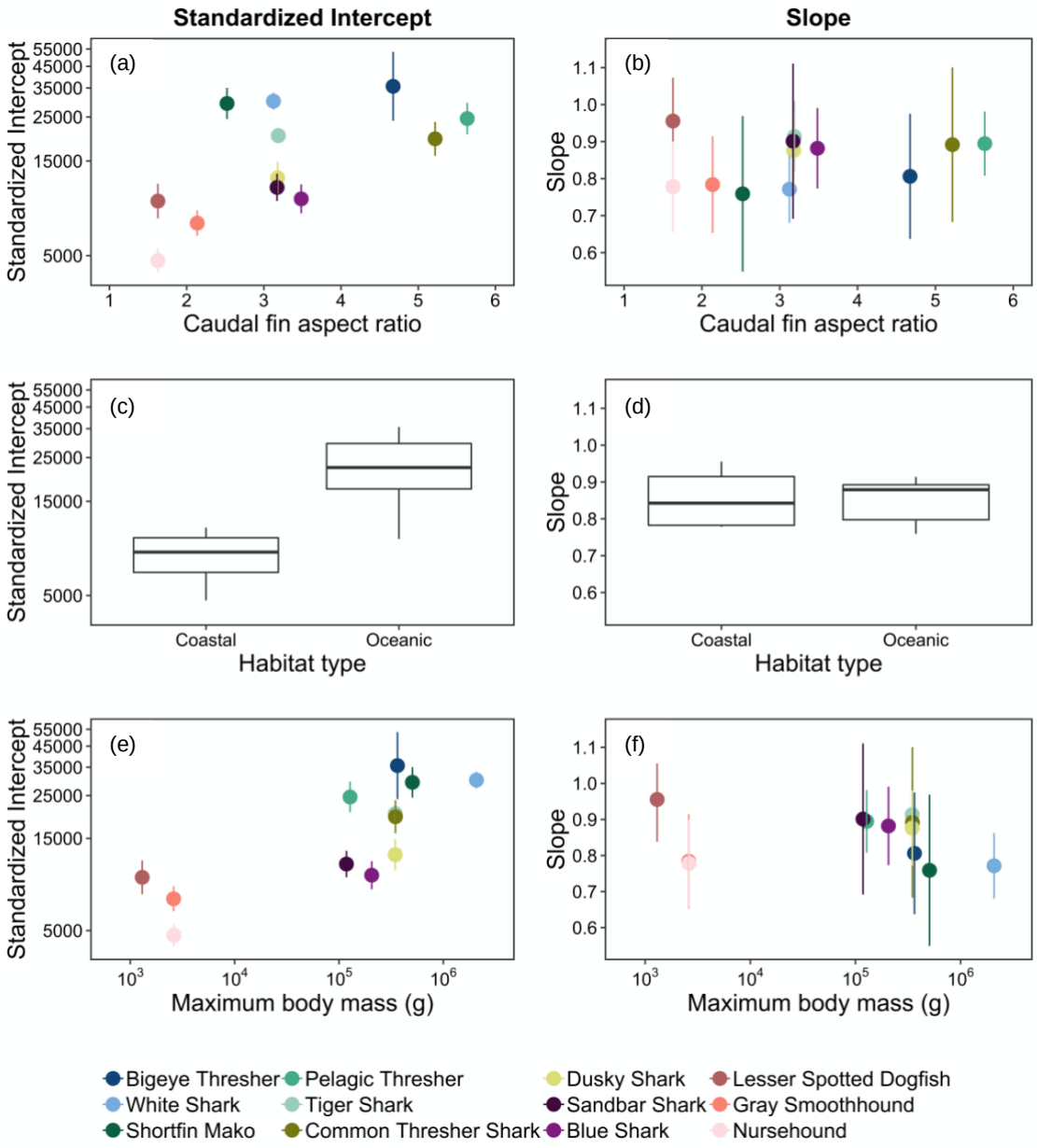

Figure 3.3 Gill surface area allometric standardized intercepts (a, c, e) and slopes (b, d, f) for 12 shark species in relation to three ecological lifestyle traits: caudal fin aspect ratio as a measure of activity level, habitat type, and maximum body mass.

3.8. References

Boylan, J. W. & Lockwood, M. (1962). Urea and thiourea excretion by dogfish kidney and gill: Effect of temperature. *Bull. Mt. Desert. Isl. Biol. Lab., 4*, 25.

Burnham, K. P. & Anderson, D. R. (2002). *Model selection and multimodel inference*. New York. NY: Springer.

Campos, D. F., Val, A. L., & Almeida-Val, V. M. F. (2018). The influence of lifestyle and swimming behavior on metabolic rate and thermal tolerance of twelve Amazon forest stream fish species. *J. Therm. Biol.*, *72*, 148-154.

Castro, J. I. (2010). *The Sharks of North America*. Oxford University Press.

De Jager, S. & Dekkers, W. (1975). Relation between gill structure and activity in fish. *Neth. J. Zool.*, *25*, 276–308.

Dulvy, N. K., Fowler, S. L., Musick, J. A., Cavanagh, R. D., Kyne, P. M., Harrison, L. R., Carlson, J. K., Davidson, L. N. K., Fordham, S. V., Francis, M. P., Pollock, C. M., Simpfendorfer, C. A., Burgress, G. H., Carpenter, K. E., Compagno, L. J. V., Ebert, D. A., Gibson, G., Heupel, M. R., Livingstone, S. R., Sanciangco, J. C., Stevens, J. D., Valenti, S., & White, W. T. (2014). Extinction risk and conservation of the world 's sharks and rays. *eLife*, 1–35.

Ebert, D. A., Fowler, S. L., & Compagno, L. J. V. (2016). *Sharks of the World: A Fully Illustrated Guide*. Wild Nature Press.

Emery, S. H. & Szczepanski, A. (1986). Gill dimensions in pelagic elasmobranch fishes. *Biol. Bull.*, *171*, 441.

Froese, R. & Pauly, D., Eds. (2000). *FishBase 2000: concepts, design and data sources.* ICLARM, Los Baños, Laguna, Philippines. 344 p.

Gillooly, J. F., Gomez, J. P., Mavrodiev, E. V., Rong, Y., & McLamore, E. S. (2016). Body mass scaling of passive oxygen diffusion in endotherms and ectotherms. *Proc. Nat. Acad. Sci. U.S.A*, *113*, 5340-5345.

Graham, J. B. (1997). *Air-Breathing Fishes*. Academic Press, San Diego.

Graham, J. B., Lee, H. L., & Wegner, N. C. (2007). Transition from water to land in an extant group of fishes: Air breathing and the acquisition sequence of adaptations for amphibious life in oxudercine gobies. In M. N. Fernandes et al. (Eds). *Fish Respiration and Environment* (p. 255-288) Science Publishers: Enfield.

Gray, I. E. (1954). Comparative study of the gill area of marine fishes. *Biol. Bull.*, *107*, 219–255.

Hakim, A., Munshi, J. S. D., & Hughes, G. M. (1978). Morphometrics of the respiratory organs of the Indian green snake-headed fish, *Channa punctata*. *J. Zool., 184*, 519-43.

Hata, D. (1993). Gill surface area in relation to growth rates and maximum size in sharks. *PhD dissertation*. Virginia Institute of Marine Science.

Heinicke M. P., Naylor, G. J. P., & Hedges, S. B. (2009). Cartilaginous fishes (Chondrichthyes). In: Hedges, S. B. & Kumar, H. D. (Eds.), The timetree of life. Oxford, pp. 320-327.

Holeton, G. F. (1976). Respiratory morphometrics of white and red blooded Antarctic fish. *Comp. Biochem. Phys. A, 54A*, 215-220.

Hughes, G. M. (1966). The dimensions of fish gills in relation to their function. *J. Exp. Biol.*, *45*, 177–195.

Hughes G. M. (1970). Morphological measurements on the gills of fishes in relation to their respiratory function. *Folia Morph.*, *18,* 78–95.

Hughes G. M. (1972). Morphometrics of fish gills. *Respir. Physiol.14*: 1–25.

Hughes, G. M. (1984a). General anatomy of the gills. In Fish Physiology Vol. 9A (eds. Hoar, W.S., Randall, D.J.) Academic Press: Orlando. pp. 1-72.

Hughes, G. M. (1984b). Scaling of respiratory areas in relation to oxygen consumption of vertebrates. *Experientia, 40*, 519-524.

Hughes, G. M. (1984c). Measurement of gill area in fishes: practices and problems. *J. Mar. Biol. Assoc. U. K.,* 64, 637–655.

Hughes, G. M. & Morgan, M. (1973). The structure of fish gills in relation to their respiratory function. *Biol. Rev.*, *48*, 419–475.

Hughes G. M., Perry S. F., & Piiper J. (1986). Morphometry of the gill of the elasmobranch *Scyliorhinus stellaris* in relation to body size. *J. Exp. Biol., 121*, 27–42

Killen, S .S., Glazier, D. S., Rezende, E. L., Clark, T. D., Atkinson, D., Willener, A. S. T., & Halsey, L. G. (2016). Ecological influences and morphological correlates of resting and maximal metabolic rates across teleost fish species. *Am. Nat.*, *187,* 592–606.

Lefevre, S., McKenzie, D. J., & Nilsson, G. E. (2017). Models projecting the fate of fish populations under climate change need to be based on valid physiological mechanisms. *Glob. Chang. Biol.*, *23*, 3449-3459.

Muir, B. S. & Hughes, G. M. (1969). Gill dimensions for three species of tunny. *J. Exp. Biol., 51,* 271–285.

Nilsson, G. E. (2010). Respiratory physiology of vertebrates: life with and without oxygen. Cambridge University Press, pp. 334.

Palomares, M. L. & Pauly, D. (1989). A multiple regression model for prediction the food consumption of marine fish populations. *Mar. Freshwater Res.*, *40*, 259-273.

Palzenberger, M. & Pohla, H. (1992). Gill surface area of water-breathmg freshwater fish. *Rev. Fish Biol. Fish.*, *2*, 187–216.

Pauly, D. (2010). Gasping Fish and Panting Squids: Oxygen. Temperature and the Growth of Water-Breathing Animals (International Ecology Institute, 2010).

Pauly, D. & Cheung, W. W. (2018). Sound physiological knowledge and principles in modeling shrinking of fishes under climate change. *Glob. Chang. Biol.*, *24*(1).

Perna, S. A. & Fernandes, M. N. (1996). Gill morphometry of the facultative air-breathing loricariid fish, *Hypostomus plecostomus* (Walbaum) with, special emphasis on aquatic respiration. *Fish Physiol. Biochem.*, *15*, 213-220.

Pinheiro, J. C. & Bates, D. M. (2000) *Mixed-Effects Models in S and S-PLUS*, Springer.

Quinn, G. P. & Keough, M. J. (2002). *Experimental design and data analysis for biologists*. Cambridge University Press.

R Core Team (2016). R: A language and environment for statistical computing. R Foundation for Statistical Computing, Vienna, Austria. URL: https://www.R-project.org/.

Sambilay Jr, V. C. (1990). Interrelationships between swimming speed, caudal fin aspect ratio and body length of fishes. *Fishbyte*, *8*, 16-20.

Santos, C. T. C., Fernandes, M. N., & Severi, W. (1994). Respiratory gill surface area of a facultative air-breathing loricariid fish, *Rhinelepis strigosa. Can. J. Zool., 72*, 2009-2013.

Satora, L. & Wegner, N. C. (2012). Reexamination of the Byczkowska-Smyk gill surface area data for European teleosts, with new measurements on the pikeperch, *Sander lucioperca*. *Rev. Fish Biol. Fish.*, *22*, 1–9.

Stein R. W., Mull, C. G. M., Kuhn, T. S., Aschilman, N. C., Davidson, L. N. K., Joy, J. B., Smith, G. J., Dulvy, N. K., & Mooers, A. O. (2018). Global priorities for conserving the evolutionary history of sharks, rays, and chimaeras. *Nat. Ecol. Evol., 2*, 288–298.

Thomson, K. S. & Simanek, D. E. (1977). Body form and locomotion in sharks. *Am. Zool.*, *17*, 343-354.

Wegner, N. C. (2011). Gill Respiratory Morphometrics. In Farrell, A. P. (Ed.), *Encyclopedia of Fish Physiology: From Genome to Environment* (Vol. 2, pp. 803–811). San Diego, CA: Academic Press.

Wegner, N.C. (2016). Elasmobranch Gill Structure. In Shadwick, R. E., Farrell, A.P., & Brauner, C.J. (Eds.), *Physiology of Elasmobranch Fishes: Structure and Interaction with Environment* (Vol. 34, pp. 102-145). Elsevier Inc.

Wegner, N.C., Lai, N. C., Bull, K. B., & Graham, J. B. (2012). Oxygen utilization and the branchial pressure gradient during ram ventialtion of the shortfin mako, *Isurus oxyrinchus:* is lamnid shark-tuna convergence constrained by elasmobranch gill morphology? *J. Exp. Biol.*, *215*, 22-28.

Wegner, N. C., Sepulveda, C. A., Olson, K. R., Hyndman, K. A., & Graham, J. B. (2010a). Functional morphology of the gills of the shortfin mako, *Isurus oxyrinchus*, a lamnid shark. *J. Morph.*, *271*, 937–948.

Wegner, N. C., Sepulveda, C. A., Bull, K. B., & Graham, J. B. (2010b). Gill morphometrics in relation to gas transfer and ram ventilation in high-energy demand teleosts: scombrids and billfishes. *J. Morph.*, *271*, 36-49.

White, C. R. & Kearney, M. R. (2014). Metabolic scaling in animals: methods, empirical results, and theoretical explanations. *Compr. Physiol.*, *4*, 231–256.

Wilson, J. M. & Laurent, P. (2002). Fish gill morphology: inside out. *J. Exp. Zool.*, *293*, 192–213.

Wootton, T. P., Sepulveda, C. A., & Wegner, N. C. (2015). Gill morphometrics of the thresher sharks (Genus Alopias): Correlation of gill dimensions with aerobic demand and environmental oxygen. *J. Morph.*, *276*, 589-600.

Xiao, X., White, E., Hooten, M., & Durham, S. (2011). On the use of log-transformation vs. nonlinear regression for analyzing biological power-laws. *Ecol.*, *92,* 1887-1894.

Chapter 4.

Forty years of gill surface area and growth performance across fishes[3]

4.1. Abstract

Life history theory dictates that an organism's maximum size and its corresponding somatic growth rate have evolved to maximize lifetime reproductive output. An intriguing theory suggests that in aquatic organisms, maximum size is constrained by the surface area of the gills, which largely control oxygen uptake. A central prediction of this theory is the tight relationship between the von Bertalanffy growth model (i.e., asymptotic size and growth coefficient) and gill surface area. Since first tested in the 1980s, however, the data and analytical methods initially used to identify these relationships have greatly advanced over the past 40 years. Here, we revisit the relationship of maximum size, growth, and gill surface area in fishes, structuring our investigation around six questions that examine limitations in the original analysis and leverage the availability of more data and advanced statistical techniques. Overall, we find that a weak relationship exists among asymptotic size, growth coefficient, and gill surface area across 132 species of fishes. Further, we found that the activity level of a fish statistically explained more variation in asymptotic size and growth coefficient across species compared to gill surface area. Additionally, we found little evidence that gill surface area is related to the variation in growth coefficients across species, especially for those who reach the same asymptotic size. Our results support the idea that in fishes, growth and maximum size is not simply related to gill surface area, and the importance of other covariates—both tractable (e.g., activity, temperature) and less tractable (e.g., predation risk, resource availability and variation)—may explain more variation in the life history traits across species.

[3] A version of this chapter is submitted to *Fish and Fisheries* as: Bigman, J.S., Wegner, N.C., & Dulvy, N.K. Forty years of gill surface area and growth across fishes.

4.2. Introduction

Formalized as life history theory, decades of work have revealed that body size, and other life history traits related to growth, survival, and reproduction, are optimized by natural selection to maximize fitness (typically measured by reproductive output in fishes; Beverton & Holt 1959; Stearns 1992; Hutchings 2002). Maximizing fitness results in tradeoffs between traits as competing processes, such as growth and reproduction, draw from the same finite pool of internal resources (e.g., time, energy; Roff 1984; Stearns 1989, Reynolds 2003). One of the classic tradeoffs between life history traits is the inverse relationship observed between maximum size (i.e., the observed maximum size of a species) and the change in body size over time, or somatic growth (Beverton & Holt 1959; Reynolds *et al.* 2001). For fishes, this inverse relationship is evident when comparing the growth parameters (growth coefficient and asymptotic size) estimated from a von Bertalanffy growth function fit to size-at-age data (Fig. 4.1; Pauly 1998). Such a comparison suggests that an individual generally can grow faster to a smaller asymptotic (final) size or grow more slowly to a larger asymptotic size (Beverton & Holt 1959). With respect to maximum size and growth trade-offs, life history theory predicts that under high mortality (e.g., in an unstable environment or under high predation risk) fitness would be maximized through a faster life history strategy, one that results in a higher reproductive output earlier in life, which would select for a smaller maximum size, faster growth, and earlier maturity (Stearns 1976; Roff 1984; Reznick *et al.* 1996). On the other hand, under low mortality (e.g., a stable environment or one with lower predation risk) fitness would be maximized through a slower life history strategy by waiting to reproduce until an organism reaches a larger size (as reproductive output increases with increasing size; Bjørkvoll *et al.* 2012; Barneche *et al*. 2018). This would select for a larger maximum size, slower growth, and later maturity (Stearns 1976; Roff 1984). While life history theory and its predictions have been widely supported by both theoretical and empirical research over the last 70 years, recent work on the effect of oxygen (i.e., balance of supply and demand) and temperature on body size and growth, especially for fishes, has inspired the proposal of a new causal mechanism that shapes body size (Pauly 2010; Forster *et al.* 2012; Cheung *et al.* 2013).

One multifaceted and intriguing theory proposes that the maximum size of aquatic, water-breathing organisms is mechanistically constrained by oxygen supply (Pauly 2010, 2021).

The central tenet of this theory, the Gill Oxygen Limitation Theory, is that the oxygen supply acquired over the surface area of the gills—which is (to a first approximation) a two-dimensional surface—cannot keep pace with the demand from a continually increasing three-dimensional volume (body mass). The proposed consequence of this mismatch in geometry is that the ontogenetic slope of the relationship of gill surface area and body mass will always be less than one (i.e., hypoallometric). This means that the ratio of gill surface area to body mass (i.e., mass-specific gill surface area) will decrease with increasing body mass. Thus, when the supply of oxygen diffused over the 'diminishing' gill surface area cannot match the demand from the growing body, the organism will stop growing and its maximum size will be reached (Pauly 2010, 2021).

A central prediction of the Gill Oxygen Limitation Theory is that a tight correlation would exist among maximum size, growth, and gill surface area (Pauly 1981, 2010). Specifically, Pauly (1981, 2010) predicted that gill area index (a measure of the amount of gill surface area for a given body size) and growth performance (an index that integrates the tradeoff between the von Bertalanffy growth coefficient and asymptotic size) would be tightly correlated. Further, it was suggested that the large amount of variation in von Bertalanffy growth coefficients both within and across species was related to gill surface area, such that an individual or a species can only grow fast to its asymptotic size if it has a larger than expected gill surface area for its body size (Pauly 1981, 2010). Although only a weak relationship between gill area index and growth performance existed in the original 42 fish species examined by Pauly (1981), this relationship has been used as evidence that gill surface area constrains growth and maximum (or asymptotic) size in fishes (Pauly 1981, 2010, 2021; Cheung *et al.* 2013; Cheung & Pauly 2016). Indeed, half of the expected 14 – 24% decline in maximum size for an individual fish (over generations) due to projected temperature increases through 2050 has been suggested to be mechanistically linked to oxygen limitation, or the mismatch between oxygen supply (gill surface area) and demand (metabolic rate; Pauly 1981, 2010; Cheung *et al*. 2013).

However, there is much debate surrounding the causal mechanisms underlying oxygen limitation, particularly with respect to gill surface area, growth, and the Gill Oxygen Limitation Theory (Lefevre *et al.* 2017, 2018; Marshall & White 2019). For example, many argue that the surface area of respiratory organs would evolve to provide the capacity needed to meet an organism's requirements, instead of (aerobic) metabolic rate being driven by, and ultimately, limited by the surface area of the gills (Lefevre *et al.* 2017, 2018;

Marshall & White 2019). Relatedly, physiologists have noted that the surface area of gills are folded surfaces and thus are not under the same strict geometric constraints as seen in spherical objects (i.e., the scaling of gill surface area and body mass could deviate from surface area-to-volume ratios; Lefevre et al. 2017, 2021). Notwithstanding these criticisms, the Gill Oxygen Limitation Theory has potentially far-reaching consequences if empirically supported. In addition to the idea that oxygen limitation and gill surface area may be behind the observed declines in maximum size in response to increasing temperature (temperature size rule), mounting evidence from broad, cross-species studies suggests that oxygen limitation may also shape species' geographic distributions and underlie the mass- and temperature-dependence of metabolic rate (Forster *et al.* 2012; Deutsch *et al*. 2020; Rubalcaba *et al*. 2020; Bigman *et al.* 2021).

To understand if oxygen limitation mediated by gill surface area is indeed occurring, and affecting growth and maximum size, predictions generated by the Gill Oxygen Limitation Theory must be tested. Yet, few predictions have been tested to-date, including the generality of the relationship among maximum size, growth, and gill surface area. Additionally, the last 40 years have seen an increase in the availability of gill surface area data and von Bertalanffy growth parameters, as well as the advancement of statistical techniques that can incorporate additional salient factors, such as phylogenetic relationships among species.

Here, we revisit the interrelationships of maximum size, growth, and gill surface area in fishes. Specifically, we ask six questions that examine limitations in the original relationship and leverage the availability of more data and advanced statistical techniques to examine these relationships in more detail (Table 4.1). For each question, we outline the relevant background, detail the data and analysis used, and present and interpret the results.

In Act I, we reconsider Pauly's (1981) original dataset (hereafter, 'Pauly dataset') of gill area index and growth performance to ask:

i. What constitutes an outlier and how sensitive is the relationship of gill area index and growth performance to outliers?

ii. What is the effect of parameterizing the relationship between gill area index and growth performance based on the predictions made by the Gill Oxygen Limitation Theory (i.e., testing if gill area index can explain variation in growth performance)?

In Act II, we build from the Pauly dataset and collate gill surface area (and associated body mass) and life history data for additional fish species (teleost, elasmobranch, and coelacanth) to ask if the relationship of maximum size, growth, and gill surface area holds across more species. Specifically, using this larger dataset, we ask:

i. Does employing more realistic metrics of gill surface area (i.e., the ontogenetic regression coefficients instead of a simplified index) provide new insight into the relationship of gill surface area and growth performance?

ii. Is evolutionary history an important factor in determining how gill surface area and growth performance are related?

iii. Does activity level better characterize the variation in growth performance across species compared to gill surface area?

iv. Do species with faster growth coefficients for their body size have larger gills?

4.3. Act I: Re-examining Pauly (1981)'s analysis

I.i. Question

In the Pauly dataset, what constitutes an outlier and how sensitive is the relationship of gill area index and growth performance to outliers?

I.i. Premise

When first examining whether a relationship existed between gill area index and growth performance, Pauly (1981) identified a compilation of both raw and mean gill surface area and (measurement) body mass for 115 fish species (teleost, elasmobranch, and coelacanth) compiled from other studies and published by Hughes & Morgan (1973). This dataset was chosen by Pauly (1981) for specific reasons: (1) it included a large number of fish species, (2) the authors (Hughes & Morgan) had checked and standardized the

data presented in a large number of publications, and (3) the use of a single data source for analysis by Pauly (1981) was thought to prevent bias. Pauly (1981) subsequently chose to only include marine species to reduce the effects of habitat heterogeneity. Of the 66 marine fish species in this dataset, 42 had published von Bertalanffy growth parameters (Pauly 1981). However, Pauly (1981) suspected that the gill surface area data for two species, West Indian Ocean Coelacanth *Latimeria chalumnae* and Atlantic Cutlassfish *Trichiurus lepturus*, were either erroneous or to reflect a specific feature of the species and were removed from further analysis.

For each species, Pauly (1981) calculated gill area index and growth performance. Gill area index is somewhat similar to the intercept of the ontogenetic relationship of gill surface area and body mass (the predicted gill surface area for a given body size resulting from a regression equation; Pauly 1981, 2010). However, gill area index is not estimated from a regression relationship but calculated as G/W^d, where G = one estimate of a species-specific mean gill surface area, W = mean body mass estimate associated with the mean gill surface area estimate, and d = the species-specific ontogenetic slope of the relationship between body mass and gill surface area (Pauly 1981, 2010). Here, the G and W are the mean of gill surface area and body mass measurements, respectively, from a (random) sample of fishes for which gill surface area was measured for one study. The parameter d must be included (which is why Pauly did so) because gill surface area usually scales hypoallometrically with body mass, such that the ratio of gill surface area to body mass for a single individual changes throughout its lifetime (De Jager & Dekkers 1975; Palzenberger & Polha 1992; Wegner 2011; Bigman *et al*. 2018). However, an empirical estimation of d requires raw gill surface area and body mass data for a number of individuals for a given species (ideally spanning the entire body size range). Due to the lack of raw data for all species, Pauly (1981) predicted the parameter d for each species from a previously estimated linear relationship between the ontogenetic slope of a relationship between body mass and gill surface area or metabolic rate and maximum observed body mass (W_{max}) for 27 species or genera of fishes, as well as average values of d for (1) “all freshwater fishes”, (2) “all marine fishes”, (3) two different average values for “fishes”, and (4) “Gray’s intermediates [various marine teleosteans]” (see pg. 264 in Pauly 1981). Growth performance is calculated as $\log_{10}(k * W_\infty)$, where k is the growth coefficient and W_∞ is asymptotic size, both estimated using the von Bertalanffy growth function (Pauly 1981, 1991; Juan-Jordá *et al.* 2013). If multiple growth functions were

available for a given species (and thus a given species had multiple values of k and W_∞), a single growth function was chosen based on sample size and data quality (D. Pauly pers. comm. August 2020).

To estimate the relationship between gill area index area and growth performance, Pauly (1981) estimated a Reduced Major Axis regression (also called a 'functional regression' or 'geometric mean functional regression') on $\log_{10}$-transformed gill area index (on the y-axis) and growth performance (already $\log_{10}$-transformed by nature of the calculation; on the x-axis) for 40 species of fish (Pauly 1981). He reported that there was a significant correlation between gill area index and growth performance, with a r = 0.431 (equivalent to an r^2 of 0.19) and a p = 0.01 (i.e., the slope does not equal zero; Pauly 1981). Three additional apparent outliers were then removed from the analysis and it was reported that the removal of these outliers "greatly improves the correlation, which increases to r = 0.661 [equivalent to an r^2 value of 0.44] (with 35 degrees of freedom)" (Pauly 1981).

Here we ask what constitutes an outlier and how sensitive is the relationship of gill area index and growth performance to outliers?

I.i. Method

A statistical outlier can be defined as an outlying or extreme observation, one that appears to deviate markedly from other members of the sample or fall unusually far from the expected value based on the model (Gelman & Hill 2007; Fahrmeir *et al.* 2013). Although checking for outliers is common practice, standardized methods across fields to identify and deal with outliers are rare (Hampel 2001; Burnham & Anderson 2002; Fahrmeir *et al.* 2013). Historically, outliers have often been removed from datasets to facilitate modeling by Ordinary Least Squares (OLS) regression methods or similar (e.g., Reduced Major Axis regression), but because there is often no way to non-arbitrarily remove outliers, it is more commonly recommended to instead refine the model to accommodate outliers (Hampel 2001; Kruschke 2014). One way of identifying outliers is to use model diagnostics such as Cook's distance for frequentist models and Pareto k for Bayesian models (Fahrmeir *et al.* 2013; Vehtari *et al.* 2017; Gabry *et al.* 2019). If a data point's Cook's distance or Pareto k value is above the threshold (0.5 for Cook's distance, 0.7 for Pareto k), it is recommended to employ robust regression – a category of regression models that relax the assumption of normality that is characteristic of the most common OLS regression models, (e.g.,

Gelman & Hill 2007; Kruschke 2014; Vehtari *et al.* 2017). Robust regression is commonly used to deal with outliers, as influential data points are down-weighted or a fat-tailed distribution such as a student-t is used instead of a normal distribution (Gelman & Hill 2007; Wang & Blei 2016; Anderson *et al*. 2017).

While many ways to estimate a robust regression exist, common frequentist methods are Quantile regression and Iteratively Reweighting Least Squares (Rousseeuw 1984; Fox & Weisberg 2012; Fahrmeir *et al.* 2013). Quantile regression (as employed in our analysis) simply models the median of the response variable as a linear function of the predictor variables (Rousseeuw 1984; Fox & Weisberg 2012; Fahrmeir *et al*. 2013). Iteratively Reweighted Least Squares down-weights outliers according to the distance from the best fit line, and iteratively refits the model (Rousseeuw 1984; Fox & Weisberg 2012). In a Bayesian framework, robust regression simply involves changing the response distribution from a normal to a student-t distribution (Lange *et al.* 1989; Wang & Blei 2016; Gelman *et al*. 2020). The normal distribution is a specific type of the student-t distribution, with the degrees of freedom parameter (*nu*) set to infinity; *nu* can either be estimated from the model directly or set to a specific value (Wang & Blei 2016).

Here, we first used model diagnostics to identify possible outliers in the Pauly dataset and second, we compared model coefficients estimated by different methods of linear and robust linear regression. To identify potential outliers using model diagnostics, we used Cook's distance and Pareto k, both of which are measures of the influence of a given observation on the model. Cook's distance values were estimated using OLS and Pareto k values were estimated using Bayesian simple linear regression (Fahrmeir *et al.* 2013; Vehtari *et al.* 2017). Second, we compared Pauly's reported model coefficients (estimated via Reduced Major Axis regression on 40 and 37 data points, respectively) to model coefficients estimated with all 42 species using (1) Reduced Major Axis regression (*lmodel2* function in the *lmodel2* package; Legendre 2018), (2) Quantile regression (*rq* function in the *quantreg* package; Koenker 2020), (3) Iteratively Reweighted Least Squares regression (*rlm* function in the *MASS* package; Venables & Ripley 2002), and (4) Bayesian regression with a student-t response distribution (*brm* function in the *brms* package; Bürkner 2017, 2018). To aid in comparison, we re-estimated the Reduced Major Axis regression for the 37 and 40 data points (reported in Pauly 1981, 2010), respectively. For the Bayesian linear regression, we estimated two models; both allowed the degrees

of freedom parameter (*nu*) to be estimated but differed in the strength of the prior on nu: one model had a strong prior on *nu* and the other had a weakly informative prior on *nu.*

I.i. Results

Based on both the Cook's distance and the Pareto k values, there is no reason to exclude any of the 42 species from the analysis of the relationship of gill area index and growth performance. This suggests that neither the West Indian Ocean Coelacanth *Latimeria chalumnae* nor the Atlantic Cutlassfish *Trichiurus lepturus* gill area index value originally suspected to be outliers in Pauly (1981) leveraged our estimated regression parameters. The West Indian Ocean Coelacanth gill surface area and body mass data were later confirmed to be accurate in a subsequent paper (Hughes 1995).

The mean slope for the relationship of gill area index and growth performance for all regression methods was positive but depended on the type of regression (Table 4.2, Fig. 4.2). Irrespective of sample size, the three Reduced Major Axis regression models yielded the greatest mean slope values, (~0.4, 95% Confidence Intervals (CI) did not overlap with zero). Although not significantly different, the mean slope estimated by Reduced Major Axis regression with all 42 species included was higher than the mean slopes estimated for 37 or 40 species. Finally, the slope value from Pauly's original reported fit estimated via Reduced Major Axis regression was also higher than any of the other Reduced Major Axis regression models (Table 4.2, Fig. 4.2).

For all models estimated here, the 95% CIs or the 95% Bayesian Credible Intervals (BCI; for the two Bayesian models) did not overlap with zero, with the exception of the lower bound of the 95% BCI for the robust Bayesian regression with a weak prior, which was equal to -0.02 (Table 4.2, Fig. 4.2). The mean slopes of all models estimated with Reduced Major Axis regression were significantly higher than the mean slopes estimated by robust regression, which had 95% CIs or BCIs that were only slightly nonzero (or for robust Bayesian regression with a weak prior on *nu*, just overlapping with zero). The four different robust regression models almost had identical mean slopes and 95% CIs or BCIs. Further, the choice of prior on *nu* for the Bayesian models did not significantly affect the mean slope estimate (Table 4.2, Fig. 4.2).

I.i. Discussion

Broadly, we found—based on Cook's distance and Pareto k values—that no outliers existed in the Pauly dataset (n = 42 species). Instead, the significance of the relationship of gill area index and growth performance depended on the type of regression used. Thus, the conclusion regarding the significance of this relationship can be drawn from either robust regression (using Quantile regression, Iteratively Reweighted Least Squares regression, or robust Bayesian regression) or Reduced Major Axis regression. These two methods, robust regression and Reduced Major Axis regression, are not typically combined (i.e., using a student-t distribution instead of a normal distribution for Reduced Major Axis regression). Instead, the measurement error in either the predictor and/or response variable in a Bayesian framework would be incorporated directly in the model (Bürkner 2017, 2018). However, as the values of gill area index from Pauly (1981) were estimated using mean gill surface area and mean body mass, error in these data is unknown. Recommendations for deciding between using Reduced Major Axis regression or OLS or similar, e.g., robust regression) in the literature are based on the biological question(s) at hand (Smith 2009; Klimer & Rodríguez 2017). One key assumption of using Reduced Major Axis regression is that the relationship between the predictor(s) (i.e., x-variable) and response (i.e., y-variable) variable is symmetric—it does not matter which variable is the predictor (x) and which is the response (y) as the resulting coefficients and relationship will be identical (McArdle 2003; Smith 2009). As the Gill Oxygen Limitation Theory makes explicit predictions about directionality—that gill surface area is constraining maximum size—we suggest that the relationship between gill area index and growth performance should not be tested in a symmetrical manner, and thus favor robust regression. We note that to draw conclusions in an asymmetrical manner between gill area index and growth performance following the Gill Oxygen Limitation Theory, the response variable and predictor variable should be flipped: growth performance would be the response variable and gill area index (or other metric of gill surface area) would be the predictor variable (we test this question below). Additionally, measurement error in both the predictors and response variables, if available, would ideally be incorporated into a robust regression.

I.ii. Question

What is the effect of parameterizing the relationship between gill area index and growth performance based on the predictions made by the Gill Oxygen Limitation Theory (i.e., testing whether gill area index can explain variation in growth performance)?

I.ii. Premise

The relationship between gill area index and growth performance in Pauly (1981) was estimated by Reduced Major Axis regression (called 'functional regression' in Pauly (1981). The Gill Oxygen Limitation Theory makes explicit predictions about the cause-effect relationship between gill area index and growth performance (Pauly 1981, 2010). Specifically, this theory argues that gill surface area is constraining growth and maximum size (Pauly 1981, 2010). Thus, Reduced Major Axis regression is not an ideal method for assessing the relationship between gill area index and growth performance in the context of the Gill Oxygen Limitation Theory.

Here, we ask what is the relationship between gill area index and growth performance if the axes are flipped (according to predictions of the Gill Oxygen Limitation Theory): growth performance is the response variable and gill area index is the predictor variable?

I.ii. Method

Using the Pauly dataset, we ask how the relationship of gill area index and growth performance would differ if parameterized according to the prediction of the Gill Oxygen Limitation Theory. As this is a different model (and outliers, as well as other diagnostics should be checked for any and all model runs), we first estimated both Cook's distance and Pareto k (see above in Question I.i.) to identify any outliers using OLS and Bayesian linear regression, respectively. If any observation was an outlier (Cook's distance > 0.5 or a Pareto k value > 0.7), we used robust regression in a Bayesian framework to estimate the slope and intercept. We did so in the same manner as in Question I.i.—we used the *brm* function in the *brms* package to estimate two Bayesian linear models with a student-t response distribution, one with a strong prior on nu and one with a weak prior on nu (Bürkner 2017, 2018). Pareto smoothed importance sampling leave- one-out cross validation (PSIS-LOO) was used to compare the two Bayesian models with different priors on nu to identify which prior provided the best fit to the data (Vehtari *et al.* 2017). Finally,

we compute an r^2 value using the bayes_R2 function in the brms package for the purpose of comparing with Pauly's reported r^2 values (Bürkner 2017, 2018).

I.ii. Results

One outlier (*Latimeria chalumnae*) was identified using Cook's distance, however, the Pareto k value of this species was < 0.7. Thus, to be conservative, we compared the results from a Bayesian robust regression to those estimated by a Bayesian simple linear regression to ask if gill area index can explain variation in growth performance for the 42 fish species in the Pauly dataset. The model fit was equivalent regardless of the model used based on the loo information criterion (*looic*, similar interpretation as AIC; robust regression weak prior = 119.6, robust regression strong prior = 120.9, Bayesian simple linear regression = 119.2; Table 4.3, Fig. 4.3).

I.ii. Discussion

Overall, we did not find that gill area index explained variation in growth performance for the 42 species of fish in the Pauly dataset (Table 4.3, Fig. 4.3). Specifically, the slope of the relationship of growth performance and gill area index, when parametrized according to the explicit predictions of the Gill Oxygen Limitation Theory—that gill area surface area constrains growth—had 95% BCIs that overlapped with zero. We note that there is a great deal of uncertainty in the relationship (the standard deviation of the slope ranges from 0.34 – 0.39, depending on the three models). It may be that with more data, we may see a stronger relationship between gill area index (or other measures of gill surface area) and growth performance, as well as less variability. This question will be assessed with more data in Questions II.i – II.iv below.

4.4. Act II: A fresh look at the relationship of maximum size, growth, and gill surface area

The foundational relationship between maximum size, growth, and gill surface area has not been re-examined in the ~40 years since Pauly (1981). A wealth of gill surface area and life history data have been published in this time, with many species possessing raw gill surface area data—or measures for multiple individuals of the same species.

Additionally, statistical advances have afforded the opportunity to explore the nuances of data and the relationship between various parameters. This increase in the availability of data and statistical techniques opens the door to a fresh look at the relationship between maximum size, growth, and gill surface area. In the following, we ask four questions that examine the relationship between gill surface area and growth performance in more detail, as well as assess if two salient factors – evolutionary history and activity level – are important in explaining variation in this relationship.

II.i. Question

Does employing more realistic metrics of gill surface area (i.e., the ontogenetic regression coefficients instead of a simplified index) provide new insight into the relationship of gill surface area and growth performance?

II.i. Premise

The original relationship of maximum size, growth, and gill surface area was estimated using gill area index (G/W^d), a simplified metric of gill surface area that does not capture the known variability in gill surface area within and across species (see Question I.i.; Pauly 1981, 2010; Bigman *et al.* 2018). First, this index is based on mean gill surface area and mean (measurement) body mass data, thus likely not representing the realized within-species relationship between gill surface and body mass (which is known to scale hypoallometrically; Palzenberger & Polha 1992; Wegner 2011; Bigman *et al.* 2018). Second, the *d* value (the ontogenetic slope value for the relationship between gill surface area and body mass) would ideally be empirically estimated from individual (i.e., raw) gill surface area estimates matched to individual body sizes. Due to a paucity of such data, Pauly (1981) first estimated gill area index using a predicted *d* value for each species from a relationship between maximum size and the slope of gill surface area or metabolic rate for a mix of species for which it was known (see above in the 'Premise' of Question I.i.). Later, Pauly (2010) estimated gill area index using the same *d* value for all species (d = 0.8). Hence, the gill area indices originally used by Pauly (1981) and (2010) may have been biased by the sizes at which gills were measured (i.e., the sizes used to generate the species' means), the prediction of the parameter *d*, and the assumption that the slope of gill surface area was constant across a broad array of species (an assumption we now know is false). Thus, comparing the empirically estimated regression coefficients (i.e., the

intercept and slope) from an ontogenetic relationship of gill surface area and body mass across species as metrics of gill surface area, in place of gill area index, provides a more detailed view of how gill surface area varies within species, and underlies the evolutionary allometry across species (Palzenberger and Polha 1992; Wegner 2011; Bigman *et al.* 2018).

Here, we ask three sub-questions that examine how sensitive the relationship of gill surface area and growth performance is to the metric of gill surface area used. First, we compare the relationship of gill area index and growth performance for the 42 species in the Pauly dataset to the same relationship estimated across a larger number of fishes (full dataset, all with mean data). Next, we take advantage of the raw gill surface area and body mass data available and examine the relationship of gill surface area and growth performance across species with two different metrics of gill surface area: the predicted gill surface area at a given size (the intercept of the ontogenetic relationship between gill surface area and body mass) and the rate at which gill surface area increases with body mass (the slope of the ontogenetic relationship between gill surface area and body mass). Finally, we examine – using those species with raw data – if gill area index, estimated with an empirically estimated *d* (as opposed to a predicted *d* value or one set to 0.8 for all species), explains variation in growth performance. We additionally assess how the method used to estimate gill area index affects the relationship between gill area index and growth performance. Specifically, we compare the effect of estimating gill area index in the two ways employed in Pauly (1981) and Pauly (2010) (predicting *d* from Pauly's relationship and setting $d = 0.8$, respectively) with our method of using an empirically estimated *d*.

II.i.a. Question

Does the relationship between gill area index and growth performance originally estimated by Pauly (1981) and again reported in Pauly (2010) still hold when examined across more species?

II.i.a. Method

Additional data collection and sources

We compiled a dataset of fish (teleost, elasmobranch, and coelacanth) gill surface area, (measurement) body mass associated with gill surface area, and von Bertalanffy growth parameters. An initial dataset was collated for those fish species with both gill surface areas and growth parameters in Fishbase (Froese and Pauly 2019). This initial dataset was then supplemented with species with published gill surface area data from other sources (if they also had published growth data). These other sources of gill surface area data were: Bigman *et al.* (2021), Gray (1954), Hughes & Morgan (1973), De Jager and Dekkers (1975), and Palzenberger & Pohla (1992) and references therein.

Gill surface area data

Raw and mean gill surface area estimates (cm^2 or mm^2) and associated body mass (g) were extracted from the original paper in which they were reported, if possible, otherwise they were extracted from Fishbase (for three species, the original paper could not be accessed). Both raw (i.e., estimates for multiple individuals of a species) and mean gill surface area data were included in our dataset. If more than one study reported raw data for a number of individuals for a given species, we included both datasets (this was only the case for three species: *Alopias vulpinus* Common Thresher, *Carcharhinus plumbeus* Sandbar Shark, *Isurus oxyrinchus* Shortfin Mako Shark). If a given species had both published raw and mean data, we preferentially chose the study that included raw data. All raw data were averaged per species to generate a species-specific mean of gill surface area and body mass (for analyses with raw data, see Question II.i.b.). If more than one study reported mean data (this was the case for four species), we chose the study with the largest sample size. Any gill surface area estimate that was not directly measured (e.g., predicted from geometric relationships) was not included in this study (for further discussion see Satora and Wegner 2012). Additionally, all species in Pauly's dataset were included in our dataset with the exception of four species for which the gill surface area data could not be verified (*Engraulis encrasicolus* European Anchovy, *Hippocampus hudsonicus* = *Hippocampus erectus* Lined Seahorse, *Scorpaena porcus* Black Scorpionfish), or the gill surface area was predicted from a regression equation and not empirically measured (Spiny Dogfish *Squalus acanthias*). For the remaining 38 species,

25 of these did not have more recent or higher quality gill surface area data available (e.g., larger sample size, raw data) and thus the data from Hughes & Morgan (1973) was included in our dataset. For the remaining 13 species, either raw data were acquired, or as Pauly's dataset included averaged mean gill surface area data (i.e., means of means), only one mean was included in the full dataset (the mean from the study with the largest sample size). All gill surface area and body mass estimates were $\log_{10}$-transformed prior to analyses.

Life history data

Using the 'rfishbase' package for Fishbase, we extracted all observations (i.e., studies reporting parameters of a von Bertalanffy growth function for a species) for each species in our dataset of k (year^{-1}), the growth coefficient and L_∞ (cm), the asymptotic length or mean length the individuals in a population would reach if they were to grow indefinitely (Froese and Pauly 2000; Boettiger *et al.* 2012). If reported, we also extracted W_∞ (g), the asymptotic mass or mean mass the individuals in a population would reach if they were to grow indefinitely. If the length type (i.e., total length, TL, fork length, FL, etc.) was not reported for an observation of L_∞, that observation (both k and L_∞) was removed from the dataset. If growth data were not available in Fishbase for any species, the primary literature was searched for published age and growth data. For most species, the asymptotic size was often reported as L_∞ and not W_∞ and thus W_∞ was estimated for each observation using length-weight regressions matched by length measure and sex downloaded from Fishbase using the 'rfishbase' package (Boettiger *et al.* 2012). For eight species, growth parameters were not available in Fishbase but were published in the literature. For seven species, sex-specific length-weight coefficients were not available for sex-specific growth parameters, and so available length-weight coefficients were averaged and then used to estimate W_∞. For 14 species, length-weight coefficients for the same length type as was used to estimate growth parameters was not available, and thus matching type-specific length-weight regressions were collated from the literature. Finally, the published estimates of W_∞ for two species were used instead of estimating them with length-weight regressions.

Growth performance was calculated for each observation as log10(k * W_∞) following Pauly (1981). For analyses, a mean of growth performance was taken for each species.

In total, our dataset (hereafter, “full dataset”) included 708 observations of gill surface area and body mass for a total of 132 fish species (teleost, elasmobranch, and coelacanth), as well as von Bertalanffy growth parameters for each of these species (species listed in Table S1). There are two considerations that necessitated generating two subsets of data to ensure our results were not biased: (1) the growth of ‘aquacultured’ species differs from wild fishes (due to food ad libitum, little predation, and aeration of aquaculture ponds, all which possibly result in faster growth; Pauly 2010), and (2) fishes that breath air (either by possessing an air-breathing organ or passive oxygen diffusion through the skin) as they have lower gill surface area for a given size compared to their non-air-breathing counterparts (Wegner 2011). Excluding aquaculture and airbreathing species had no effect on our results (for more detail, see Tables S3 – S9 in the Supplementary Information).

Estimating gill area index

The gill area index first estimated in Pauly (1981) was calculated for each species using mean gill surface area and body mass data, as well as a species-specific predicted d value based on a previously estimated linear relationship between d and maximum observed body mass (Wmax; see earlier text in the ‘Premise’ of Question I.i. and Pauly (1981). Subsequently, Pauly (2010) estimated gill area index with a value of d = 0.8 for all species. For this question (assessing whether the relationship between gill area index and growth performance still holds with more data), we chose to set d = 0.8 (but also examined sensitivity to different d values to estimate gill area index in Question II.i.c. below). For those species with raw gill surface area and raw body mass data, a species-specific mean of both were calculated prior to estimating gill area index following Pauly (1981, 2010). Thus, one gill area index value is estimated for each species.

Statistical analysis

We used simple linear regression estimated in a Bayesian framework using the *brm* function in the *brms* package to estimate regression coefficients for the relationship of gill area index and growth performance for the Pauly dataset and the full dataset (Bürkner 2017, 2018; R Core Team 2020). For these models, growth performance was the response variable and gill area index was the predictor variable (see Question 2 above).

We examined the existence of outliers in all models using Cook's distance (as estimated by OLS) and Pareto k (see Question I.i. above).

II.i.a. Results

In Pauly's dataset of 42 species, one outlier was identified (*Latimeria chalumnae,* Cook's distance > 0.5, but Pareto k value < 0.7). Thus, to be conservative, we compared the results from two Bayesian robust regressions (differed only in prior on *nu; see above*) to those estimated by a Bayesian simple linear regression (i.e., a linear regression in *brms* using the Gaussian distribution). All three models were equivalent, and thus, we compared the results from a Bayesian simple linear regression using Pauly's dataset of 42 species and the full dataset of 132 species. No outliers were identified in the relationship of gill area index and growth performance estimated using the full dataset.

The relationship of gill area index (as estimated by setting d = 0.8) and growth performance parametrized according to the predictions of the Gill Oxygen Limitation Theory was positive and significant irrespective of the number of species included in a dataset (Fig. 4.4). For the Pauly dataset, the mean slope = 0.83 (95% BCI 0.19 – 1.47) and for the full dataset, the mean slope = 0.87 (95% BCI 0.52 – 1.23). The slopes were statistically indistinguishable from each other as the slopes of both models fell within the 95% BCI of the other (Fig. 4.4).

II.i.a. Discussion

Overall, we found a positive and significant relationship between gill area index and growth performance, irrespective of the number of species included in the analysis. We note that the r^2 value is still low (0.16 for the full dataset, 0.15 for the Pauly dataset) and that there remains a great deal of uncertainty in the relationship, as indicated by the range of growth performance values for a given gill area index.

In Question II.i.a., we still used gill area index, which relies on mean data and a predicted (or set) value of d. However, the raw gill surface area and body mass data now available through the updated data acquired herein allow us to further examine the relationship of gill surface area and growth performance using two different metrics of gill surface area, both estimated on individual-level data: (1) the predicted gill surface area at a given body size (the intercept of the ontogenetic relationship between gill surface area and body mass

for a single species) and (2) the rate at which gill surface area increases with body mass (the slope of the ontogenetic relationship between gill surface area and body mass for a single species). We can thus ask:

II.i.b. Question

Does growth performance vary with gill surface area at a given size (ontogenetic intercept) and the rate at which gill surface area increases with body mass (ontogenetic slope)?

II.i.b. Method

Data filtering

We filtered our full dataset (see previous section) for those species that had raw gill surface area data for at least eight individuals (hereafter, "raw dataset"). This threshold of eight individuals was based on simulations (see SI) and other studies that have assessed the effect of sample size on regression parameters (Jenkins & Quintana-Ascencio 2020). In order to facilitate comparison across models with and without a phylogeny (Question II.ii., see below), we further restricted our dataset to include only those species that have a resolved phylogenetic position on the *Fish Tree of Life* or on a recently published Chondrichthyan phylogeny (Rabosky *et al.* 2018; Stein *et al.* 2018; Chang *et al.* 2019). Of the 132 species that have published gill surface area and life history traits in our full dataset, only 32 species met our criteria (raw gill surface area data with at least eight individuals, known growth parameters, and resolved position on the phylogeny) and were included in the raw dataset (Table S2, used in this analysis and the analysis for Questions II.ii. and II.iv.). To ensure our results were not sensitive to the choice of estimating gill surface area allometric coefficients (ontogenetic intercept and slope) using only species with at least 8 individuals, we also created an additional raw dataset in which we filtered for those species that had a body size range of at least an order of magnitude. Using this additional raw dataset had no effect on our results (Table S6).

Statistical analysis

To assess whether growth performance varied with gill surface area at a given size and the rate at which gill surface area increased with body mass, we employed a Bayesian multilevel modeling framework that included two levels of models. The first level of the model estimated the ontogenetic allometry of gill surface area and body mass for each

species, resulting in a species-specific posterior distribution of the intercept and a species-specific posterior distribution of the ontogenetic slope. To ensure that intercepts are estimated accurately across the broad size range of species included in the dataset, body mass data were centered on the mean value of body mass for all 32 species in the dataset (300 g). The second level of this model then examined whether the species-specific gill surface area at a given body size (intercept of the ontogenetic allometry) or the species-specific rate at which gill surface area increases with body mass (slope of the ontogenetic allometry) explained variation in growth performance across species. Thus, two multilevel models were run – one with growth performance as the response variable and the species-specific intercepts as the predictor variable and one with growth performance as the response variable and the species-specific slopes as the predictor variable. In both models, the species-specific slopes and intercepts were standardized using the z-score transformation for input in the second level of the model, which facilitated model convergence and parameter estimation. The strength of using such a multilevel modeling approach is that the uncertainty in the species-specific intercepts and ontogenetic slopes estimated in the first level of the model are propagated across levels of the model as each iteration of all levels of the model happens in succession (Bigman *et al.* 2021). All models were fit in R using *rstan* (Stan Development Team 2019; R Core Team 2020; see the SI for more detail on our modeling approach.

II.i.b. Results

The relationship of gill surface area and growth performance was not significant for either metric of gill surface area– the ontogenetic intercept (i.e., the species-specific gill surface area at 300 g of body mass) or the ontogenetic slope (i.e., the species-specific rate at which gill surface area increased with body mass; Table 4.4, Fig. 4.5a, b). Both relationships yielded similar mean slope values and the 95% BCIs overlapped with zero: the mean slope for the relationship of growth performance and the ontogenetic intercept = 0.36 (95% BCI -0.11 to 0.83) and for the ontogenetic slope, the mean slope = 0.33 (95% BCI -0.20 to 0.83, Table 4.4, Fig. 4.5a, b).

II.i.b. Discussion

The finding that there was no relationship between gill surface area and growth performance when considering gill surface area decomposed into its allometric

components, the ontogenetic intercept and the ontogenetic slope, is in stark contrast to Pauly's originally estimated relationship. These results are also in contrast to those in Question II.i.a. (the relationship of gill area index and growth performance across more species [132 species in full dataset] parameterized as growth performance ~ gill area index). This relationship (II.i.a.) was significant, such that species with a higher growth performance had a higher gill area index. The fact that we did not find a significant relationship with growth performance and either the ontogenetic intercept or ontogenetic slope may be due to the amount of uncertainty in the ontogenetic-level regression coefficients or the variation in ontogenetic regression coefficients across species. Although estimating a regression with eight individuals has been found to be suitable for our purposes, ensuring that the size range of each species is broad may decrease the uncertainty in the allometric coefficients. In addition, analyses across a larger number of species (i.e., > 32) would also help us understand how gill surface area and growth performance are related.

Last, with raw data, we can now calculate an 'empirical' value of gill area index (i.e., not use a set *d* value or one predicted from a relationship). While this gill area index calculation still employs mean data, comparing gill area indices estimated using different values of *d* provides insight into understanding how variable this metric of gill surface area can be:

II.i.c. Question

When estimating gill area index with the empirically estimated *d*, do we still see a significant relationship between gill area index and growth performance?

II.i.c. Method

To assess if growth performance varied with gill area index as calculated with empirically estimated slope values, we built on the approach used in the previous question (Question II.i.b.). We again used the raw dataset and altered the Bayesian multilevel model to estimate gill area index using the species-specific slopes estimated in the first level and then altered the second level of the model to examine whether the species-specific gill area index explained variation in growth performance. Thus, this model estimated species-specific slopes in the first level, calculated gill area index for each species (using the species-specific mean gill surface area, mean body mass associated with the mean gill surface area, and slope estimated in the first level of the model), and then estimated a

model in the second level that examined if gill area index explains variation in growth performance. The gill area index was $\log_{10}$-transformed and standardized (using a z-score) prior to the second level of the model. Importantly, this approach allowed us to not fit subsequent models as each iteration of each model happens in succession. Thus, the uncertainty in the species-specific slopes, and thus in gill area index, is propagated to all levels of the model. See the SI for more detail on our modeling approach. To ensure our results were not sensitive to the choice of estimating gill surface area ontogenetic slopes (and thus gill area indices) using only species with at least 8 individuals, we also ran the same model on the additional raw dataset that only included those species that had a body size range of at least an order of magnitude. Our model output did not change when using this additional raw dataset (Table S6).

Finally, we compared the results from these models – where gill area index was calculated using empirically estimated *d* values – to models in which gill area index was estimated (1) following Pauly (1981; *d* predicted from Pauly's relationship between *d* and maximum observed body mass, see Question I.i.) and (2) following Pauly (2010; using $d = 0.8$). These models differed from those in Question II.i.a. only by the number of data points – here, we only used species in the raw dataset for purposes of comparison with the model that calculates gill area index using empirically estimated *d* values (which can only be done for species with raw (individual) gill surface area and body mass data).

II.i.c. Results

The relationship of gill area index and growth performance was not significant, regardless of how the gill area index was estimated (the 95% BCI of the slope overlapped with zero for all models Table 4.4, 4.5, Fig. 4.5c, 4.6). In other words, choosing different forms of *d* did not affect significance. When gill area index was estimated with empirically estimated *d* values (using the multilevel model), the mean slope = 0.13 (95% BCI -0.40 to 0.65; Table 4.5, Fig. 4.6a). When gill area index was estimated with $d = 0.8$, the mean slope = 0.44 (95% BCI 0.00 to 0.88; Table 4.5, Fig. 4.6b), and when the gill area index was estimated using the relationship of *d* and maximum size for other species, the mean slope = 0.06 (95% BCI -0.43 to 0.54; Table 4.5, Fig. 4.6c). We note that for the relationship where gill area index was estimated with $d = 0.8$, the slope was slightly higher when excluding those species that are traditionally used in aquaculture (Table S7).

II.i.c. Discussion

The finding that there was no relationship of gill area index and growth performance is again in contrast to Pauly's original estimated relationship. These results are also in contrast to those in Question II.i.a. (the relationship of gill area index and growth performance across more species [132 species in full dataset] parameterized as growth performance ~ gill area index). This relationship (II.i.a) was significant, such that species with a higher growth performance had a higher gill area index. The fact that we did not find a significant relationship with gill area index and growth performance when estimating gill area index using species-specific empirically estimated *d* values – or the other two ways gill area index has been estimated in the past –suggests that the relationship of gill area index and growth performance is sensitive to the composition of a dataset. However, all results for species with raw data align, suggesting that growth performance is not simply (or only) related to gill surface area – whether gill surface area is measured by the ontogenetic intercept, ontogenetic slope, or gill area index (Fig. 4.5).

II.ii. Question

Is evolutionary history an important factor in determining how gill surface area and growth performance are related?

II.ii. Premise

When examining a relationship across different species, it is important to take into account their shared evolutionary history (Freckleton 2009). Species are not statistically independent from one another; instead, they share varying parts of evolutionary trajectories that can be traced back through deep time, and thus closely related species share more evolutionary history than more distantly related ones (Freckleton 2009). Thus, using typical linear regression methods (OLS, robust regression) to assess a relationship between traits across species violates the assumption that observations are independent of each other (Freckleton 2009; Revell 2010). Phylogenetic comparative methods were designed to account for the shared evolutionary history among species and can now be implemented with relative ease (Freckleton 2009; Symonds & Blomberg 2014; Bürkner 2017, 2018). These methods estimate parameter values that account for the interspecific autocorrelation due to relatedness (Symonds & Blomberg 2014). When phylogenetically

correcting a linear regression, the phylogenetic component is typically included in the model as a random effect, thus accounting for any pattern among the residuals as (i.e., residual error) as opposed to the trait itself (Symonds & Blomberg 2014). As the relationship of gill surface area and growth performance is being assessed across species (i.e., an evolutionary allometry at the second level of the model), the phylogenetic structure of the data may be an important aspect to consider. Here, we add a phylogeny to the analyses of gill surface area and growth performance to account for species' shared evolutionary history.

II.ii. Method

To incorporate a phylogeny into our analyses of gill surface area and growth performance, we built on the Bayesian multilevel modeling framework used in previous questions above. Specifically, we incorporated a random effect of phylogeny in the second level of each model, when examining whether the species-specific regression coefficients (i.e., the slope or intercept) of gill surface area explains variation in growth performance (the evolutionary allometry). To do so, we first constructed a new supertree with species from our dataset using two published phylogenies -- one for teleosts (Rabosky *et al.* 2018; Chang *et al*. 2019) and one for Chondrichthyans (Stein *et al*. 2018). Then, we reran three models: both multilevel models in Question II.i.b (first level estimates the species-specific gill surface area ontogenetic slopes and intercepts and the second level estimates if either the slopes or intercepts explain variation in growth performance) and the multilevel model in Question II.i.c (first level estimates the species-specific gill surface area ontogenetic slopes and intercepts, the slopes are used to estimate gill area index, and the second level estimates if gill area index explains variation in growth performance) with an addition of a phylogenetic random effect (see SI for more details on the modeling approach).

II.ii. Results

Overall, we found that including a phylogeny in the three models of growth performance and gill surface area, specifically as measured by the (1) the ontogenetic intercept, (2) the ontogenetic slope, and (3) gill area index (using empirically estimated *d* values) did not change the resulting parameter estimates of the respective models (Table 4.4, Fig. 4.5, compare panels a-c with d-f). The effect size of the phylogenetic signal (Pagel's lambda,

λ) for all three models was approximately equal to 0.5, with wide 95% BCIs that nearly spanned the entire range of possible values (0 to 1, Table 4.4).

II.ii. Discussion

The finding that including a random effect of phylogeny in our analyses of gill surface area and growth performance did not change our results suggests that including a phylogenetic effect, while prudent, does not affect the relationship between growth performance and gill surface area (as parameterized here and on the set of species included in the analysis). The apparent lack of an underlying phylogenetic structure in this relationship could be for two reasons. First, commonly implemented methods to account for underlying phylogenetic structure in datasets rely on the Brownian motion model of trait evolution to model the expected variance and covariance between species (Felsenstein 1985; Freckleton 2009; Harmon 2018). This model of evolution assumes that traits evolve along the phylogeny through a random-walk process (Harmon 2018). Thus, species that are more closely related have had less time to diverge and thus will have trait values that are more similar (i.e., they co-vary) compared to distantly related species, whose trait values have been randomly drifting for a longer period of time (Symonds & Blomberg 2014). Other, and perhaps better, models of trait evolution exist, yet implementing them in practice is nontrivial (Harmon 2018). However, rapid advancements in the implementation of more complex comparative methods are occurring, which will undoubtedly open the door to exploring trait evolution in a broader sense, to include employing other models of trait evolution (Pennell & Harmon 2013). Second, it may be that evolutionary history truly does not explain remaining variation in growth performance after gill surface area has been accounted for. It could be that variation in growth performance across species may be entirely related to ecological and physiological processes that are independent of shared ancestry. Few studies examine patterns of growth across a large number of species; of those that have, it seems that whether or not phylogeny is important may be related to the taxa in question (Grady *et al.* 2014; van Denderen *et al.* 2020). Future work comparing growth patterns across species could examine this in more detail, as well as identify if other models of trait evolution are more relevant to explaining patterns of growth or gill surface across species.

II.iii. Question

Does activity level better characterize the variation in growth performance across species compared to gill surface area?

II.iii. Premise

In addition to growth performance, other factors have been suggested to relate closely to gill surface area and growth across species. For example, Pauly (2010) flagged that 'fish can either grow a lot or swim a lot, but not both'. Indeed, the activity level of a fish has historically been thought of as the most important predictor of a species' gill surface area (Gray 1954; Hughes 1966). As more and more gill surface area data have been published, it is now well known that active, pelagic species have larger gill surface areas for a given size than their less active, benthic counterparts (Palzenberger & Pohla 1992; Wegner 2011; Bigman *et al.* 2018). Further, it has been suggested that no relationship exists between growth performance and gill area surface area – as measured by gill area index – when activity level is accounted for. Blier *et al.* (1992) re-examined Pauly's original dataset of growth performance and gill area index and found that when excluding species designated as 'good swimmers,' no relationship of growth performance and gill area index existed. When Pauly (2010) subsequently added activity level, as measured by the 'swimming capacity index' (the sustained swimming speed of a fish multiplied by its body length), into his examination of the relationship of gill area index and growth performance, he found that both gill area index and the swimming capacity index explained variation in growth performance across fishes. However, the (unstandardized) effect size of his metric of activity level (= 0.049) was larger than the effect size of gill area index (= 0.011; Pauly 2010). Thus, it remains unclear if gill surface area explains significant variation in growth performance across species, above and beyond what can be attributed to activity level.

Here, we ask if gill surface area, as measured by the ontogenetic intercept of the relationship of gill surface area and body mass, the ontogenetic slope of the relationship of gill surface area and body mass, and gill area index (calculated with an empirically estimated d value), explains more variation in growth performance compared to activity level. For this question, we again use species with raw gill surface area and body mass data, which allows us to estimate species-specific ontogenetic intercepts and slopes.

II.iii. Method

Data collection

To include a standardized, objective, and quantitative metric of activity level in our analyses, we followed established methods and estimated the caudal fin aspect ratio – a morphological correlate of swimming speed and activity – of each species in the raw dataset (Palomares & Pauly 1989; Sambilay 1990; Bigman *et al.* 2018). Caudal fin aspect ratio (A) was calculated for each species as $A = h^2/s$, where h is the height and s is the surface area of the caudal fin from anatomically correct field guide illustrations (Palomares & Pauly 1989; Sambilay 1990, Bigman *et al.* 2018). We obtained anatomically correct field guide illustrations from Sharks of the World (Ebert *et al.* 2016) for elasmobranch species and from FAO field guides for teleost species. For some teleost species, FAO images were not available (n = 7) and thus alternative field guides were used. If alternative guides were used, we generated an average of CFAR from up to four field guide illustrations (if available). Of the 32 species used in previous analyses, CFAR could only be estimated for 30 species as one species was a batoid and one was an eel (both do not have traditional caudal fin morphology).

Although shortcomings exist with this approach (e.g., tail shape may change slightly with growth), using caudal fin aspect ratio as a quantitative metric for activity level improves the rigor of analyses regarding the relationship of gill surface area and activity, as most previous gill surface area studies have only examined broad, descriptive categories of activity level (e.g., 'sluggish,' 'moderate activity') based on the perceived, subjective activity of each species (e.g., Gray 1954; Wegner 2011).

Statistical analysis

To assess whether activity level explained more variation in growth performance compared to gill surface area, we fit three multilevel Bayesian models in which all predictors in the second level (which examined what factors explained variation in growth performance) were standardized for inferring the relative importance of each predictor. The first level of all three models estimated the species-specific posterior distribution of the ontogenetic intercepts and slopes of the relationship of gill surface area and centered body mass (at 300 g, see Question II.i.b.). The second level of the three models examined

whether caudal fin aspect ratio or the ontogenetic gill surface area intercept (model 1), ontogenetic gill surface area slope (model 2), or gill area index (model 3) explained more variation in growth performance. We estimated the correlation and variance inflation factors (VIF) for all three models to ensure that activity level and gill surface area, as parameterized in our models, were not colinear or correlated. Additionally, we compared models with and without the inclusion of a phylogenetic random effect.

II.iii. Results

In all three models, caudal fin aspect ratio explained more variation in growth performance across fishes compared to the ontogenetic intercept, the ontogenetic slope, or gill area index, respectively (Table 4.6, Fig. 4.7). As with the previous models in Questions II.i and II.ii, gill surface area, regardless of metric, did not explain variation in growth performance across species as the 95% BCI for all three overlapped with zero (Table 4.6). Based on the mean effect size estimates (slope values in Table 4.6) caudal fin aspect ratio explained 5.5 times more variation than the ontogenetic intercept, 3.3 times more variation than the ontogenetic slope, and 16 times more variation than gill area index (calculated using empirically estimated *d* values, Table 4.6, Fig. 4.7). Additionally, no multicollinearity or correlation was detected for any model that included both caudal fin aspect ratio and gill surface area based on VIFs or correlation indices (whether measured by the gill surface area ontogenetic intercept, the gill surface area ontogenetic slope, or gill area index, Table 4.6). Finally, the inclusion of a phylogeny did not change parameter estimates for any model (Table 4.6).

II.iii. Discussion

Our results highlight that activity – as measured by the caudal fin aspect ratio of a species – better explains variation in growth performance compared to gill surface area, regardless of the gill surface area metric used (intercept, slope, or gill area index). Thus, activity level, and not gill surface area, appears to be a better predictor of variation in growth and maximum size across species. Of course, gill surface area is highly intertwined with activity, as decades of work have uncovered that more active species have larger gill surface areas than their less active counterparts (Gray 1954; Palzenberger & Pohla 1992; Wegner 2011; Bigman *et al.* 2018). Thus, it is non-trivial to partition variance between activity and gill surface area, which may be reflected in our results despite the low

correlation found between the specific predictors used for gill surface area and growth performance used in our models. Further work examining other, possibly more refined measures of both activity level, such as swimming speed or even aerobic scope, and growth (we used von Bertalanffy growth coefficients) may shed more light on the relationship of gill surface area, activity, and growth. Additionally, other factors not considered here (e.g., environmental temperature, diet and food availability) are known to affect growth and size in fishes (Morais & Bellwood 2018; van Denderen *et al*. 2020). Exploring the relationships among gill surface area in conjunction with these other salient factors are fruitful avenues for future inquiry that may help us understand how other factors (e.g., temperature, food, and oxygen) affect growth across species.

II.iv. Question

Do species with faster growth rates for their size have larger gills (does gill surface area explain the variation in growth coefficients for fishes that grow to the same asymptotic size)?

II.iv. Premise

One inherent prediction resulting from the assertion that maximum size, growth, and gill surface area are tightly correlated is that fishes with large gills will grow rapidly to their maximum size (Pauly 2010). In other words, variation in growth (as measured by the von Bertalanffy growth coefficient in fishes, k) for individuals or species that grow to the same asymptotic sizes (W_∞) may be explained by differences in gill surface areas across species. When examining this relationship using gill area index across 52 species, Pauly (2010) found that gill area index did indeed explain variation in growth performance across species, above and beyond what can be attributed to asymptotic size (Pauly 2010). Now that more gill surface area data is available, we can test to what extent this relationship still holds.

II.iv. Method

To assess whether gill surface area, in addition to asymptotic size, explained variation in growth coefficients across species, we fit three multilevel Bayesian models. The first level of all three models estimated the species-specific posterior distribution of the ontogenetic

intercepts and slopes of the relationship of gill surface area and body mass (centered at 300 g, see above). The second level of the three models examined if the ontogenetic intercept (model 1), ontogenetic slope (model 2), or gill area index (model 3) explained additional variation in the relationship between the von Bertalanffy growth coefficient and asymptotic size across species. Both predictors (the gill surface area metric and asymptotic size) in the second level of the model were standardized (by z-score) in order to facilitate comparison among them and infer the relative importance of a given predictor in explaining variation in growth coefficients. We estimated the correlation and variance inflation factors (VIF) between gill surface and asymptotic size for all three models to ensure that these traits, as parameterized in our models, were not colinear or correlated. Additionally, we compared models with and without the inclusion of a phylogenetic random effect. For more details on our modeling approach, see the SI.

II.iv. Results

Gill surface area did not explain variation in growth coefficients across species, regardless of which gill surface area metric was used: the ontogenetic intercept, the ontogenetic slope, or gill area index (Table 4.7, Fig. 4.8). Specifically, the 95% BCI of the gill surface area metric in each of the three models overlapped with zero (Table 4.7). In contrast, asymptotic size did explain variation in growth coefficients across species in all three models (Table 4.7). Based on the mean effect size estimates (slope values in Table 4.7) asymptotic size explained 3.25 times more variation than the ontogenetic intercept, 5.4 times more variation than the ontogenetic slope, and 9.33 times more variation than gill area index (estimated using empirically estimated d values, Table 4.7). Additionally, no multicollinearity or correlation was detected between gill surface area and asymptotic size in any of the three models (Table 4.7). Finally, the inclusion of a phylogeny did not significantly change parameter estimates for any model (Table 4.7).

II.iv. Discussion

These results suggest that gill surface area does not explain the variation in the von Bertalanffy growth coefficient for individuals or species that grow to the same asymptotic sizes. As such, we do not find evidence in support of the idea that fishes with large gills grow rapidly to their maximum size. Our results show that asymptotic size explained more variation in growth coefficients across fishes compared to gill surface area. As stated

earlier, other factors – such as activity (as examined in this study), temperature, or food availability – are likely more important predictors of growth and maximum size across fishes.

4.5. Overall discussion

Overall, we found that gill surface area explained little variation in growth and maximum size across fishes, and that other variables – particularly activity, were more important in explaining variation in these life history traits. While we used many approaches in this study to assess whether gill surface area explained variation in growth and maximum size across species, all the models were in agreement and supported the idea that variation in growth and maximum size across fishes cannot simply be explained by gill surface area alone. We note that all models were quite noisy and had a great deal of residual error. This may provide support that activity level (as tested here), as well as other factors (environmental temperature, food availability) likely play a larger role in fish growth compared to gill surface area (Morais & Bellwood 2018; Audzijonyte *et al.* 2019; van Denderen *et al.* 2020). From a life history perspective, our study thus suggests that gill surface area likely does not determine maximum size in fishes, as predicted by the Gill Oxygen Limitation Theory. Instead, other mechanisms may underlie the suggested pattern of oxygen limitation on growth under warmer temperatures or in larger species (Hoefnagel & Verberk 2015; Audzijonyte *et al.* 2019, Rubalcaba *et al.* 2020). By extension, our work suggests that the hypoallometric scaling of gill surface area does not confer a limitation on the oxygen supply required for aerobic metabolism. However, we caution that the Gill Oxygen Limitation Theory is multifaceted (Pauly 1981, 2010). Our work only tested one prediction of this theory, leaving much to be done to evaluate this theory in its entirety (Pauly 1981, 2010). We focus the remainder of our discussion on the importance of recognizing data types and choosing statistical analyses, as well as lay out a path forward to further understand the interplay among gill surface area (and more broadly, oxygen) and life histories across fishes.

A strength of this study and general approach is the comparison of ontogenetic/intraspecific relationships across species. The central tenet of the Gill Oxygen Limitation Theory is that the hypoallometric ontogenetic scaling of gill surface area and body mass limits the supply of oxygen for growth as an organism increases in size,

ultimately determining its maximum size (Pauly 1981, 2010, 2021). Thus, it is necessary to examine the relationship of growth and maximum size in the context of an allometry (or scaling), as opposed to simply using a metric such as gill area index or a mass-specific measure of gill surface area (Pauly 1981, 2010, 2021). Another important reason why a scaling approach is necessary is evident when considering scale: the Gill Oxygen Limitation Theory is focused on how the scaling of gill surface area within species drives patterns across species, while other theories surrounding the role that oxygen plays in structuring life histories, population dynamics, and ecosystem functioning, among other processes, are largely centered on species-level mean data (i.e., the Metabolic Theory of Ecology; Brown *et al*. 2004). A combined approach that has the flexibility to incorporate raw and mean data, such as the modeling approach developed here, will help us to understand how raw data, and the ontogenetic scaling relationships they confer, scale up to structure patterns across species, communities, and ecosystems. Indeed, understanding the role that oxygen plays in the ecology, physiology, and evolution of fishes will require an integrated approach that allows us to scale up individual-level physiological and ecological data to species- and ecosystem-level patterns.

To this end, we outline three areas for future research that would help us to understand the role that gill surface area, and more broadly, oxygen, may play in structuring the growth, maximum size, and more broadly, the life histories of fishes. First, there is an underappreciated complexity in estimating accurate and reliable ontogenetic regression slopes. Ideally, species-specific raw data that spans the entire body size range of a species would be used to estimate an ontogenetic slope, yet these data are rarely available. Estimating accurate slope values is central to testing whether the scaling of gill surface area (or other size-dependent traits such as metabolic rate) affect ecological, physiological, and evolutionary patterns across species. Here, we took care to identify the number of individuals of a given species that were required to produce a reliable and reasonable slope estimate, and only used data to estimate regression coefficients for species that had the minimum number of individuals. We urge other researchers to take a similar approach when estimating ontogenetic slope values. Future work could build off of our simulations to identify the minimum proportion of a species' size range needed to estimate a reliable and reasonable slope value. Second, future studies should examine other factors (e.g., temperature, food availability, metabolic rate) that may underlie life history traits and maximum size across species and assess whether and how oxygen

plays a role in structuring these processes (Audzijonyte *et al.* 2019; Verberk *et al.* 2020). Indeed, we have not dealt with environmental temperature, a factor known to be important in explaining variation in growth across fishes (van Denderen *et al.* 2020). Future work could examine the relationships among gill surface area, environmental temperature, and growth to assess whether gill surface area varies with environmental temperature (as does metabolic rate), and whether this interaction explains variation in growth. Third, without complementary experimental studies that can manipulate abiotic factors such as oxygen, temperature, and food availability, it is difficult to identify the mechanisms that confer the observed correlational patterns (Audzijonyte *et al.* 2019, Bigman *et al.* 2021). Marrying correlational and experimental work will help us understand the role that oxygen plays in structuring growth and other life history characteristics, and more broadly, the ecology, physiology, and evolution of organisms (Audzijoynte *et al.* 2018). Such work is incredibly timely in light of the uncertainty regarding how the physiology and ecology of fishes will determine the response of species to continued global environmental change (Verberk *et al.* 2020, Lefevre *et al.* 2021).

4.6. Tables

Table 4.1 The six questions we ask to examine the relationship of maximum body size, growth, and gill surface area in fishes.

Research question
Act I In the original dataset Pauly (1981) uses to examine the relationship between gill surface area and growth: i. What constitutes an outlier and how sensitive is the relationship of gill area index and growth performance to outliers? ii. What is the effect of parameterizing the relationship between gill area index and growth performance based on the predictions made by the Gill Oxygen Limitation Theory (i.e., testing if gill area index can explain variation in growth performance)? Act II When including the gill surface area and growth data that has become available in the 40 years since this relationship was first tested (i.e., broadly across fishes): i. Does employing more realistic metrics of gill surface area (i.e., the ontogenetic regression coefficients instead of a simplified index) provide new insight into the relationship of gill surface area and growth performance (note there are three sub questions within this question)? ii. Is evolutionary history an important factor in determining how gill surface area and growth performance are related? iii. Does activity level better characterize the variation in growth performance across species compared to gill surface area? iv. Do species with faster growth rates for their body size have larger gills?

Table 4.2 Comparison of model coefficients estimated by various regression methods. The number of species used in each model is indicated by 'n ='.

Model name	Regression method	Intercept (95% CI)	Slope (95% CI)	n =
Pauly (1981) reported fit with no outliers	Reduced major axis (i.e., "functional") regression"	-0.53 (not given)	0.57 (not given)	37
Pauly (1981) reported fit with 2 outliers excluded	Reduced major axis	not given	not given	40
Reduced major axis: 37 species	Reduced major axis regression	-0.06 (-0.40 – 0.19)	0.40 (0.31– 0.53)	37
Reduced major axis: 40 species	Reduced major axis regression	0.02 (-0.34 – 0.28)	0.40 (0.30 – 0.54)	40
Reduced major axis: 42 species	Reduced major axis regression	-0.26 (-0.71– 0.08)	0.47 (0.35 – 0.65)	42
Quantile regression	Robust regression	0.63 (0.38 – 0.86)	0.17 (0.05 – 0.24)	42
Iteratively reweighted least squares	Robust regression	0.64 (0.31 – 0.98)	0.14 (0.02 – 0.26)	42
Robust Bayesian regression weak prior on nu	Bayesian robust regression	0.68 (0.29 – 1.08)	0.13 (-0.02 – 0.27)	42
Robust Bayesian regression strong prior on nu	Bayesian robust regression	0.63 (0.27 – 1.00)	0.15 (0.02 – 0.28)	42

Table 4.3 Comparison of Bayesian model coefficients and their 95% Bayesian Credible Intervals (BCI) estimated for the relationship of gill area index and growth performance, as parameterized according to the predictions made by the GOLT (growth performance ~ gill area index).
Model selection was conducted using Pareto-smoothing importance sampling leave-one-out cross validation (PSIS-LOO) using the *loo* package in R v.5.3.1 and v.4.0.1. *looic* = LOO information criterion value (similar to Akaike Information Criterion [AIC]).

Regression method	Intercept (95% BCI)	Slope (95% BCI)	looic
Bayesian robust regression with strong prior on nu	2.03 (1.20 – 2.86)	0.58 (-0.19 – 1.34)	120.9
Bayesian robust regression with weak prior on nu	2.16 (1.38 – 2.91)	0.48 (-0.21 – 1.20)	119.6
Bayesian regression with gaussian distribution	2.22 (1.50 – 2.95)	0.43 (-0.23 – 1.10)	119.2

Table 4.4 Comparison of all coefficients and their 95% Bayesian Credible Intervals (BCI) estimated from models parameterized with growth performance as the response variable and either the species-specific slope or intercept as the response variable (differentiated in the 'Model parameterization' column) with and without the inclusion of a phylogeny.
A Bayesian multilevel modeling framework was used to estimate all parameters in Stan using the package *rstan* in R v.4.0.2. All intercepts and slopes were standardized in the model prior to the second level (see text and SI).

Model parameterization	Intercept (95% BCI)	Slope (95% BCI)	Phylogenetic signal (λ)
Growth performance ~ intercept	3.08 (2.63 to 3.53)	0.36 (-0.11 to 0.83)	--
Growth performance ~ intercept	3.08 (2.62 to 3.52)	0.36 (-0.13 to 0.83)	0.50 (0.03 to 0.98)
Growth performance ~ slope	3.08 (2.63 to 3.53)	0.33 (-0.20 to 0.83)	--
Growth performance ~ slope	3.08 (2.63 to 3.52)	0.33 (-0.21 to 0.84)	0.50 (0.03 to 0.98)
Growth performance ~ gill area index	3.08 (2.61 to 3.54)	0.13 (-0.40 to 0.65)	--
Growth performance ~ gill area index	3.08 (2.62 to 3.54)	0.13 (-0.39 to 0.63)	0.50 (0.03 to 0.97)

Table 4.5 Comparison of coefficients and their 95% Bayesian Credible Intervals (BCI) for the relationship of growth performance and the gill area index as calculated using (1) empirically estimated *d* values, (2) *d* = 0.8, and (3) *d* predicted from the relationship of *d* and maximum size in Pauly (1981).

The model where gill area index was calculated using empirically estimated ontogenetic slope values was estimated using a Bayesian multilevel modeling framework in *rstan* in R v.4.0.2 and the models where gill area index was calculated using either *d* = 0.8 or *d* predicted from Pauly (1981) were estimated using a Bayesian linear regression using the *brms* package in R.v.4.0.2. All slopes were standardized in the model prior to estimating gill area index, which was $\log_{10}$-transformed prior to the second level of the (see text and SI).

Estimation of gill area index in model for growth performance ~ gill area index	Intercept (95% CI)	Slope (95% CI)
Empirically estimated	3.08 (2.61 to 3.54)	0.13 (-0.40 to 0.65)
d = 0.8	3.08 (2.64 to 3.53)	0.44 (0.00 to 0.88)
Predicted d	3.08 (2.62 to 3.54)	0.06 (-0.43 to 0.54)

Table 4.6 Comparison of coefficients and their 95% Bayesian Credible Intervals (BCI) for the relationship of growth performance, activity level (as measured by caudal fin aspect ratio), and gill surface area, as measured by (1) the ontogenetic intercept, (2) the ontogenetic slope, and (3) gill area index.

All models were estimated using a Bayesian multilevel modeling framework in Stan using the package *rstan* in R v.4.0.2. All predictors in the second level of the model were standardized and thus the effect sizes for the slopes are relative to each other (see text and SI). GP = growth performance, CFAR = caudal fin aspect ratio, GSA = gill surface area, VIF = variance inflation factor, and COR = correlation matrix value.

Model parameterization of the second level	Intercept (95% CI)	CFAR Slope (95% CI)	GSA slope (95% CI)	Phylogenetic signal (λ)	Relative importance of CFAR vs. gill surface area	VIF	COR
growth performance ~ activity level +							
intercept	2.95 (2.51 to 3.38)	0.60 (0.21 to 1.00)	0.11 (-0.35 to 0.58)	--	0.60/0.11 = 5.5	1.16	0.29
intercept	2.95 (2.52 to 3.39)	0.60 (0.20 to 1.00)	0.11 (-0.38 to 0.58)	0.50 (0.03 to 0.98)	--	--	--
slope	2.95 (2.52 to 3.38)	0.62 (0.25 to 0.99)	0.19 (-0.29 to 0.67)	--	0.62/0.19 = 3.3	1.02	0.25
slope	2.95 (2.52 to 3.39)	0.62 (0.24 to 0.99)	0.19 (-0.29 to 0.65)	0.50 (0.02 to 0.98)	--	--	--
gill area index	2.95 (2.51 to 3.39)	0.64 (0.27 to 1.02)	-0.04 (-0.52 to 0.43)	--	0.64/0.04 = 16	1.05	0.09
gill area index	2.94 (2.52 to 3.38)	0.64 (0.26 to 1.03)	-0.04 (-0.52 to 0.44)	0.50 (0.03 to 0.97)	--	--	--

Table 4.7 Comparison of coefficients and 95% Bayesian Credible Intervals (BCI) for the relationship of the growth coefficients (*k*), asymptotic size (W_∞), and gill surface area, as measured by (1) the ontogenetic intercept, (2) the ontogenetic slope, and (3) gill area index.

All models were estimated using a Bayesian multilevel modeling framework in Stan using the package rstan in R v.4.0.2. All predictors in the second level of the model were standardized and thus the effect sizes for the slopes are relative to each other (see text and SI). GSA = gill surface area, VIF = variance inflation factor, and COR = correlation matrix value.

Model parameterization of the second level	Intercept (95% CI)	W_∞ Slope (95% CI)	GSA slope (95% CI)	Phylogenetic signal (λ)	Relative importance of W_∞ vs. gill surface area	VIF	COR
$k \sim W_\infty +$							
intercept	-0.55 (-0.68 to -0.42)	-0.26 (-0.38 to -0.13)	-0.08 (-0.22 to 0.06)	--	-0.26/-0.08 = 3.25	1.14	0.35
intercept	-0.55 (-0.68 to -0.42)	-0.26 (-0.39 to -0.14)	-0.06 (-0.20 to 0.07)	0.50 (0.03 to 0.97)	--	--	--
slope	-0.55 (-0.68 to -0.42)	-0.27 (-0.40 to -0.14)	-0.05 (-0.19 to 0.09)	--	-0.27/-0.05 = 5.4	1.08	0.27
slope	-0.55 (-0.68 to -0.41)	-0.28 (-0.40 to -0.15)	-0.03 (-0.17 to 0.12)	0.50 (0.03 to 0.97)	--	--	--
gill area index	-0.55 (-0.69 to -0.41)	-0.28 (-0.40 to 0.15)	-0.03 (-0.17 to 0.11)	--	-0.28/-0.03=9.33	1.02	0.13
gill area index	-0.55 (-0.68 to -0.41)	-0.28 (-0.40 to -0.15)	-0.03 (-0.17 to 0.11)	0.50 (0.02 to 0.98)	--	--	--

4.7. Figures

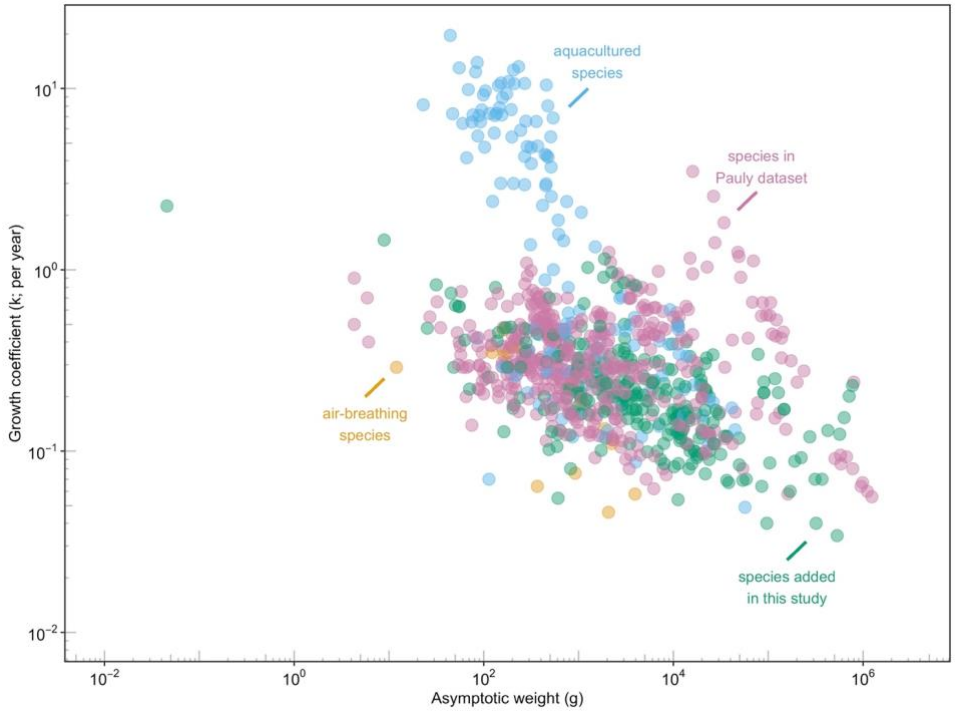

Figure 4.1 The somatic growth coefficient and asymptotic weight from the von Bertalanffy growth function are inversely related across the 132 fish species included in our reanalysis of the relationship between growth performance and gill surface area.

Each data point represents a single species-specific estimate of the ($\log_{10}$) growth coefficient and ($\log_{10}$) asymptotic weight and all estimates for each of the 132 species recorded in Fishbase are plotted separately (thus a given species could have multiple data points). Colors indicate the category or type of species: species traditionally used in aquaculture (blue), species that are known to be capable of air-breathing (yellow), species included in the original analysis of Pauly (1981; light purple), and species that were added to Pauly (1981)'s dataset (green).

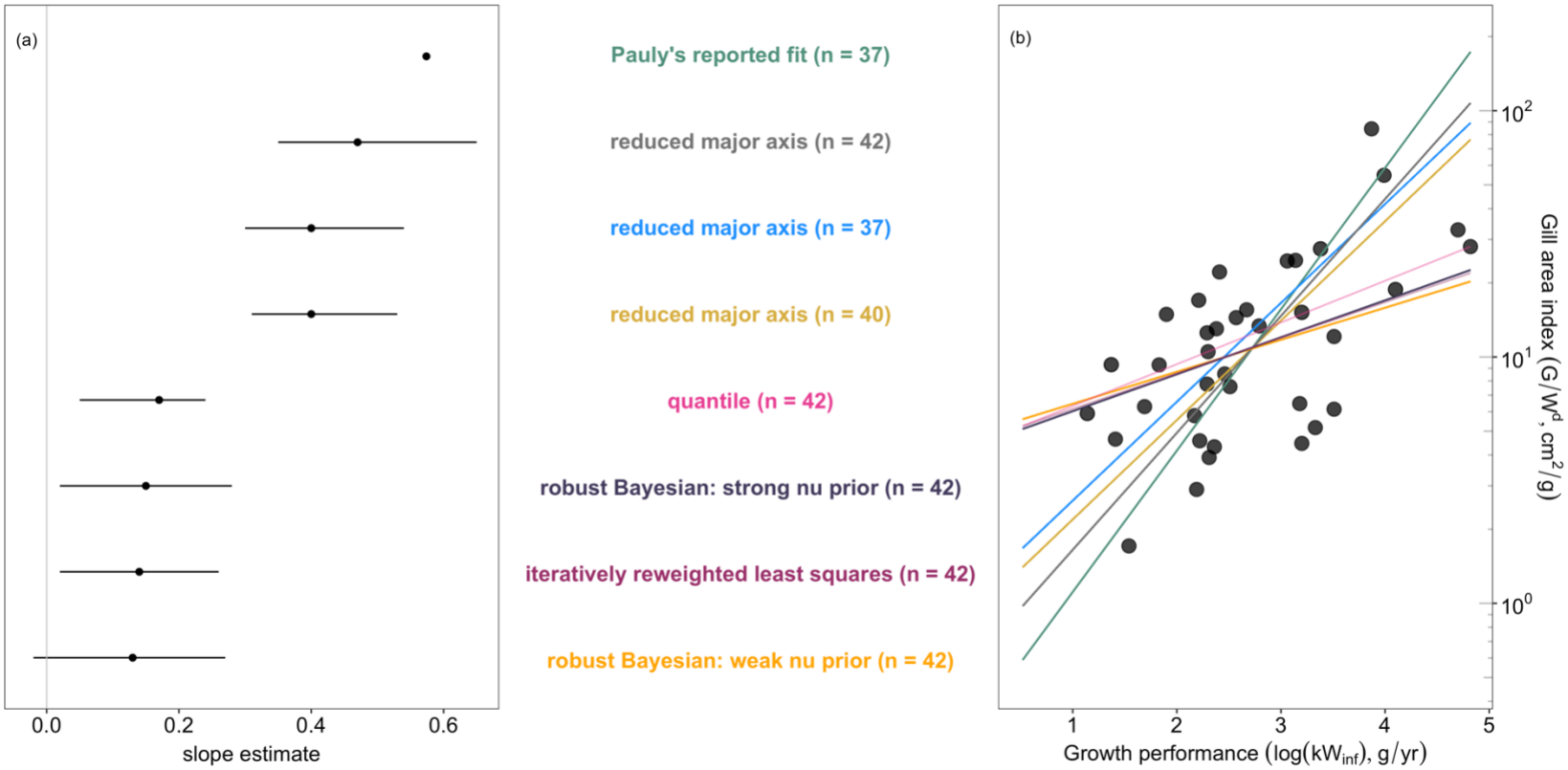

Figure 4.2 The significance of the relationship of growth performance and gill area index is dependent upon the type of regression used.

(a) A coefficient plot of the mean slope (black dot) and 95% intervals (confidence intervals for all non-Bayesian models, credible intervals for all Bayesian models) for all models examined. The vertical grey line indicates zero. (b) The relationship of ($\log_{10}$) growth performance and ($\log_{10}$) gill area index depending on various regression methods.

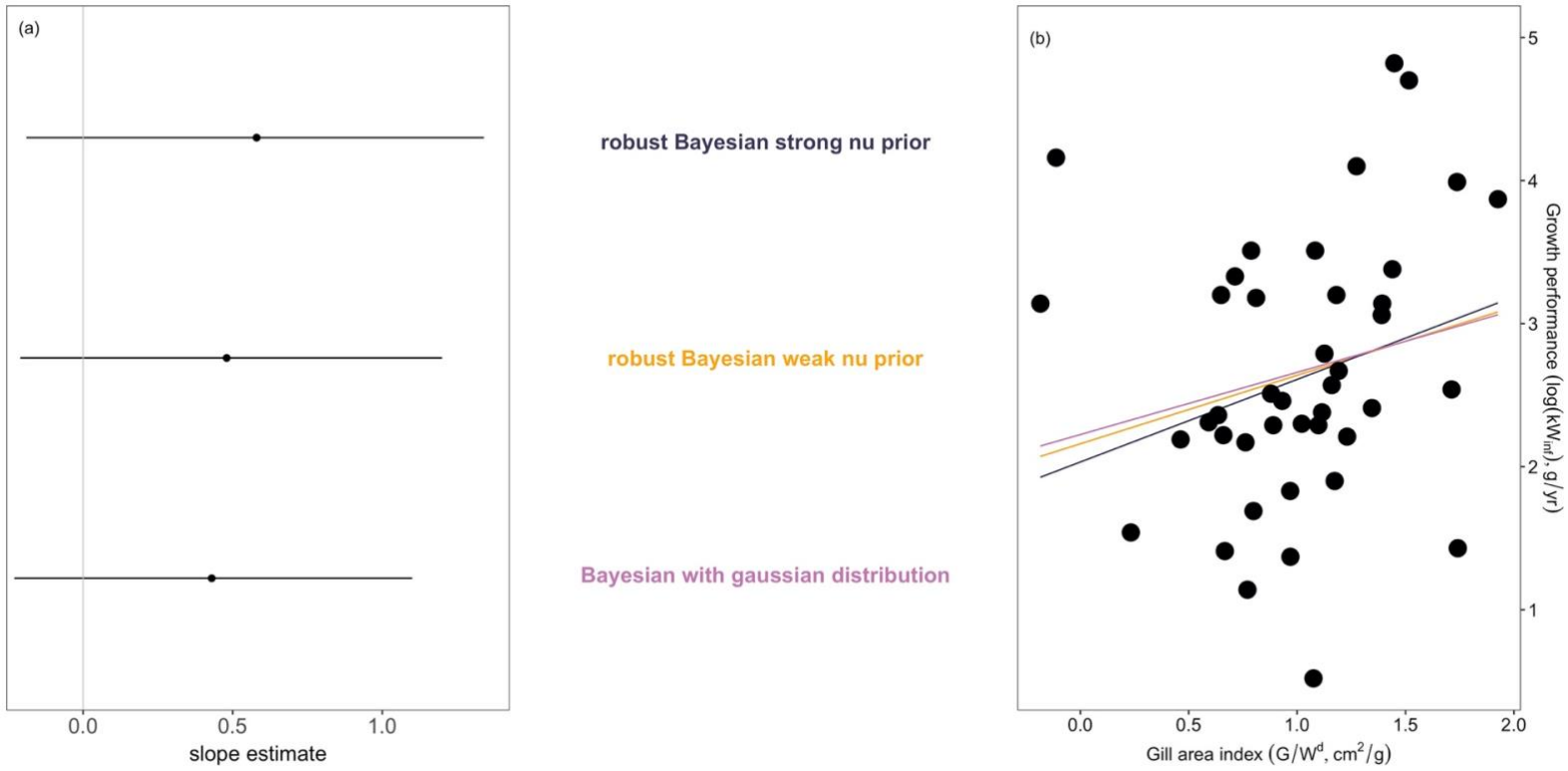

Figure 4.3 The relationship of growth performance and gill area index for the 42 fish species in the Pauly (1981) dataset as parameterized according to the GOLT's prediction that gill surface area constrains growth in fishes.
(a) A coefficient plot of the mean slope (black dot) and 95% Bayesian Credible Intervals (BCIs) for both Bayesian robust regression models (weak versus strong prior on nu) and the Bayesian regression with a Gaussian distribution. The vertical grey line indicates zero. (b) The relationship of ($\log_{10}$) gill area index and ($\log_{10}$) growth performance for those three same models. The model fit is equivalent regardless of model; the 95% BCIs for all three models overlap with zero.

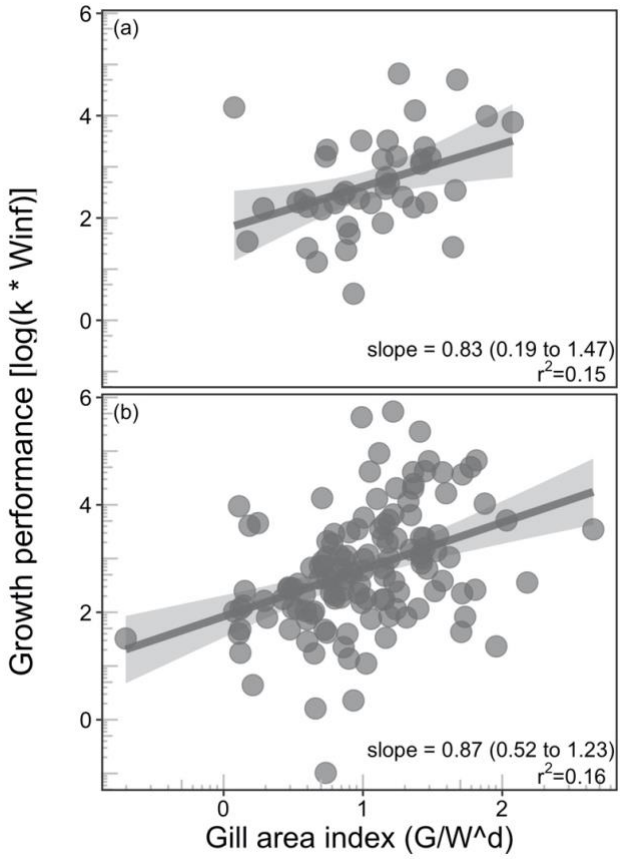

Figure 4.4 The relationship bwtween (log_{10}) growth performance and (log_{10}) gill area index does not significantly differ between the (a) 42 fish species in the Pauly (1981) dataset and the (b) 132 fish species in which gill surface area data has become available in the forty years since this relationship was first examined.
The model was parameterized according to the GOLT's prediction that gill surface area constrains growth in fishes and with gill area index estimated using *d = 0.8.* The model fits were estimated Bayesian linear regression using the *brm* function in the *brms* package in R.v.4.0.2.

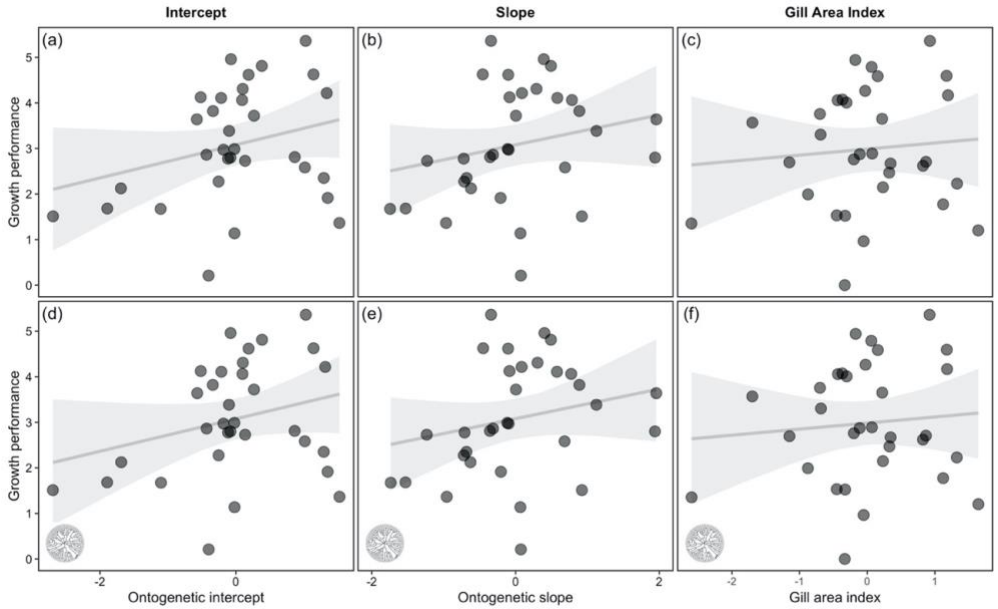

Figure 4.5 Little to no relationship of (log_{10}) growth performance and gill surface area exists when decomposing the allometry of gill surface area into the (a) ontogenetic intercept (the species-specific gill surface area at 300 g of body mass) and (b) the ontogenetic slope (the species-specific rate of increase in gill surface area with body mass), (d,e) with or (a,b) without a phylogeny.

There is also no relationship between (log_{10}) growth performance and the gill area index regardless of whether a phylogeny is included (c,f). Species-specific ontogenetic regression coefficients and their relationships with growth performance were estimated in a Bayesian multilevel model where the first level estimated the ontogenetic regression coefficients, and the second level estimated the relationship of growth performance and the ontogenetic intercept or the ontogenetic slope. The relationship between growth performance and gill area index was also estimated using a Bayesian multilevel model in which gill area index for each species was estimated from the ontogenetic slope (and mean gill surface area and mean body mass data) resulting from the first level of the model, and then the second level estimated the relationship between growth performance and those gill area index estimates. Intercepts and slopes were standardized in the model prior to the second level and the gill area index was log_{10}-transformed (see text and SI for more detail). The fit lines represent the fitted growth performance for each value of the respective gill surface area measure, and the grey shaded region represents the 95% Bayesian Confidence Interval. The 95% BCIs for all models overlapped with zero (see Table 4). The phylogenetic tree in the lower left corner of the bottom row indicates the model incorporated a phylogenetic tree.

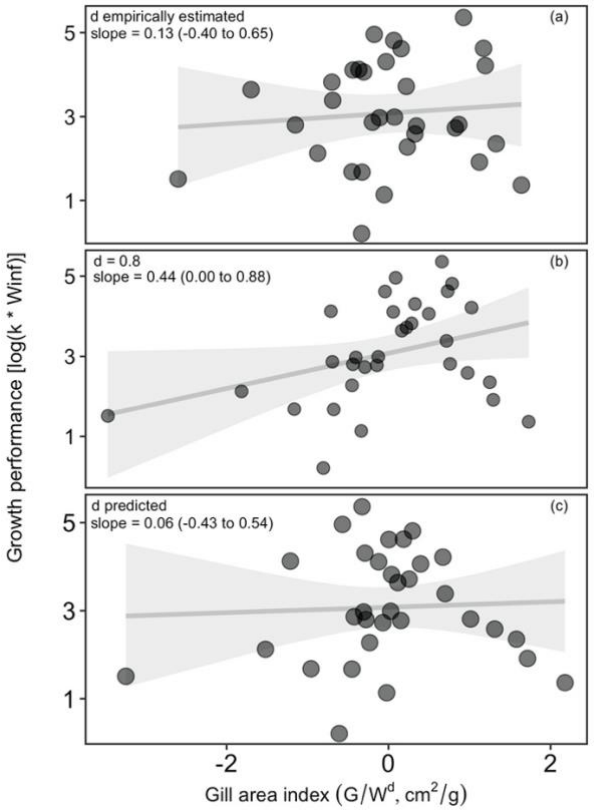

Figure 4.6 The relationship between (log_{10}) growth performance and (log_{10}) gill area index is not significant regardless of how gill area index is calculated: (a) gill area index calculated from empirically estimated *d* values, (b) gill area index calculated using *d* = 0.8, and (c) gill area index calculated from the relationship of *d* and maximum size from Pauly (1981).

All models were estimated using the 'raw dataset' of 32 species with raw gill surface area and body mass data. The relationship in (a) was estimated using a Bayesian multilevel modeling framework (see text), and the relationship in (b) and (c) was estimated using Bayesian linear regression (see text). The fit lines represent the fitted growth performance for each value of gill area index and the grey shaded region represents the 95% Bayesian Confidence Interval. The 95% BCIs for all models overlapped with zero.

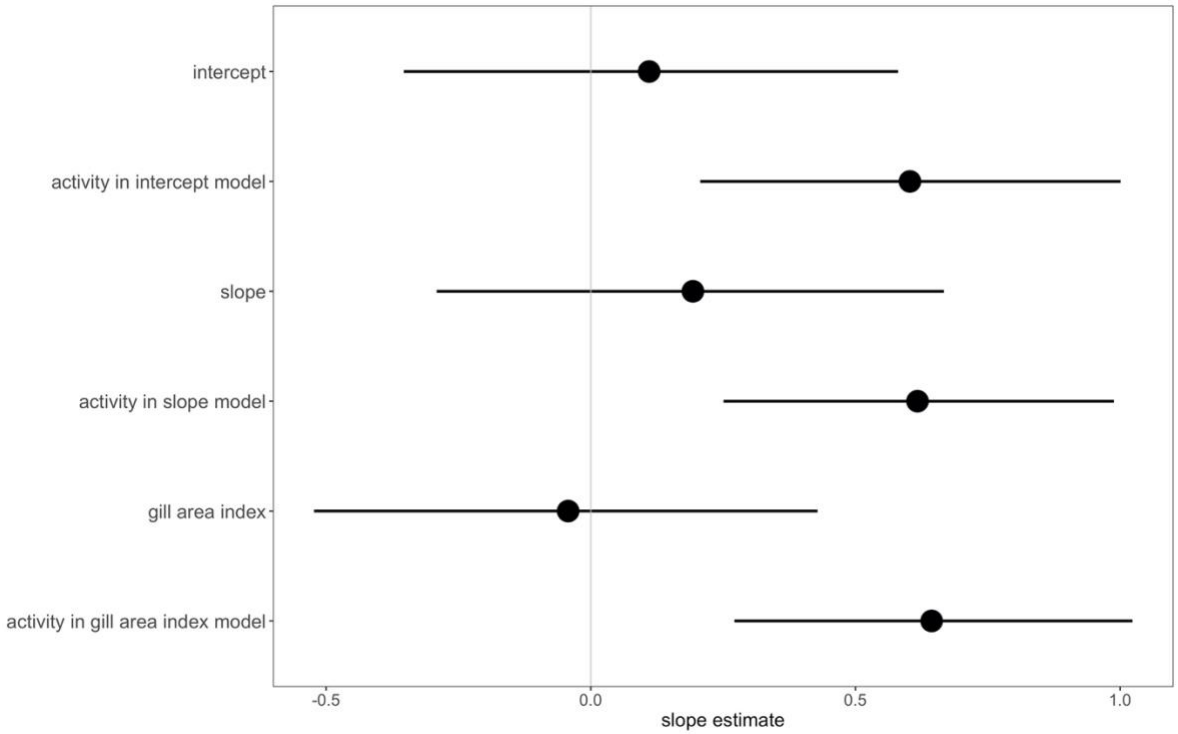

Figure 4.7 Activity level (as measured by caudal fin aspect ratio) explains more variance in growth performance compared to gill surface area as measured by the ontogenetic intercept, ontogenetic slope, or gill area index

The mean (black dot) and 95% Bayesian Credible Interval (BCI, black line) of the standardized effect sizes for the slope values in all three models as estimated by a Bayesian multilevel modeling framework (see text and SI). In all three models, the slope value for the metric of gill surface area overlapped with zero, but the slope value for activity did not.

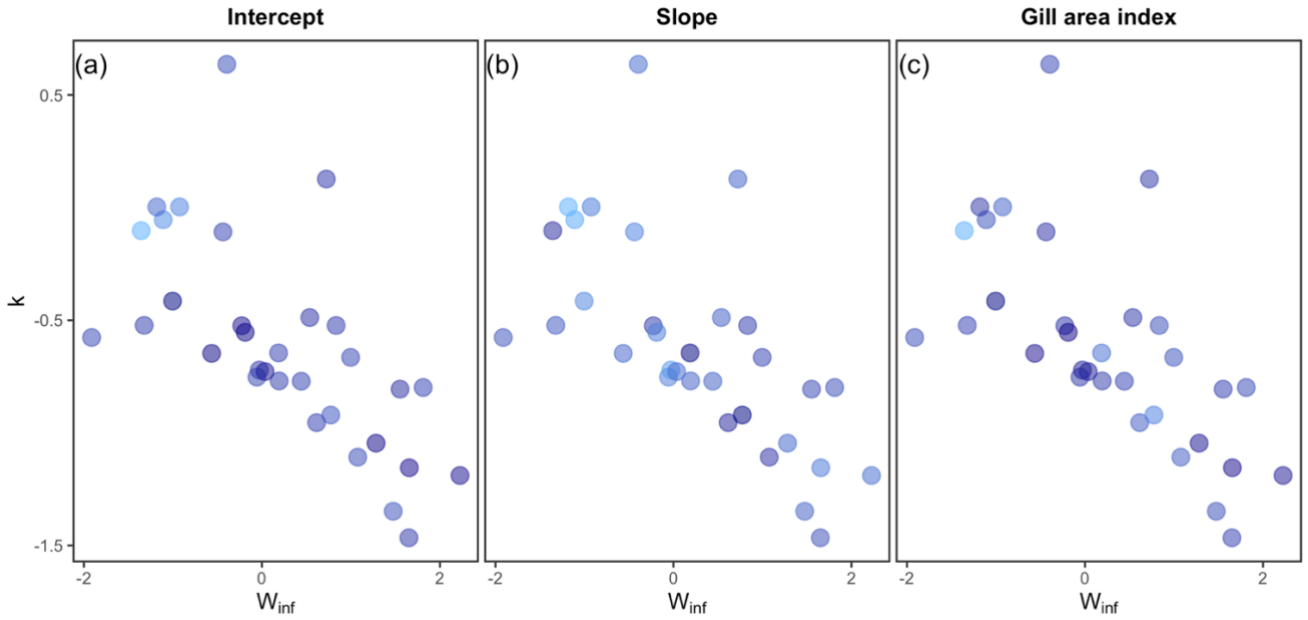

Figure 4.8 Gill surface area, as measured by the species-specific (a) ontogenetic intercept or (b) ontogenetic slope of the relationship of gill surface area and body mass, or the (c) gill area index, does not differ across fishes that differ in von Bertalanffy growth coefficients (*k*) and asymptotic sizes (W_∞).

Gill surface area is indicated by a gradient of color, with darker blue indicating a higher intercept, slope, or gill area index, and lighter blue indicating a lower intercept, slope, or gill area index. Species-specific ontogenetic regression coefficients and their relationships with k and W_∞ were estimated in a Bayesian multilevel model where the first level estimated the ontogenetic regression coefficients, and the second level estimated the relationship of k, W_∞, and the ontogenetic intercept or the ontogenetic slope. The relationship between k, W_∞, and gill area index was also estimated using a Bayesian multilevel model in which gill area index for each species was estimated from the ontogenetic slope (and mean gill surface area and mean body mass data) resulting from the first level of the model, and then the second level estimated the relationship between growth performance and those gill area index estimates. Intercepts and slopes were standardized in the model prior to the second level and the gill area index was $\log_{10}$-transformed (see text and SI for more detail.

4.8. References

Anderson, S.C., Branch, T.A., Cooper, A.B. and Dulvy, N.K. (2017) Black-swan events in animal populations. *Proc. Nat. Acad. Sci.* **114**, 3252-3257.

Audzijonyte, A., Barneche, D.R., Baudron, A.R., Belmaker, J., Clark, T.D., Marshall, C.T., Morrongiello, J.R., van Rijn, I. (2019) Is oxygen limitation in warming waters a valid mechanism to explain decreased body sizes in aquatic ectotherms? *Glob. Ecol. Biogeogr.*, *28*, 64-77.

Barneche, D. R., Robertson, D. R., White, C. R., & Marshall, D. J. (2018). Fish reproductive-energy output increases disproportionately with body size. *Science*, *360*(6389), 642-645.

Beverton, R. J. H., & Holt, S. J. (1959). A review of the lifespans and mortality rates of fish in nature, and their relation to growth and other physiological characteristics. In *CIBA Foundation colloquia on ageing* (Vol. 5, pp. 142-180).

Bigman, J.S., M'Gonigle, L.K., Wegner, N.C., & Dulvy, N.K. (2021). Respiratory capacity is twice as important as temperature in driving patterns of metabolic rate across the vertebrate tree of life. *Sci. Adv.*

Bigman, J. S., Pardo, S. A., Prinzing, T. S., Dando, M., Wegner, N. C., & Dulvy, N. K. (2018). Ecological lifestyles and the scaling of shark gill surface area. *J. Morph.*, *279*(12), 1716-1724.

Blier, P. U., Pelletier, D., & Dutil, J. D. (1997). Does aerobic capacity set a limit on fish growth rate? *Rev. Fish. Sci.*, *5*(4), 323-340.

Boettiger, C., Lang, D. T., and Wainwright, P. C. (2012) rfishbase: exploring, manipulating and visualizing FishBase data from R. *J. Fish Biol.*, *81.6*, 2030-2039.

Brown, J. H., Gillooly, J. F., Allen, A. P., Savage, V. M., & West, G. B. (2004). Toward a metabolic theory of ecology. *Ecology*, *85*(7), 1771-1789.

Bürkner, P.C. (2017). *brms*: An R Package for Bayesian Multilevel Models Using Stan. *J. Stat. Softw.*, *80*(1), 1-28.

Bürkner, P.C. (2018). Advanced Bayesian Multilevel Modeling with the R Package *brms*. *The R Journal*, *10*(1), 395-411.

Burnham. K.P., Anderson. D.R. (2002) Model selection and multimodel inference: a practical information theoretic approach, 2nd edn. New York, NY: Springer.

Chang, J., Rabosky. D.L., Smith. S.A., Alfaro, M.E. (2019). An R package and online resource for macroevolutionary studies using the ray-finned fish tree of life. *Methods Ecol. Evol.*, *10*(7), 1118-1124.

Cheung, W. & Pauly, D. (2016) *in* Explaining ocean warming: Causes, Scale, Effects and Consequences (*eds*. Laffoley, D. & Baxter, J.) 239–253. International Union for Conservation of Nature.

Cheung, W.W., Sarmiento, J.L., Dunne, J., Frölicher, T.L., Lam, V. W., Palomares, M. D., Watson, R., & Pauly, D. (2013). Shrinking of fishes exacerbates impacts of global ocean changes on marine ecosystems. *Nat. Clim. Change*, *3*(3), 254-258.

De Jager, S., & Dekkers, W. J. (1975). Relations between gill structure and activity in fish. *Neth. J. Zool.*, *25*(3), 276-308.

Deutsch, C., Penn, J. L., & Seibel, B. (2020). Metabolic trait diversity shapes marine biogeography. *Nature*, *585*(7826), 557-562.

Ebert, D. A., Fowler, S. L., & Compagno, L. J. V. (2016). Sharks of the world: A fully illustrated guide. Portland, Oregon: Wild Nature Press.

Fahrmeir, L., Kneib, T., Lang, S., & Marx, B. (2013). Regression models. In *Regression* (pp. 21-72). Springer, Berlin, Heidelberg.

Felsenstein, J. (1985). Phylogenies and the comparative method. *Am. Nat.*, *125*(1), 1-15.

Forster, J., Hirst, A. G., & Atkinson, D. (2012). Warming-induced reductions in body size are greater in aquatic than terrestrial species. *Proc. Nat. Acad. Sci., 109*(47), 19310-19314.

Fox, J., & Weisberg, S. (2012). Robust regression. *An R and S-Plus companion to applied regression*, *91*: 1 – 16.

Freckleton, R. P. (2009). The seven deadly sins of comparative analysis. *J. Evol. Biol.*, *22*(7), 1367-1375.

Froese, R. and D. Pauly. Editors. (2020). FishBase. World Wide Web electronic publication.
www.fishbase.org, version (12/2020).

Gabry, J., Simpson, D., Vehtari, A., Betancourt, M., & Gelman, A. (2019). Visualization in Bayesian workflow. *J. R. Stat. Soc. Ser. A Stat. Soc.*, *182*(2), 389-402.

Gelman, A. & Hill, J. (2007) Data analysis using regression and multilevel/hierarchical models. Cambridge University Press, 625 pgs.

Gelman, A., Hill, J., & Vehtari, A. (2020). *Regression and other stories*. Cambridge University Press.

Grady, J. M., Enquist, B. J., Dettweiler-Robinson, E., Wright, N. A., & Smith, F. A. (2014). Evidence for mesothermy in dinosaurs. *Science*, *344*(6189), 1268-1272.

Gray, I. E. (1954). Comparative study of the gill area of marine fishes. *Biol. Bull.*, 107, 219–255.

Hampel, F. R. (2001). Robust statistics: A brief introduction and overview. In *Research report/Seminar für Statistik, Eidgenössische Technische Hochschule (ETH)* (Vol. 94). Seminar für Statistik, Eidgenössische Technische Hochschule.

Harmon, L. (2018). Phylogenetic comparative methods: learning from trees. Online book. https://lukejharmon.github.io/pcm/

Hoefnagel, K. N., & Verberk, W. C. (2015). Is the temperature-size rule mediated by oxygen in aquatic ectotherms? *J. Therm. Biol.*, *54*, 56-65.

Hughes, G. M. (1966). The dimensions of fish gills in relation to their function. *J. Exp. Biol.*, *45*(1), 177-195.

Hughes G.M. (1995). The gills of the coelacanth, *Latimeria chalumnae,* a study in relation to body size. *Phil. Trans.: Biol. Sci. 347*(1322), 427 – 438.

Hughes, G.M. & Morgan, M. (1973). Supplement 90005 to The structure of fish gills in relation to their respiratory function. Supplement 90005 to *Biol. Rev.*, 48, 419 – 475.

Hutchings, J. A. (2002). Life histories of fish. *Handbook of Fish Biology and Fisheries: Fish Biology*, 149-174.

Jenkins, D. G., & Quintana-Ascencio, P. F. (2020). A solution to minimum sample size for regressions. *PloS One*, *15*(2), e0229345.

Kilmer, J. T., & Rodríguez, R. L. (2017). Ordinary least squares regression is indicated for studies of allometry. *J. Evol. Biol.*, *30*(1), 4-12.

Koenker, R. (2020). quantreg: Quantile Regression. R package version 5.73. <https://CRAN.R-project.org/package=quantreg>

Kruschke, J.K. (2014). Doing Bayesian Data Analysis: A Tutorial with R, JAGS, and Stan. Elsevier, 759 pgs.

Juan-Jordá, M. J., Mosqueira, I., Freire, J., & Dulvy, N. K. (2013). Life in 3-D: life history strategies in tunas, mackerels and bonitos. *Rev. Fish Biol. Fish.*, *23*(2), 135-155.

Lange, K. L., Little, R. J., & Taylor, J. M. (1989). Robust statistical modeling using the t distribution. *J. Am. Stat. Assoc.*, *84*(408), 881-896.

Lefevre, S., McKenzie, D. J., & Nilsson, G. E. (2017). Models projecting the fate of fish populations under climate change need to be based on valid physiological mechanisms. *Glob. Chang. Biol.*, *23*(9), 3449-3459.

Lefevre, S., McKenzie, D. J., & Nilsson, G. E. (2018). In modelling effects of global warming, invalid assumptions lead to unrealistic projections. *Glob. Chang. Biol.*, *24*(2), 553-556.

Lefevre, S., Wang, T., & McKenzie, D. J. (2021). The role of mechanistic physiology in investigating impacts of global warming on fishes. *J. Exp. Biol.*, *224*.

Legendre, P. (2018). lmodel2: Model II Regression. R package version 1.7-3. <https://CRAN.R-project.org/package=lmodel2>

Marshall, D. J., & White, C. R. (2019). Aquatic life history trajectories are shaped by selection, not oxygen limitation. *Trends Ecol. Evol.*, *34*(3), 182-184.

McArdle, B. H. (2003). Lines, models, and errors: regression in the field. *Limnol. Oceanogr.*, *48*(3), 1363-1366.

Morais, R. A., & Bellwood, D. R. (2018). Global drivers of reef fish growth. *Fish Fish.*, *19*(5), 874-889.

Palomares, M. L., & Pauly, D. (1989). A multiple regression model for prediction the food consumption of marine fish populations. *Mar. Freshwater Res.*, *40*(3), 259-273.

Palzenberger, M., & Pohla, H. (1992). Gill surface area of water-breathing freshwater fish. *Rev. Fish Biol. Fish., 2*, 187–216.

Pauly, D. (1981). The relationships between gill surface area and growth performance in fish: a generalization of von Bertalanffy's theory of growth. Berichte der Deutschen Wissenchaftlichen Kommission für *Meeresforschung 28*(4): 251-282.

Pauly, D. (1991). Growth performance in fishes: rigorous description of patterns as a basis for understanding causal mechanisms. *Aquabyte, Newsletter of the Network of Tropical Aquaculture Scientists, 4*(3):3-6.

Pauly, D. (1998). Tropical fishes: patterns and propensities. *J. Fish Biol.*, *53*, 1-17.

Pauly, D. (2010). Gasping fish and panting squids: oxygen, temperature and the growth of water-breathing animals. Excellence in Ecology, Vol. 22. International Ecology Institute, 216 pgs.

Pauly, D. (2021). The gill-oxygen limitation theory (GOLT) and its critics. *Sci. Adv.*, *7*(2), eabc6050.

Pennell, M. W., & Harmon, L. J. (2013). An integrative view of phylogenetic comparative methods: connections to population genetics, community ecology, and paleobiology. *Ann. N.Y. Acad. Sci.*, *1289*(1), 90-105.

R Core Team (2020). R: A language and environment for statistical computing. R Foundation for Statistical Computing, Vienna, Austria. URL http://www.R-project.org/

Rabosky, D. L., Chang, J., Title, P. O., Cowman, P. F., Sallan, L., Friedman, M., Kashner, K., Garilao, C., Near, T. J., Coll, M., Alfaro, M. E. (2018). An inverse latitudinal gradient in speciation rate for marine fishes. *Nature, 559*(7714), 392–395.

Revell, L. J. (2010). Phylogenetic signal and linear regression on species data. *Methods Ecol. Evol.*, *1*(4), 319-329.

Reynolds, J. D. (2003). Life histories and extinction risk. Chapter 11 in *Macroecology. Blackwell Publishing, Oxford, UK*, pgs. 195-217.

Reynolds, JD, Jennings, S & Dulvy, NK. (2001). Life histories of fishes and population responses to exploitation. In: Conservation of Exploited Species (eds. JD Reynolds, GM Mace, KH Redford & JG Robinson), pp 148-168. Cambridge University Press, Cambridge.

Reznick, D. (1985). Costs of reproduction: an evaluation of the empirical evidence. *Oikos*, 257-267.

Reznick, D. N., Butler IV, M. J., Rodd, F. H., & Ross, P. (1996). Life-history evolution in guppies (Poecilia reticulata) 6. Differential mortality as a mechanism for natural selection. *Evolution*, *50*(4), 1651-1660.

Roff, D. A. (1984). The evolution of life history parameters in teleosts. *Can. J. Fish. Aquat. Sci.*, *41*(6), 989-1000.

Rousseeuw, P. J. (1984). Least median of squares regression. *J. Am. Stat. Assoc.*, *79*(388), 871-880.

Rubalcaba, J. G., Verberk, W. C., Hendriks, A. J., Saris, B., & Woods, H. A. (2020). Oxygen limitation may affect the temperature and size dependence of metabolism in aquatic ectotherms. *Proc. Nat. Acad. Sci.*, *117*(50), 31963-31968.

Sambilay Jr, V. C. (1990). Interrelationships between swimming speed, caudal fin aspect ratio and body length of fishes. *Fishbyte*, *8*(3), 16-20.

Satora, L., & Wegner, N. C. (2012). Reexamination of the Byczkowska-Smyk gill surface area data for European teleosts, with new measurements on the pikeperch, Sander lucioperca. *Rev. Fish Biol. Fish., 22*(1), 1-9.

Smith, R. J. (2009). Use and misuse of the reduced major axis for line-fitting. *Am. J. Phys. Anthropol.*, *140*(3), 476-486.

Stan Development Team. 2019. *Stan Modeling Language Users Guide and Reference Manual*, Version 2.19.2. http://mc-stan.org

Stearns, S. C. (1976). Life-history tactics: a review of the ideas. *Q. Rev. Biol.*, *51*(1), 3-47.

Stearns, S. C. (1989). Trade-offs in life-history evolution. *Funct. Ecol.*, *3*(3), 259-268.

Stearns, S. C. (1992). *The evolution of life histories* (No. 575 S81).

Stein, R. W., Mull, C. G., Kuhn, T. S., Aschliman, N. C., Davidson, L. N., Joy, J. B., Smith, G. J., Dulvy, N. K., and Mooers, A. O. (2018). Global priorities for conserving the evolutionary history of sharks, rays and chimaeras. *Nat. Ecol. Evol.*, *2*(2), 288-298.

Symonds, M. R., & Blomberg, S. P. (2014). A primer on phylogenetic generalised least squares. In *Modern phylogenetic Comparative Methods and Their Application in Evolutionary Biology* (pp. 105-130). Springer, Berlin, Heidelberg.

Tsuboi, M., van der Bijl, W., Kopperud, B.T., Erritzøe, J., Voje, K.L., Kotrschal, A., Yopak, K.E., Collin, S.P., Iwaniuk, A.N., and Kolm, N. Breakdown of brain–body allometry and the encephalization of birds and mammals. *Nat. Ecol. Evol.,* 2**,** 1492–1500 (2018).

van Denderen, D., Gislason, H., van den Heuvel, J., & Andersen, K. H. (2020). Global analysis of fish growth rates shows weaker responses to temperature than metabolic predictions. *Glob. Ecol. Biogeogr.*, *29*(12), 2203-2213.

Vehtari, A., Gelman, A., & Gabry, J. (2017). Practical Bayesian model evaluation using leave-one-out cross-validation and WAIC. *Stat. Comput.*, *27*(5), 1413-1432.

Venables, W. N. & Ripley, B. D. (2002) Modern Applied Statistics with S. Fourth Edition. Springer, New York. ISBN 0-387-95457-0

Verberk, W. C., Atkinson, D., Hoefnagel, K. N., Hirst, A. G., Horne, C. R., & Siepel, H. (2020). Shrinking body sizes in response to warming: explanations for the temperature–size rule with special emphasis on the role of oxygen. *Biol. Rev.*, *96*(1), 247-268.

Wang, C., & Blei, D. M. (2018). A general method for robust Bayesian modeling. *Bayesian Anal.*, *13*(4), 1163-1191.

Wegner, N. C. (2011). Gill respiratory Morphometrics. In A. P. Farrell (Ed.), Encyclopedia of fish physiology: From genome to environment (Vol. 2, pp. 803–811). San Diego, CA: Academic Press.

4.9. Supplementary Information

4.9.1. Supplementary Methods

Model overview

Model parameterization

We constructed and compared phylogenetic Bayesian multilevel (i.e., hierarchical) linear regression models in R v.4.0.2 in Stan using the package *rstan* (Stan Development Team 2019; R Core Team 2020).

All multilevel models constructed in this study shared the same foundation and then were built upon to either add additional covariates (e.g., activity level) or a phylogenetic random effect. After the first level of the model, the relevant gill surface area metric was extracted (ontogenetic intercept or ontogenetic slope of gill surface area for each species) or calculated (gill area index). See text for a more detailed overview of how gill area index is estimated.

Basic parametrization

First level of the model:

$GSA_i = \alpha + \Sigma_j \beta_j x_{i,j} + \varepsilon_i$

$\hat{\varepsilon} \sim \text{normal}\ (0, \sigma_e^2)$

$\alpha \sim$ student-t (3, 0, 10)

$\beta_{mass} \sim$ student-t (3, 0, 10)

$\sigma_e^2 \sim$ half-Cauchy (0, 10)

Here, GSA_i is the response variable (mean whole-organism gill surface area), α is the intercept, and β_{mass} is the slope of the body mass associated with gill surface area, x_{mass}.

The priors on the intercept, α, slope, β_{mass}, and error, σ_e^2, are also reported and our choice of priors is explained below.

Second level of the model:

$Y_i = \alpha + \Sigma_j \beta_j x_{i,j} + \varepsilon_i$

$\hat{\varepsilon} \sim$ multivariate normal $(0, \sigma_e^2)$

$\alpha \sim$ student-t (3, 0, 10)

$\beta_j \sim$ student-t (3, 0, 10)

$\sigma_e^2 \sim$ half-Cauchy (0, 10)

Here, Y_i is the response variable (growth performance for Questions II.i. – II.iii., k for Question II.iv.), α is the intercept, and β_j is the slope of the predictor (either the ontogenetic intercept or the ontogenetic slope of gill surface area, or, the gill area index for each species), $x_{i,j}$ for each species. The priors on the intercept, α, slope, β_j, and error, σ_e^2, are also reported and our choice of priors is explained below.

Other covariates (caudal fin aspect ratio for question II.iii. and asymptotic weight for question II.iv.) were added on as needed.

<u>Models with phylogenetic parameterization</u>

Second level of the model:

$Y_i = \alpha + \Sigma_j \beta_j x_{i,j} + \varepsilon_i$

$\hat{\varepsilon} \sim$ multivariate normal $(0, \sigma_e^2 * C_{phylo})$

$C_{phylo} = \lambda * V + (1 - \lambda) * I$

α ~ student-t (3, 0, 10)

β_j ~ student-t (3, 0, 10)

σ_e^2 ~ half-Cauchy (0, 10)

Here, the first level of the model does not change, but the second level does. The second level of the model is as described above with the change in the residual error structure. Following (Frishkoff *et al*. 2017), we assumed the residual error, ε_i, to be distributed according to a multivariate normal distribution, where $\hat{0}$ is a vector with length N, σ_e^2 is the variation in responses to the predictors ($\beta_j x_{i,j}$), and C_{phylo} is the N×N correlation matrix resulting from the phylogeny. The strength of the phylogenetic signal, λ, in the residuals under a model of evolution of Brownian motion is estimated according to $C_{phylo} = \lambda * V + (1 - \lambda) * I$, where V is the variance covariance matrix from the phylogeny, and I is an identity matrix of N×N values with σ_e^2 on the diagonal.

Choice of priors

We used weakly informative regularizing priors based on recommendations for Stan (https://github.com/stan-dev/stan/wiki/Prior-Choice-Recommendations). As λ (phylogenetic signal) has an equal chance of taking any value within the bounds of zero to one, we used a prior with a uniform distribution from zero to one. As σ_e^2 (variation in responses to the predictors ($\beta_j x_{i,j}$) can only be positive, we used a half-Cauchy prior with a location of zero and a scale of ten. Priors are also shown below for each set of models.

Simulations

To assess the number of individuals required to estimate a reliable slope estimate for the relationship between gill surface area and growth, we simulated how the estimated slope (and intercept) value varied with the number of individuals included in its estimation, based on a simple linear regression ($y = \beta_0 + \beta_1 * x_1 + \varepsilon$).

To do so, we first defined a dataset of 100 individuals that ranged in body mass over four orders of magnitude (10g – 100000g). Next, we simulated the gill surface area data for these individuals at their given body mass based on simulated random errors and defined regression coefficients. For this, we simulated random errors for each unique observation (n = 100) from a normal distribution with a mean of zero and a standard deviation of 0.08.

This value for the standard deviation was chosen as it was the mean standard deviation (sigma) for all gill surface area – body mass regressions for all species in our dataset with at least eight individuals (this threshold was chosen based on Jenkins & Quintana-Ascencio 2020). Similarly, we set the regression coefficients (intercept and slope) to the mean values estimated from these same regressions (mean slope = 0.85, mean intercept = 0.90). Next, we simulated the regression using the body mass and gill surface area data 1000 times and assessed the accuracy of the predicted regression coefficients (i.e., did the estimated regression coefficients match the defined regression coefficients?).

Second, we repeated these simulations 1000 times each on subsets of the dataset where a specified number of individuals (0 – 97) were dropped. In other words, we simulated a regression 1000 times on a random subset of three individuals (the minimum number to obtain a standard error on the regression coefficients), then four individuals, then five, etc., all the way up to 100 individuals. Finally, we plotted the standard error of the mean slope and intercept for each of these regressions (Fig. S1).

Our simulations suggested that a threshold of eight individuals was sufficient for estimating reliable ontogenetic slope coefficients. We note, however, that this threshold of eight individuals, at least in our data simulations, is for a random spread of gill surface area and body mass (e.g., selecting individuals at random) as opposed to selecting a range of body size (e.g., individuals that span at least 33% of size range of species). Thus, a threshold of eight individuals of the same species to estimate an ontogenetic slope is likely conservative (i.e., fewer individuals may also result in a reliable slope based on the size range encompassed) yet produced reliable slope estimates that are within the known range of gill surface area slope values.

4.9.2. Supplementary Figures

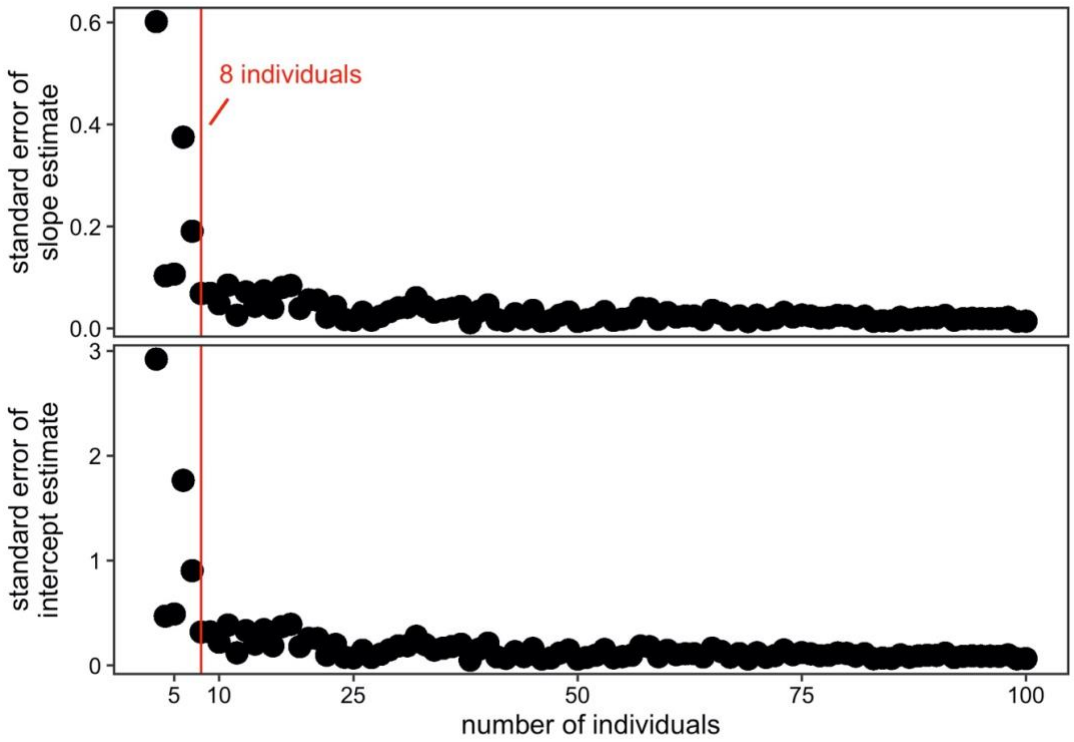

Figure S1. The change in the standard error of the slope (top row) and intercept (bottom row) resulting from simulations of the ontogenetic relationship between gill surface area and body mass with an increasing number of data points (individuals) included. The vertical red line on each plot indicates the threshold of eight individuals. For more detail, please see the Supplementary Methods.

4.9.3. Supplementary Tables

Table S1. The list of the 132 species in the full dataset (see text).

Taxon	Binomial	Common name
Chondrichthyan	*Alopias pelagicus*	Pelagic Thresher
Chondrichthyan	*Alopias superciliosus*	Bigeye Thresher
Chondrichthyan	*Alopias vulpinus*	Common Thresher Shark
Chondrichthyan	*Carcharhinus acronotus*	Blacknose Shark
Chondrichthyan	*Carcharhinus isodon*	Finetooth Shark
Chondrichthyan	*Carcharhinus limbatus*	Blacktip Shark
Chondrichthyan	*Carcharhinus obscurus*	Dusky Shark
Chondrichthyan	*Carcharhinus plumbeus*	Sandbar Shark
Chondrichthyan	*Carcharodon carcharias*	White Shark
Chondrichthyan	*Galeocerdo cuvier*	Tiger Shark
Chondrichthyan	*Galeorhinus galeus*	Tope Shark
Chondrichthyan	*Isurus oxyrinchus*	Shortfin Mako
Chondrichthyan	*Prionace glauca*	Blue Shark
Chondrichthyan	*Rhinoptera bonasus*	Cownose Ray
Chondrichthyan	*Rhizoprionodon terraenovae*	Atlantic Sharpnose Shark
Chondrichthyan	*Scyliorhinus canicula*	Lesser Spotted Dogfish
Chondrichthyan	*Sphyrna lewini*	Scalloped Hammerhead
Chondrichthyan	*Sphyrna tiburo*	Bonnethead Shark
Chondrichthyan	*Torpedo marmorata*	Marbled Electric Ray
Chondrichthyan	*Triakis semifasciata*	Leopard Shark
Chondrichthyan	*Raja clavata*	Thornback Ray
Lobe-finned fish	*Latimeria chalumnae*	Coelacanth
Teleost	*Acanthocybium solandri*	Wahoo
Teleost	*Acipenser transmontanus*	White Sturgeon
Teleost	*Ameiurus nebulosus*	Brown Bullhead
Teleost	*Anabas testudineus*	Climbing Perch
Teleost	*Anguilla anguilla*	European Eel
Teleost	*Anguilla rostrata*	American Eel
Teleost	*Anoplopoma fimbria*	Sablefish
Teleost	*Archosargus probatocephalus*	Sheepshead
Teleost	*Balistes capriscus*	Grey Triggerfish
Teleost	*Barbatula barbatula*	Stone Loach
Teleost	*Boleophthalmus boddarti*	Boddart's Goggle-Eyed Goby
Teleost	*Brevoortia tyrannus*	Atlantic Menhaden
Teleost	*Callionymus lyra*	Common Dragonet
Teleost	*Caranx crysos*	Blue Runner

Taxon	Binomial	Common name
Teleost	*Carassius auratus*	Goldfish
Teleost	*Careproctus melanurus*	Blacktail Snailfish
Teleost	*Catostomus commersonii*	White Sucker
Teleost	*Centropristis striata*	Black Sea Bass
Teleost	*Chaenocephalus aceratus*	Blackfin Icefish
Teleost	*Channa punctata*	Spotted Snakehead
Teleost	*Channa striata*	Striped Snakehead
Teleost	*Cirrhinus mrigala*	Mgrial Carp
Teleost	*Clarias batrachus*	Philippine Catfish
Teleost	*Clupea harengus*	Atlantic Herring
Teleost	*Cobitis taenia*	Spined Loach
Teleost	*Comephorus dybowskii*	Little Baikal Oilfish
Teleost	*Conger conger*	European Conger
Teleost	*Coryphaena hippurus*	Dolphinfish
Teleost	*Cottocomephorus grewingkii*	Baikal Yellowfin
Teleost	*Cottus gobio*	European Bullhead
Teleost	*Ctenopharyngodon idella*	Grass Carp
Teleost	*Cynoscion regalis*	Weakfish
Teleost	*Echeneis naucrates*	Sharksucker
Teleost	*Glyptocephalus zachirus*	Rex Sole
Teleost	*Esox lucius*	Northern Pike
Teleost	*Euthynnus affinis*	Mackerel Tuna
Teleost	*Euthynnus alletteratus*	False Albacore
Teleost	*Eutrigla gurnardus*	Grey Gurnard
Teleost	*Gadus morhua*	Atlantic Cod
Teleost	*Gobius niger*	Black Goby
Teleost	*Gymnocephalus cernua*	Ruffe
Teleost	*Heteropneustes fossilis*	Stinging Catfish
Teleost	*Hoplias malabaricus*	Trahira
Teleost	*Hyperoglyphe perciformis*	Barrelfish
Teleost	*Kajikia audax*	Striped Marlin
Teleost	*Katsuwonus pelamis*	Skipjack Tuna
Teleost	*Labeo rohita*	Rohu
Teleost	*Labrus merula*	Brown Wrasse
Teleost	*Limanda limanda*	Common Dab
Teleost	*Lipophrys pholis*	Shanny
Teleost	*Lophius piscatorius*	Angler
Teleost	*Lota lota*	Burbot
Teleost	*Merlangius merlangus*	Whiting
Teleost	*Micropterus dolomieu*	Smallmouth bass

Taxon	Binomial	Common name
Teleost	*Microstomus pacificus*	Dover Sole
Teleost	*Misgurnus fossilis*	Weatherfish
Teleost	*Mistichthys luzonensis*	Sinarapan
Teleost	*Mola mola*	Ocean Sunfish
Teleost	*Mormyrus kannume*	Elephant-snout Fish
Teleost	*Morone saxatilis*	Striped Bass
Teleost	*Mugil cephalus*	Jumping Mullet
Teleost	*Myoxocephalus scorpius*	Shorthorn Sculpin
Teleost	*Nezumia liolepis*	Smooth Grenadier
Teleost	*Oncorhynchus mykiss*	Rainbow Trout
Teleost	*Opsanus tau*	Oyster toadfish
Teleost	*Oreochromis niloticus*	Nile Tilapia
Teleost	*Paralichthys dentatus*	Summer Flounder
Teleost	*Peprilus triacanthus*	Atlantic Butterfish
Teleost	*Perca flavescens*	American Yellow Perch
Teleost	*Perca fluviatilis*	European Perch
Teleost	*Periophthalmus barbarus*	Atlantic Mudskipper
Teleost	*Petrocephalus catostoma*	Churchill
Teleost	*Platichthys flesus*	European Flounder
Teleost	*Pleuronectes platessa*	European Plaice
Teleost	*Pollachius virens*	Saithe
Teleost	*Pomatomus saltatrix*	Bluefish
Teleost	*Prionotus carolinus*	Northern SeaRobin
Teleost	*Prionotus evolans*	Striped Searobin
Teleost	*Pseudopleuronectes americanus*	Winter Flounder
Teleost	*Rutilus rutilus*	Roach
Teleost	*Salmo trutta*	Brown Trout
Teleost	*Sander lucioperca*	Pike-perch
Teleost	*Sander vitreus*	Walleye
Teleost	*Sarda chiliensis*	Eastern Pacific Bonito
Teleost	*Sarda sarda*	Atlantic Bonito
Teleost	*Scomber japonicus*	Pacific Chub Mackerel
Teleost	*Scomber scombrus*	Common Mackerel
Teleost	*Scomberomorus maculatus*	Spanish Mackerel
Teleost	*Sebastes diploproa*	Splitnose Rockfish
Teleost	*Sebastolobus alascanus*	Shortspine Thornyhead
Teleost	*Seriola lalandi*	Yellowtail Amberjack
Teleost	*Seriola quinqueradiata*	Yellowtail
Teleost	*Sphoeroides maculatus*	Northern Puffer
Teleost	*Spicara maena*	Blotched Picarel

Taxon	Binomial	Common name
Teleost	*Stenotomus chrysops*	Scup
Teleost	*Symphodus melops*	Corkwing Wrasse
Teleost	*Taurulus bubalis*	Longspined Bullhead
Teleost	*Tautoga onitis*	Tautog
Teleost	*Tenualosa ilisha*	Hilsa shad
Teleost	*Thunnus albacares*	Yellofin Tuna
Teleost	*Thunnus thynnus*	Bluefin Tuna
Teleost	*Tinca tinca*	Tench
Teleost	*Trachurus trachurus*	Atlantic Horse Mackerel
Teleost	*Trichiurus lepturus*	Largehead Hairtail
Teleost	*Xiphias gladius*	Swordfish
Teleost	*Zeus faber*	John Dory
Teleost	*Zoarces viviparus*	Eelpout
Teleost	*Bathygobius soporator*	Frillfin Goby
Teleost	*Mancopsetta maculata*	Antarctic Armless Flounder
Teleost	*Periophthalmus chrysospilos*	Mudskipper

Table S2. The 32 species for which raw gill surface area and body mass data is available for at least 8 individuals (see text).

All models using this raw dataset were also compared with and without the inclusion of those species traditionally used in aquaculture (Table S3) and with and without those species capable of air-breathing (Table S4). ⁺Aquaculture, *Air-breather.

Scientific name	Common name
Acanthocybium solandri	Wahoo
Acipenser transmontanus	White Sturgeon
Alopias superciliosus	Bigeye Thresher
Alopias vulpinus	Common Thresher
*Anabas testudineus**	Climbing Perch
*Anguilla anguilla**	European Eel
Barbatula barbatula	Stone Loach
*Boleophthalmus boddarti**	Boddart's Goggle-Eyed Goby
Carcharhinus acronotus	Blacknose Shark
Carcharhinus isodon	Finetooth Shark
Carcharhinus limbatus	Blacktip Shark
Carcharhinus obscurus	Dusky Shark
Carcharhinus plumbeus	Sandbar Shark
Carcharodon carcharias	White Shark
Cirrhinus mrigala⁺	Mgrial Carp
*Cobitis taenia**	Spined Loach
Galeocerdo cuvier	Tiger Shark
Gymnocephalus cernua	Ruffe
*Heteropneustes fossilis**	Stinging Catfish
Hoplias malabaricus	Trahira
Isurus oxyrinchus	Shortfin Mako
*Lipophrys pholis**	Shanny
Micropterus dolomieu	Smallmouth Bass
Opsanus tau	Oyster Toadfish
Oreochromis niloticus⁺	Nile Tilapia
Petrocephalus catostoma	Churchill
Prionace glauca	Blue Shark
Rhizoprionodon terraenovae	Atlantic Sharpnose Shark
Scomber japonicus	Pacific Chub
Sphyrna tiburo	Bonnethead Shark
Tinca tinca⁺	Tench
Torpedo marmorata	Marbled Electric Ray

Table S3. The 10 species determined to be those often used in aquaculture. The results of all models using the full dataset, or the raw dataset were compared with and without the inclusion of the species in this table to ensure that our results were not biased.

Scientific name	Common name
Ameiurus nebulosus	Brown Bullhead
Channa punctata	Spotted Snakehead
Channa striata	Snakehead Murrel
Cirrhinus mrigala	Mrigal
Clarias batrachus	Walking Catfish
Ctenopharyngodon idella	Grass Carp
Oncorhynchus mykiss	Rainbow Trout
Oreochromis niloticus	Nile Tilapia
Salmo trutta	Brown trout
Tinca tinca	Tench

Table S4. The 15 species determined to be capable of air-breathing. The results of all models using the full dataset, or the raw dataset were compared with and without the inclusion of the species in this table to ensure that our results were not biased.

Scientific name	Common name
Anabas testudineus	Climbing Perch
Anguilla anguilla	European Eel
Anguilla rostrata	American Eel
Boleophthalmus boddarti	Boddart's Goggle-Eyed Goby
Channa punctata	Spotted Snakehead
Channa striata	Striped Snakehead
Clarias batrachus	Philippine Catfish
Cobitis taenia	Spined Loach
Heteropneustes fossilis	Stinging Catfish
Lipophrys pholis	Shanny
Misgurnus fossilis	Weatherfish
Periophthalmus barbarus	Atlantic Mudskipper
Periophthalmus chrysospilos	Gold-spotted Mudskipper
Taurulus bubalis	Longspined Bullhead
Zoarces viviparus	Eelpout

Table S5. Comparison of coefficients and their 95% Bayesian Credible Intervals (BCI) for the relationship of growth performance and gill area index estimated for (1) all species in the full dataset, (2) the full dataset excluding those species that are used in aquaculture, and (3) the full dataset excluding those species that are capable of air-breathing.
Both models were estimated using Bayesian linear regression using the *brm* function in the *brms* package in Rv.4.0.2.

Model parameterization	Dataset	Intercept (95% CI)	Slope (95% CI)	Sample size
growth performance ~ log gill area index	full	1.92 (1.53 to 2.32)	0.87 (0.52 to 1.23)	132
growth performance ~ log gill area index	excluding aquaculture species	1.88 (1.47 to 2.30)	0.90 (0.53 to 1.27)	122
growth performance ~ log gill area index	excluding air-breathing species	2.08 (1.62 to 2.54)	0.78 (0.39 to 1.17)	117

Table S6. Comparison of coefficients and their 95% Bayesian Credible Intervals (BCI) for the relationship of growth performance and the (1) ontogenetic intercept, (2) ontogenetic slope, and (3) gill area index estimated with the (a) full dataset, (b) full dataset excluding those species that are used in aquaculture, and the (c) full dataset excluding those species that are capable of air-breathing.

The gill area index here was empirically estimated (see text). Both models were estimated using a Bayesian multilevel modeling framework in Stan using the package *rstan* in R v.4.0.2 All intercepts were standardized in the model prior to the second level (see text and SI).

Model parameterization of the second level	Intercept (95% CI)	Slope (95% CI)	Dataset	Sample size
GP ~				
intercept	3.08 (2.63 to 3.53)	0.36 (-0.11 to 0.83)	full	32
intercept	3.06 (2.56 to 3.55)	0.35 (-0.18 to 0.87)	excluding aquaculture species	29
intercept	3.40 (2.94 to 3.87)	-0.05 (-0.56 to 0.46)	excluding air-breathing species	26
intercept	3.22 (2.81 to 3.63)	0.40 (-0.05 to 0.83)	species with a body size range of at least an order of magnitude	34
slope	3.08 (2.63 to 3.53)	0.33 (-0.20 to 0.83)	full	32
slope	3.05 (2.56 to 3.54)	0.32 (-0.27 to 0.88)	excluding aquaculture species	29
slope	3.40 (2.94 to 3.84)	0.23 (-0.33 to 0.78)	excluding air-breathing species	26
slope	3.22 (2.79 to 3.65)	0.20 (-0.29 to 0.67)	species with a body size range of at least an order of magnitude	34
gill area index	3.08 (2.61 to 3.54)	0.13 (-0.40 to 0.65)	full	32
gill area index	3.06 (2.56 to 3.55)	0.16 (-0.41 to 0.72)	excluding aquaculture species	29
gill area index	3.40 (2.94 to 3.85)	-0.17 (-0.69 to 0.35)	excluding air-breathing species	26
gill area index	3.21 (2.78 to 3.64)	0.21 (-0.28 to 0.67)	species with a body size range of at least an order of magnitude	34

Table S7. Comparison of coefficients and their 95% Bayesian Credible Intervals (BCI) for the relationship of growth performance and the gill area index as estimated using (1) empirically estimated *d* values, (2) *d* = 0.8, and (3) *d* predicted from the relationship of *d* and maximum size in Pauly (1981) estimated with and without those species that are used in aquaculture.

The models where gill area index was estimated using empirically estimated ontogenetic slope values were estimated using a Bayesian multilevel modeling framework in Stan using the package *rstan* in R v.4.0.2. For the models where gill area index was estimated using either *d* = 0.8 or *d* predicted from Pauly (1981), a Bayesian linear model was estimated using the *brm* function in the *brms* package in R v.4.0.2. All slopes were standardized in the model prior to the second level (see text and SI).

Estimation of gill area index	Intercept (95% CI)	Slope (95% CI)	Dataset	Sample size
empirically estimated	3.08 (2.61 to 3.54)	0.13 (-0.40 to 0.65)	full	32
empirically estimated	3.06 (2.56 to 3.55)	0.16 (-0.41 to 0.72)	excluding aquaculture species	29
empirically estimated	3.40 (2.94 to 3.85)	-0.17 (-0.69 to 0.35)	excluding air-breathing species	26
d = 0.8	3.08 (2.64 to 3.53)	0.44 (0.00 to 0.88)	full	32
d = 0.8	3.06 (2.60 to 3.52)	0.51 (0.05 to 0.97)	excluding aquaculture species	29
d = 0.8	3.41 (2.95 to 3.87)	0.05 (-0.42 to 0.51)	excluding air-breathing species	26
predicted d	3.08 (2.62 to 3.54)	0.06 (-0.43 to 0.54)	full	32
predicted d	3.06 (2.56 to 3.56)	0.10 (-0.41 to 0.62)	excluding aquaculture species	29
predicted d	3.40 (2.98 to 3.82)	-0.42 (-0.86 to 0.02)	excluding air-breathing species	26

Table S8. Comparison of coefficients and their 95% Bayesian Credible Intervals (BCI) for the relationship of growth performance, caudal fin aspect ratio, and gill surface area, as measured by (1) the ontogenetic intercept, (2) the ontogenetic slope, (3) gill area index for models with the (a) full dataset, (b) full dataset excluding those species that are used in aquaculture, and the (c) full dataset excluding those species that are capable of air-breathing.

All models were estimated using a Bayesian multilevel modeling framework in Stan using the package *rstan* in R v.4.0.2 All predictors in the second level of the model were standardized and thus the effect sizes for the slopes are relative to each other (see text and SI). GP = growth performance, CFAR = caudal fin aspect ratio, GSA = gill surface area, and GAI = gill area index.

Model parameterization of the second level	Intercept (95% CI)	CFAR Slope (95% CI)	GSA metric slope (95% CI)	Dataset	Sample size
GP ~ CFAR +					
intercept	2.95 (2.51 to 3.38)	0.60 (0.21 to 1.00)	0.11 (-0.35 to 0.58)	full	30
intercept	2.88 (2.41 to 3.35)	0.63 (0.22 to 1.05)	0.11 (-0.41 to 0.62)	excluding aquaculture species	27
intercept	3.19 (2.71 to 3.64)	0.50 (0.13 to 0.89)	-0.15 (-0.62 to 0.33)	excluding air-breathing species	25
slope	2.95 (2.52 to 3.38)	0.62 (0.25 to 0.99)	0.19 (-0.29 to 0.67)	full	30
slope	2.87 (2.42 to 3.33)	0.65 (0.28 to 1.02)	0.21 (-0.30 to 0.70)	excluding aquaculture species	27
slope	3.20 (2.75 to 3.64)	0.48 (0.10 to 0.86)	0.20 (-0.29 to 0.70)	excluding air-breathing species	25
gill area index	2.95 (2.51 to 3.39)	0.64 (0.27 to 1.02)	-0.04 (-0.52 to 0.43)	full	30
gill area index	2.86 (2.39 to 3.34)	0.68 (0.28 to 1.08)	-0.05 (-0.56 to 0.45)	excluding aquaculture species	27
gill area index	3.19 (2.74 to 3.64)	0.51 (0.14 to 0.87)	-0.23 (-0.71 to 0.23)	excluding air-breathing species	25

Table S9. Comparison of coefficients and their 95% Bayesian Credible Interval (BCI) for the relationship of the growth coefficients (*k*), asymptotic size (W_∞), and gill surface area, as measured by (1) the ontogenetic intercept, (2) the ontogenetic slope, (3) gill area index for models with the (a) full dataset, (b) full dataset excluding those species that are used in aquaculture, and the (c) full dataset excluding those species that are capable of air-breathing.

All models were estimated using a Bayesian multilevel modeling framework in Stan using the package *rstan* in R v.4.0.2 All predictors in the second level of the model were standardized and thus the effect sizes for the slopes are relative to each other (see text and SI). GSA = gill surface area.

Model parameterization of the second level	Intercept (95% BCI)	W_∞ slope (95% BCI)	GSA slope (95% BCI)	Dataset	Sample size
$k \sim W_\infty +$					
intercept	-0.55 (-0.68 to -0.42)	-0.26 (-0.38 to -0.13)	-0.08 (-0.22 to 0.06)	full	30
intercept	-0.62 (-0.71 to -0.52)	-0.26 (-0.35 to -0.17)	-0.06 (-0.17 to 0.04)	excluding aquaculture species	27
intercept	-0.50 (-0.67 to -0.33)	-0.34 (-0.50 to -0.18)	-0.07 (-0.22 to -0.08)	excluding air-breathing species	25
slope	-0.55 (-0.68 to -0.42)	-0.27 (-0.40 to -0.14)	-0.05 (-0.19 to 0.09)	full	30
slope	-0.61 (-0.71 to -0.52)	-0.27 (-0.36 to -0.18)	-0.01 (-0.12 to 0.11)	excluding aquaculture species	27
slope	-0.50 (-0.67 to -0.33)	-0.34 (-0.50 to -0.18)	-0.01 (-0.17 to 0.15)	excluding air-breathing species	25
gill area index	-0.55 (-0.69 to -0.41)	-0.28 (-0.40 to -0.15)	-0.03 (-0.17 to 0.11)	full	30
gill area index	-0.62 (-0.71 to -0.52)	-0.27 (-.36 to -0.18)	-0.04 (-0.14 to 0.06)	excluding aquaculture species	27
gill area index	-0.50 (-0.67 to -0.33)	-0.35 (-0.51 to -0.19)	-0.05 (-0.21 to 0.11)	excluding air-breathing species	25

Chapter 5.

Discussion

This thesis aimed to contribute to our understanding regarding the generality of the relationships among oxygen, ecology, and life history in fishes and other vertebrates. In doing so, I have built on and empirically tested existing theory, as well as examined the relationships among oxygen acquisition and use, ecological lifestyle, and life histories. In the following, I review the main findings of each chapter, highlight the significance of the thesis (with an emphasis on the novelty of each chapter as the relevance of each chapter's main findings are detailed in each chapter's respective discussion section), outline future directions, and end with concluding thoughts.

5.1. Main findings

Broadly speaking, my thesis took a macroecological approach to examining the links among traits related to oxygen acquisition (respiratory surface area) and use (metabolic rate), ecology (activity, habitat), and life histories (somatic growth, maximum size). While the approach and analyses were indeed macroecological, I coupled field collections, laboratory dissections, and meta-analysis and modeling to understand the generality of patterns related to oxygen, ecology, and life histories. In doing so, I (along with my collaborators) (1) collected > 200 individual elasmobranch specimens for gill surface area measurements, (2) measured gill surface area for twelve species (> 71 individuals) that did not have these data previously, and (3) developed novel quantitative methods that enabled me to address knowledge gaps by combining data across scales (individuals, species), multiple size-dependent phenomena (metabolic rate, respiratory surface area), and salient covariates including the evolutionary history among species.

In Chapter 2, I revealed that respiratory surface area explained patterns of metabolic rate across the vertebrate tree of life. For this chapter, I developed the initial phylogenetic Bayesian hierarchical modeling framework, which allowed me to combine size-mismatched metabolic rate and respiratory surface area data for over 100 vertebrate species from all major lineages. I found that despite the difference in the scaling of metabolic rate between endotherms and ectotherms, the scaling of respiratory surface

area did not differ between the two groups, and compared to temperature, explained twice the variation in metabolic rate across vertebrates.

In Chapter 3, I brought gill surface area comparisons across species into a scaling context and quantified how gill surface area related to ecological lifestyles across shark species. Here, I uncovered that larger-bodied, active, and pelagic species had greater gill surface areas for a given size (ontogenetic intercept) compared to their small-bodied, less active, benthic counterparts. Conversely, the rate at which gill surface area increased with body mass (ontogenetic slope) was the same for all species, regardless of activity level or habitat type.

In Chapter 4, I tested a central prediction of the Gill Oxygen Limitation Theory – that gill surface area is related to growth and maximum size across fishes, as parametrized by the von Bertalanffy growth model. For this chapter, I first re-examined an original dataset used to first establish this relationship over 40 years ago. Second, I conducted a meta-analysis that included data from over 130 fish species to assess if gill surface area – in a scaling context – explained the incredible variation in growth and maximum size observed across fishes. To do so, I expanded the phylogenetic Bayesian hierarchical modeling framework from Chapter 2 to include both individual- and species-level data. I found that gill surface area, regardless of the metric used for this trait, was not strongly correlated to growth and maximum size, and instead, was more related to activity level.

Collectively, this body of work highlights the complexities of integrating data across scales and illustrates that oxygen acquisition and use are tightly corelated with activity level, but the relationships with life histories are less straightforward, not least due to the size-dependent nature of metabolic rate and respiratory surface area.

5.2. Significance

There are three distinct areas in which I feel that my thesis made significant advancements and contributions to the fields of ecology and physiology. First, I filled in knowledge gaps regarding the relationship among traits related to oxygen acquisition (respiratory surface area) and use (metabolic rate), ecological lifestyle (activity, habitat), and life history (somatic growth and maximum size). In Chapter 2, I bridged the gap between physiology and macroecology by incorporating respiratory surface area and thermoregulatory

strategy into metabolic scaling (Bigman *et al.* 2021). As originally proposed, metabolic scaling was thought to be explained by the effects of body mass (through the fractal nature of distribution networks) and temperature (West *et al.* 1999; Gillooly *et al.* 2001; Brown *et al.* 2004). However, physiologists, and more recently, macroecologists and macrophysiologists have recognized the importance of respiratory structures to metabolic rate (e.g., Hughes 1978, 1984; Gillooly *et al.* 2016; Rubalcaba *et al.* 2020). Yet, incorporating respiratory surface area – a size-dependent trait – into metabolic scaling (inherently dependent on size) was complicated by these size-dependencies and other necessary covariates (e.g., thermoregulatory strategy, evolutionary history). Solving this issue with a bespoke modeling framework allowed me to reveal that respiratory surface area explained twice the variation, compared to temperature, in metabolic scaling across the vertebrate tree of life (Bigman *et al.* 2021). In Chapter 3, I brought gill surface area into a scaling context to identify patterns of gill surface area and ecological lifestyle among shark species (Bigman *et al.* 2018). Prior to this work, gill surface area was often quantified as a mass-specific measure (gill surface area per gram of body mass). While a mass-specific metric is suitable for traits that scale isometrically with body mass, it is not suitable for traits that have hypoallometric scaling (e.g., gill surface area, metabolic rate). I examined how both components of an ontogenetic allometry – the slope (rate at which gill surface area increases with body mass) and the intercept (the gill surface area for a given size) – varied with activity level, habitat type, and maximum size. In addition, I improved upon metrics of activity level used in analyses with gill surface area. Specifically, I employed caudal fin aspect ratio as a quantitative metric of activity level instead of the qualitative, subjective categories (e.g., “sluggish” or “intermediate”) used previously (Gray 1954; Wegner 2011). Finally, in Chapter 4, I tested a central prediction of the Gill Oxygen Limitation Theory – that gill surface area is tightly correlated to somatic growth and maximum size. I collated the largest database of high-quality teleost and elasmobranch gill surface area (in addition to measuring gill surface area to supplement this dataset) that will be published to-date. I emphasized the importance of choosing appropriate analytical methods and considering the scaling of traits, instead of a simplified metric. Additionally, I expanded the modeling framework developed in Chapter 2 to be flexible enough to include data across scales—both within and across species.

Second, the phylogenetic Bayesian hierarchical modeling framework developed and expanded upon herein solved two (related) problems inherent in macroecological and

macrophysiological analyses. First, this modeling framework offers the opportunity to more appropriately extend both traditional and novel macroecological and macrophysiological questions to ectothermic organisms. Historically, most macroecological work has been focused on mammals and birds, which grow determinately (Gaston & Blackburn 2008). Thus, employing species-mean data (i.e., a mean metabolic rate and mean body mass for a given species) is not too problematic, as long as the trait or factor was measured at or after a stage in which it was relatively stable (i.e., maturity). However, most ectothermic species continue to grow throughout their lifetimes and thus species-mean data becomes problematic. This problem is often overlooked in macroecological analyses and is exacerbated when working with traits or factors that also change with body size ontogenetically (e.g., metabolic rate, respiratory surface area). It is ideal to examine these traits in the context of their ontogenetic allometries, and then assess how these allometries vary across species. However, doing so requires raw data (i.e., estimates of a trait value for multiple individuals of the same species) that spans almost the entire size range of a species. These data are rarely available, resulting in the second problem. When one must use mean data, examining multiple size-dependent traits (metabolic rate, respiratory surface area) simultaneously is problematic unless the traits (or factors) were measured in the same individuals. For the majority of macroecological analyses, this will not be the case. The modeling framework presented here allows for the incorporation of both body size estimates by accounting for the effect of body mass on one trait or factor in one level of the model and propagating the uncertainty in this relationship to the other levels. Additionally, a random effect of phylogeny is also incorporated into the hierarchical models, further advancing the field of macroecology. Notably, the development of such a modeling framework would not have been possible without the advancement of statistical techniques in recent years, particularly Stan, which has offered a platform for solving these (and many other) analytical problems (Stan Development Team 2019).

Last, prior to this thesis, only 14 shark species had published estimates of gill surface area, with only 10 having enough data (at least 8 individuals) to estimate an ontogenetic allometry of gill surface area and body mass (Hughes 1972; Emery & Sczcepanski 1985; Hughes *et al.* 1986; Hata 1993; Wegner *et al.* 2010; Wootton *et al.* 2015; Wegner 2016; Bigman *et al.* 2018). Now, following my thesis work, 25 shark species have gill surface area estimates, with at least seven additional species having enough data to estimate an

ontogenetic allometry. While this may not seem like much, comparatively, over 100 teleost species have published gill surface area data.

5.3. Future directions

My thesis has generated more questions than I have answered, but alas, that is science. Although each chapter spawned multiple research questions (most of which are in the discussion section of each chapter and not repeated here), the one big question that lingers is the directionality between metabolic rate and respiratory surface area – which is driving which? Unfortunately, this thesis cannot answer that question, nor should it. Broad scale work such as that presented in this thesis cannot identify mechanisms by itself; instead, it serves to test predictions generated by theory and identify broad patterns. Such work must be coupled with other work that can identify the causal mechanisms underlying such patterns. In the context of oxygen's role in the physiology, ecology, and evolution of organisms, this would require a collaboration among experimental physiologists and macroecologists (and macrophysiologists). As my thesis work has placed me somewhere in the middle of these fields and perspectives, I can appreciate the challenging nature of such a collaboration. Yet, it will be necessary to understand the intricacies surrounding the interplay among oxygen, physiology, ecology, and evolution.

There are almost infinite opportunities for future research in the context of the role of oxygen in the physiology, ecology, and evolution of organisms, some of which were generated by this thesis and some by the data or modeling frameworks made available by this thesis. First, it is somewhat paradoxical that gill surface area, as it is related to metabolic rate, did not relate to growth and maximum size across fishes (and that my colleague generally found weak relationships among metabolic rate and life histories across fishes, Wong *et al.* 2021). Theoretically, metabolic rate (and other traits related to oxygen acquisition and use) should be tightly correlated to life histories as metabolic rate governs the available energy for growth, survival, and reproduction (e.g., Brown *et al*. 2004). After all, this is an assumption of many macroecological theories – Metabolic Theory of Ecology, Gill Oxygen Limitation Theory, Oxygen- and Capacity-Limited Thermal Tolerance, as well as other general theories of oxygen limitation (Brown *et al*. 2004; Pauly 2010; Forster *et al.* 2012; Pörtner *et al.* 2017; Verberk *et al.* 2020). While stronger relationships between metabolic rate (or respiratory surface area, presumably) have been

found in other taxa, particularly birds and mammals, fewer such connections have been documented for fishes (e.g., Henneman 1983; White & Seymour 2004; Ton & Martin 2016). Continuing down this path of exploring the relationships among gill surface area, metabolic rate, and life histories in fishes will no doubt prove useful and enlightening, not least due to the continued increase in availability of data and advancement of statistical techniques. One of the main challenges that remains (and perhaps why I and my colleagues have not found strong relationships among gill surface area, metabolic rate, and life histories) is due to the difficulty in partitioning variance among size as a life history trait and measurement size (the size at which metabolic rate/gill surface area was measured).

Second, this thesis is largely agnostic to environmental temperature. While I did not intend this to be the case, extracting meaningful and accurate environmental temperature data is no small task. It is clear that environmental temperature (and environmental oxygen) would relate to patterns of metabolic rate, respiratory surface area, and life histories, and this will be a fruitful avenue of future research (e.g., Morais & Bellwood 2018; van Denderen *et al.* 2020; Pardo & Dulvy 2021). These relationships also may provide a cohesive link from oxygen limitation (if it is occurring) and the temperature-size rule to James' Rule and Bergmann's Rule (Audzijonyte *et al.* 2019). Third, a natural extension of life histories is population dynamics. Temperature is linked to the maximum intrinsic rate of population increase (r_{max}) and extending the scope of such a relationship to include metabolic rate and respiratory surface area may help identify whether oxygen relates to population dynamics (Pardo & Dulvy 2020). Finally, employing the modeling framework developed herein offers the opportunity to bridge experimental physiology and macro-ecology and macrophysiology—an endeavor that is sorely needed. At present, studies focusing on the interrelationships of oxygen, physiology, and ecology within species are largely disconnected from those across species and often, draw divergent conclusions. Broader, macroecological scale studies often do find evidence for oxygen limitation (although not all of them; Forster *et al.* 2012; Audzijonyte *et al.* 2020; Rubalcaba *et al.* 2020). However, within species studies show a much more complicated relationship among oxygen acquisition and use, physiological performance, and life histories (e.g., Clark *et al.* 2008; Lefevre *et al.* 2017; Prinzing *et al.* in prep). Integrating individual-level data into analyses across species to understand how responses at the individual level

scale up to create patterns across species will be key to predicting species' responses to climate change.

5.4. Concluding thoughts

Understanding the role that oxygen plays in the physiology, ecology, and evolution of organisms is paramount to predicting how aquatic species, particularly those in the marine realm, will respond to a changing climate. While it is an especially exciting time to be part of such an endeavor due to the recent resurgence of research in this area, it is also a frustrating one. There are seemingly infinite avenues one could take to contribute to understanding the role of oxygen and aerobic metabolism in explaining species' observations and responses, as well as higher-level patterns. Further, work in this area is disconnected (experimental physiology, meta-analysis and modeling) and at best, polarizing (e.g., Metabolic Theory of Ecology, Gill Oxygen Limitation Theory; Brown *et al.* 2004; Pauly 2010). It was extremely difficult to choose what avenues to pursue and which puzzle pieces to fit together. Yet, I had the opportunity to not only work on these questions myself but guide other graduate students in the lab to other questions that could not be part of my own PhD but would contribute to the greater question at hand. It is my hope that my work (and other collaborations on this topic in the Dulvy lab) contributes a small part to our understanding regarding how oxygen may relate to ecology and life histories in fishes and other vertebrates.

5.5. References

Audzijonyte, A., Barneche, D. R., Baudron, A. R., Belmaker, J., Clark, T. D., Marshall, C. T., Morrongiello, J.R., & van Rijn, I. (2019). Is oxygen limitation in warming waters a valid mechanism to explain decreased body sizes in aquatic ectotherms? *Glob. Ecol. Biogeogr.*, 1–31.

Audzijonyte, A., Richards, S. A., Stuart-Smith, R. D., Pecl, G., Edgar, G. J., Barrett, N. S., Payne, N., & Blanchard, J. L. (2020). Fish body sizes change with temperature but not all species shrink with warming. *Nature Ecol. Ecol.*, *4*(6), 809-814.

Bigman, J.S., M'Gonigle, L.K., Wegner, N.C., & Dulvy, N.K. (2021). Respiratory capacity is twice as important as temperature in driving patterns of metabolic rate across the vertebrate tree of life. *Sci. Adv.*

Bigman, J. S., Pardo, S. A., Prinzing, T. S., Dando, M., Wegner, N. C., & Dulvy, N. K. (2018). Ecological lifestyles and the scaling of shark gill surface area. *J. Morphol.*, *279*(12), 1716–1724.

Brown, J. H., Gillooly, J. F., Allen, A. P., Savage, V. M., & West, G. B. (2004). Toward a metabolic theory of ecology. *Ecol.*, *85*(7), 1771–1789.

Clark, T. D., Sandblom, E., Cox, G. K., Hinch, S. G., & Farrell, A. P. (2008). Circulatory limits to oxygen supply during an acute temperature increase in the Chinook salmon (Oncorhynchus tshawytscha). *Am. J. Physiol-Reg I*, *295*(5), R1631-R1639.

Emery, S. H. & Szczepanski, A. (1986). Gill dimensions in pelagic elasmobranch fishes. *Biol. Bull.*, *171*, 441.

Forster, J., Hirst, A. G., & Atkinson, D. (2012). Warming-induced reductions in body size are greater in aquatic than terrestrial species. *Proc. Nat. Acad. Sci.*, *109*(47), 19310–19314.

Gaston, K., & Blackburn, T. (2008). *Pattern and process in macroecology*. John Wiley & Sons.

Gillooly, J. F., Brown, J. H., West, G. B., Savage, V. M., & Charnov, E. L. (2001). Effects of size and temperature on metabolic rate. *Science*, *293*(5538), 2248–2251.

Gillooly, J. F, Gomez, J. P., Mavrodiev, E. V., Rong, Y., & McLamore, E. S. (2016). Body mass scaling of passive oxygen diffusion in endotherms and ectotherms. *Proc. Nat. Acad. Sci., U.S.A., 113*(19), 5340–5345.

Gray, I. E. (1954). Comparative study of the gill area of marine fishes. *Biol. Bull.*, *107*, 219–255.

Hata, D. (1993). Gill surface area in relation to growth rates and maximum size in sharks. *PhD dissertation*. Virginia Institute of Marine Science.

Hennemann, W.W. (1983). Relationship among body mass, metabolic rate and the intrinsic rate of natural increase in mammals. *Oecologia*, *56*(1), 104–108.

Hughes G. M. (1972). Morphometrics of fish gills. *Respir. Physiol.14*: 1–25.

Hughes, G. M. (1984). Scaling of respiratory areas in relation to oxygen consumption of vertebrates. *Experientia, 40*, 519-524.

Hughes G. M., Perry S. F., & Piiper J. (1986). Morphometry of the gill of the elasmobranch *Scyliorhinus stellaris* in relation to body size. *J. Exp. Biol., 121*, 27–42,

Lefevre, S., McKenzie, D. J., & Nilsson, G. E. (2017). Models projecting the fate of fish populations under climate change need to be based on valid physiological mechanisms. *Glo. Chang. Biol.*, *23*(9), 3449-3459.

Morais, R. A., & Bellwood, D. R. (2018). Global drivers of reef fish growth. *Fish Fish.*, *19*(5), 874-889.

Pardo, S. A. & Dulvy, N. K. (2021). Body mass, temperature, and depth shape the maximum intrinsic rate of population increase in sharks and rays. bioRxiv 2021.03.02.433372; doi: https://doi.org/10.1101/2021.03.02.433372.

Pauly, D. (2010). *Gasping fish and panting squids: oxygen, temperature, and the growth of water-breathing animals*. International Ecology Institute.

Pörtner, H. O., Bock, C., & Mark, F. C. (2017). Oxygen-and capacity-limited thermal tolerance: bridging ecology and physiology. *J. Exp. Biol.*, *220*(15), 2685-2696.

Prinzing, T.S., Bigman, J.S., Skelton, Z.R., Dulvy, N.K., and Wegner, N.C. in prep. The allometric scaling of oxygen supply and demand in California Horn Shark *Heterodontus francisci.*

Rubalcaba, J. G., Verberk, W. C., Hendriks, A. J., Saris, B., & Woods, H. A. (2020). Oxygen limitation may affect the temperature and size dependence of metabolism in aquatic ectotherms. *Proc. Nat. Acad. Sci. U.S.A.*, *117*(50), 31963-31968.

Ton, R., & Martin, T. E. (2016). Metabolism correlates with variation in post-natal growth rate among songbirds at three latitudes. *Funct. Ecol.*, *30*(5), 743-748.

van Denderen, D., Gislason, H., van den Heuvel, J., & Andersen, K. H. (2020). Global analysis of fish growth rates shows weaker responses to temperature than metabolic predictions. *Glob. Ecol. Biogeogr.*, *29*(12), 2203-2213.

Verberk, W. C., Atkinson, D., Hoefnagel, K. N., Hirst, A. G., Horne, C. R., & Siepel, H. (2020). Shrinking body sizes in response to warming: explanations for the temperature–size rule with special emphasis on the role of oxygen. *Biol. Rev.*, *96*(1), 247-268.

Wegner, N. C. (2011). Gill Respiratory Morphometrics. In Farrell, A. P. (Ed.), *Encyclopedia of Fish Physiology: From Genome to Environment* (Vol. 2, pp. 803–811). San Diego, CA: Academic Press.

Wegner, N.C. (2016). Elasmobranch Gill Structure. In Shadwick, R. E., Farrell, A.P., & Brauner, C.J. (Eds.), *Physiology of Elasmobranch Fishes: Structure and Interaction with Environment* (Vol. 34, pp. 102-145). Elsevier Inc.

Wegner, N. C., Sepulveda, C. A., Olson, K. R., Hyndman, K. A., & Graham, J. B. (2010a). Functional morphology of the gills of the shortfin mako, *Isurus oxyrinchus*, a lamnid shark. *J. Morph.*, *271*, 937–948.

West, G B, Brown, J. H., & Enquist, B. J. (1999). The fourth dimension of life: fractal geometry and allometric scaling of organisms. *Science*, *284*(5420), 1677–1679.

White, C. R., & Seymour, R. S. (2004). Does basal metabolic rate contain a useful signal? Mammalian BMR allometry and correlations with a selection of physiological, ecological, and life-history variables. *Physiol. Biochem. Zool.*, *77*(6), 929-941

Wong, S., Bigman, J. S., & Dulvy, N. K. (2021). The metabolic pace of life histories across fishes.
bioRxiv 2020.11.16.385559; doi: https://doi.org/10.1101/2020.11.16.385559.

Wootton, T. P., Sepulveda, C. A., & Wegner, N. C. (2015). Gill morphometrics of the thresher sharks (Genus Alopias): Correlation of gill dimensions with aerobic demand and environmental oxygen. *J. Morph.*, *276*, 589-600.